STUDIES IN FLUIDIZED BED REACTORS FOR COMPLEX SYSTEMS

Thesis

Submitted in partial fulfilment of the requirements

for the degree of

DOCTOR OF PHILOSOPHY

by

RAIOMOND K.IRANI

Department of Chemical Engineering

INDIAN INSTITUTE OF TECHNOLOGY, BOMBAY

1980

THESIS APPROVAL SHEET

Thesis entitled: 'STUDIES IN FLUIDIZED BED REACTORS FOR COMPLEX SYSTEMS' by RAIOMOND K. IRANI is approved for the degree of DOCTOR OF PHILOSOPHY

Examiners

Supervisor(s)

Chairman

(Date)
23.12.80

THESIS APPROVAL SHEET

Thesis entitled: 'STUDIES IN FLUIDIZED BED REACTORS FOR COMPLEX SYSTEMS' by RAIOMOND K. IRANI is approved for the degree of DOCTOR OF PHILOSOPHY

Examiners

_____

_____

_____

_____

Supervisor(s)

_____

_____

Chairman

(Date) _____

CONTENTS

CONTENTS (CONTINUED)

CONTENTS (CONTINUED)

CONTENTS (CONTINUED)

LIST OF TABLES

LIST OF FIGURES

LIST OF FIGURES (CONTINUED)

LIST OF FIGURES (CONTINUED)

NOMENCLATURE

a	term defined by Equation (5.31)
A,B,R,S,T,U	reaction components
b	mass transfer parameter correlating exponent
C_A	concentration of A in the bubble phase (g mol/cm^3)
C_{Ao}	inlet concentration of A (g mol/cm^3)
C_A, C_R, C_S, C_T	concentration of A,R,S and T respectively (g mol/cm^3)
C_A^*, C_R^*	equilibrium concentration of A and R (g mol/cm^3)
$\bar{C}_A, \bar{C}_R, \bar{C}_S, \bar{C}_T$	fractional concentration of A,R,S, and T
$\bar{C}_A^*$, $\bar{C}_R^*$	fractional equilibrium concentration of A and R
d_b	effective bubble diameter (cm)
D_e	effective diffusivity for gas (cm^2/sec)
D_A, D_R	molecular diffusivity for gas (cm^2/sec)
D_t	diameter of reactor (cm)
e	modified contacting efficiency in a fluid bed
E	contacting efficiency in a fluid bed
F_{Ao}	molar feed rate of reactant A (g mol/hr)
g	acceleration due to gravity (cm/sec^2)
G	mass flux (g/hr cm^2)
k, k_i	rate constants for a first order reaction (sec^{-1})

k_s	rate constant for a first order heterogeneous reaction based on mass of solids (cm^3/g sec)
k'	rate constant for a first order heterogeneous reaction based on mass of active catalyst (cm^3/g sec)
k_1'	rate constant for a zero order reaction (g mol/cm^3 sec)
K	effective rate constant in a fluid bed defined by Equation (2.3) (sec^{-1})
$K_{bc}{}^j$	gas interchange coefficient between bubble and cloud-wake for species j (sec^{-1})
$K_{ce}{}^j$	gas interchange coefficient between cloud-wake and emulsion for species j (sec^{-1})
K_A	adsorption c onstant for ethanol (atm^{-1})
K_i	modified rate constant in a fluid bed defined by Equation (2.13) (sec^{-1})
K_{ii}	modified rate constant def ned by Equation (2.31) (sec^{-1})
K_w	adsorption constant for water (atm^{-1})
K_j'	modified rate constant defined by Equation (2.23) (sec^{-1})
K'_{jj}	modified rate constants defined by Equation (2.31) and in Table 2.1 (sec^{-1})

$K_{[12]}$, $K_{[12]_{12}}$	modified rate constants defined in Table 2.1 (sec^{-1})
$K_{[1+2]}$, $K_{[1+2]_{1+2}}$	modified rate constants defined in Table 2.1 (sec^{-1})
$K'_{[1+2]}$, $K'_{[1+2]1+2}$	modified rate constants defined in Table 2.1 (sec^{-1})
K''_{11}	modified rate constant defined in Table 2.1 (sec^{-1})
l	height in a fluid bed (cm)
L, L_f	height of a bubbling fluid bed (cm)
N_A	moles of A in reactor per unit time (g mol/sec)
N_{Ao}	moles of A entering reactor per unit time (g mol/sec)
N_j	moles of inert in reactor per unit time (g mol/sec)
N'_{Re}	Reynolds number
P, P_1, P_2, P_3	terms defined by Equations (2.37), (2.40), (2.41) and (2.42) respectively
P_g	partial pressure of component in the bulk phase (atm)
P_T	pressure at the top of the fluid bed (atm)
$P', P'(1), P'(z)$	pressure at a given height in the fluid bed (atm)
ΔP	partial pressure gradient of component between bulk phase and catalyst-fluid interface (atm)

r'	observed overall reaction rate (g/hr cm^2)
R'	mass of total solids in the fluid bed/mass of active catalyst in the bed; also mass of catalyst in the undiluted bed/mass of catalyst in the diluted bed
t	residence time in the fluid bed (sec)
u_b	volumetric bubble flow rate per unit area (cm/sec)
u_{br}	velocity of a bubble with respect to the emulsion phase (cm/sec)
u_{mf}	superficial velocity at minimum fluidization (cm/sec)
u_o	superficial entering gas velocity (cm/sec)
v_o	volumetric entering flow rate of gas (cm^3/sec)
V_b	volume of a gas bubble (cm^3)
V_w	volume of bubble wake (cm^3)
W	weight of solids in the bed (g)
x_o	mole fraction of ethanol in the feed
X_A	fractional conversion of reactant A
y_A	mole fraction of A in the bed
y_{Ao}	mole fraction of A entering the bed
y_j	mole fraction of inerts in the bed
z	fractional height in the fluid bed

Greek Letters

α	term defined by Equation (5.23)
α_w	volume of wake/volume of bubble

β	stoichiometric coefficient of change in moles during reaction
γ	term defined by Equation (5.35)
γ_i	volume of solids in region i/volume of bubbles in the bed
δ	volume of bubbles/volume of bed
ε_e	void fraction of the emulsion phase
ε_{mf}	void fraction in a fluid bed at minimum fluidizing conditions
ε_{packed}	void fraction of a packed bed
λ_1	term defined by Equation (3.7)
λ_2	term defined by Equation (3.12)
ρ_a	bulk density of alumina catalyst (g/cm^3)
ρ_g	bulk density of glass powder (g/cm^3)
ρ_s	bulk density of solids (g/cm^3)
ϕ_i	terms defined by Equations (3.18), (2.26) and (2.27) respectively
ϕ'_1	term defined by Equation (2.31)
ϕ'_{11}	term defined by Equation (2.31)
Ψ_i	terms defined by Equation (2.24) and in Table 2.1 respectively
$\Psi_{[1+2]}$	term defined in Table 2.1

Subscripts

b	bubble phase
c	cloud phase
cr	critical value of the parameter at which reactant concentration is reduced to zero
e	emulsion phase
max	value of the parameter corresponding to maximum concentration of the intermediate species
opt	optimum
mf	minimum fluidizing conditions

CHAPTER - 1

INTRODUCTION

1. INTRODUCTION

Several models have been presented in the literature to account for the main features of a catalytic fluidized bed. These include the earlier homogeneous models in which the role of mixing is accounted for by a longitudinal dispersion coefficient, two region models, and bubbling bed models. The last appear to be the most rigorous in that they explicitly recognize the role of the bubble in the analysis of the fluidized bed. Among the bubbling bed models are those of Davidson and Harrison[1], and Kunii and Levenspiel.[2, 3] These have been modified by several workers over the years, e.g. the Toor-Calderbank[4] modification of the Davidson model[5] and the Fryer-Potter[6] extension of the Kunii-Levenspiel model. Other bubbling bed models which characterize the fluidized bed include the compartment model of Kato and Wen[7], which incorporates the effect of changing bubble size along the height of the fluid bed, and the Mori-Wen[8] modification of this model. The models presented by Partridge and Rowe[9], Toor and Calderbank[4], Kato and Wen[7], Mori and Muchi[10], and Fryer and Potter[6] consider bubble coalescence in the bed. Other models such as those of Orcutt *et al.*[11], Kunii and Levenspiel[2, 3], and Kobayashi *et al.*[12] employ the concept of a single average bubble diameter throughout the bed.

Zenz[13], and Behie and Kehoe[14] have shown that the jets formed just above a perforated plate distributor may have a significant effect on the conversion profile in the bed. The model proposed by Miyauchi[15, 16] incorporates the concept of a dilute phase in the bed.

1.1 CHOICE OF MODEL

The salient features of some of the models proposed have been outlined in Table 1.1. All these models are concerned with simple first order reactions. The various models simulate the fluid bed reactor performance at different levels of complexity. Whereas a more complex model serves to present a more realistic picture of the fluidized bed, it has been shown[8] that for slow reactions, when the mass exchange from the bubble to the emulsion phase is not controlling, the two-phase concept of a fluid bed could be effectively replaced by a simpler model incorporating a single phase, and even a simple homogeneous model for describing fluid bed behaviour could be termed adequate.

The experimental results of Chavarie and Grace[17, 18] on the ozone reaction (known to conform to the first order reaction scheme A---->R), in which concentration profiles obtained in the bubble, cloud and emulsion phase were compared with those predicted by the various models, clearly showed

TABLE 1.1

SALIENT FEATURES OF SOME BUBBLING BED MODELS PROPOSED IN THE LITERATURE

Model	Single effective/ variable bubble diameter	Mode of estimation of bubble diameter	Bubble/cloud phase	Emulsion phase	Mass transfer from bubble to cloud/ emulsion	Mass transfer from cloud to emulsion	Remarks
1	2	3	4	5	6	7	8
Orcutt et al.[11]	Single effective diameter	Fitted	No cloud; bubble completely mixed	Plug flow, or completely mixed	To emulsion	--	Simple model requiring relatively few computations. Reaction occurs in the emulsion phase and both bubble and emulsion phase contributions are considered.
Partridge and Rowe[9]	Sectional average size	X-ray data on bubble size distribution	Completely mixed	Plug flow	On the basis of a rigid sphere model	--	X-ray data required for computations. Reaction occurs in cloud and emulsion. Bubble phase gas contribution is also incorporated.
Toor and Calderbank[4]	Variable bubble diameter	Empirical equation employed for bubble size increase	Bubble/ cloud completely mixed	Plug flow, completely mixed or with back mixing coefficient	To emulsion	--	Reaction occurs in the emulsion phase. Contributions from both bubble and emulsion phases are considered.
Kunii and Levenspiel[2,3]	Single effective diameter	Fitted	Bubble in plug flow	Flow reversal in emulsion phase, Plug flow	To cloud	To emulsion	Reaction occurs in bubble/ cloud and emulsion phases. Representative of back mixing models. The bubble phase gas contribution alone is considered.
Kato and Wen[7]	Variable bubble diameter. Bed is divided into compartments	Empirical equation. The size of each compartment corresponds to the bubble diameter at that level	Bubble/ cloud phase completely mixed	Completely mixed	From bubble/ cloud to emulsion	--	Elaborate computational procedure with no adjustable parameters. Contribution from bubble phase gas alone is considered.

contd...

1	2	3	4	5	6	7	8
Fryer and Potter[6]	Variable bubble size	Empirical equation employed	No mixing in bubble and cloud/ wake phases	Plug flow	To cloud/ wake	To emulsion. Flow reversal in this phase	Reaction occurs in bubble, cloud/wake and emulsion phases. The bubble and cloud/wake phase gas contributions are considered.
Behie and Kehoe[14]	Jetting region followed by single effective diameter	Fitted	No cloud; bubble in plug flow	Completely mixed	To emulsion	--	For fast reactions conversion takes place primarily in the jetting region as the mass transfer coefficient in the grid region is higher than for the rest of the bed. Experimental measurements of the mass transfer coefficient in the grid region for various grid designs and gas mixtures are required.
Miyauchi[15,16]	Single effective diameter	Fitted	Bubble in plug flow	Plug flow	To emulsion	--	Incorporation of a dilute phase above the bubbling region of the bed. Adsorption of gas on the catalyst is also considered.
Mori and Wen[8]	Jetting region followed by variable bubble diameter	Empirical equation. presented by Mori and Wen[8]. Compartmental model as per Kato and Wen[7]	Bubble/ cloud phase completely mixed	Completely mixed	To emulsion	--	No adjustable parameters. Model on basis of Kato and Wen[7] model but incorporation of jetting region improves production of conversion for fast reactions.

that the Kunii-Levenspiel (KL) model best characterized the performance of a fluidized bed reactor. In view of the above, and the fact that the KL model incorporates the main features of the fluidized bed while retaining an inherent simplicity, the present study was undertaken to extend this model to a variety of complex first order reaction schemes occurring in a fluid bed and to present a unified development for both conversion and product distribution thereof.

1.2 COMPLEX REACTIONS IN FLUIDIZED BEDS

The models presented in the literature have mainly been concerned with simple first order reactions and only a few extensions to complex reaction schemes have been presented. These have been mentioned in the subsequent chapter. However, simple reactions are the exception rather than the rule in fluidized bed operation, as can be seen from the examples of industrial fluid bed reactions mentioned below :

As an illustration of reversible complex reactions occurring in fluidized bed operation the isomerization reaction in fluid catalytic reforming is complex and reversible in nature. Fluid coking and fluid catalytic cracking may also feature reversible reactions in addition to being reactions in which a change in number of moles and hence an attendant volume change occur.

The production of phthalic anhydride from naphthalene conforms to a complex reaction scheme and fluid bed plants having a convertible feed (naphthalene or o-xylene) are in operation[19]. Other industrial fluid bed reactions which include the effect of complex reactions or change in number of moles during reaction pertain to the production of acrylonitrile[20], ethylene by ethanol dehydration[21, 22], chloromethanes[23], chlorosilanes[24], high density polyethylene[25], isophthalonitrile[26], per- and trichloroethylene[27] and chlorofluoromethanes[28].

In a majority of these reactions the intermediate is the desired product and thus selectivity of intermediate formation is an important consideration. Fluidized operation is beset with the problem of lower selectivity of intermediate formation for complex first order reactions as compared to a fixed bed reactor, for the same level of conversion.

1.3 SCOPE OF PRESENT WORK

The present study was undertaken with the objective of considering the analysis of fluidized beds for complex reaction schemes and the KL model was used for this purpose. Accordingly Chapter 2 deals with the development of the performance equations for complex first order reversible and irreversible schemes occurring in a fluidized bed. The most

general successive, parallel and simultaneous reaction schemes are considered, and by setting the appropriate rate constants equal to zero a variety of simplified reaction schemes can be obtained. On the basis of these performance equations the conversion and product distribution in the bed can be obtained along with the effect of bubble diameter and gas residence time thereon.

The analysis in Chapter 2 has shown the advantage of operating with smaller bubble diameters in the fluid bed, as this leads to a lesser deviation from the ideality of plug flow conditions. Whereas the desirability of operating with smaller bubble diameters is not in doubt, this often has to yield to the constraint that in industrial systems a certain minimum bubble size is involved. The ensuing Chapter 3 deals with the interaction between gas residence time, bubble diameter and maximum concentration of the intermediate, and a technique is evolved for optimizing the production of intermediate at the bed exit for any given value of gas residence time or bubble diameter.

The related problem of selectivity of intermediate formation in complex reactions is next considered in Chapter 4. Catalyst dilution has been shown earlier by Caldwell and Calderbank[29] to improve fixed bed reactor performance by affording a means of temperature control in the bed.

In a fluidized bed temperature control poses no problem as near isothermal conditions exist therein. Catalyst dilution results in an improvement in the efficiency of fluidized bed contacting, and hence the dilution of catalyst is shown to increase the selectivity of intermediate formation in a fluid bed without resulting in a major loss in conversion. Thus overall production of intermediate can often be increased in a fluid bed reactor by keeping all other parameters unchanged, and employing dilution of catalyst in the bed, such that the total mass of solids in the bed remains unaltered. This concept has been experimentally tested in Chapter 6 for the complex reaction scheme pertaining to the dehydration of ethanol to diethyl ether and ethylene on alumina catalyst.

The application of the models mentioned earlier to reactor design is nearly always demonstrated by considering a simple first order chemical reaction. Many industrially important reactions involve a change in volume of the gas phase due to the stoichiometry of the reaction, and some of the typical systems in this respect are the dehydration of alcohol, manufacture of high density polyethylene, absorption of sulphur dioxide in lime etc. The conversion predicting equations hitherto arrived at for simple first order systems are inapplicable for a system wherein volume change due to reaction is inherent, and a generalized model incorporating

the effect of change in moles due to reaction on the fluidized bed performance is yet to be developed. It is the objective of Chapter 5 to develop a model based on the postulates of the simple KL model, and which incorporates the effect of change in number of moles in the performance equation for the bed. On the basis of the generalized equations developed, the effect of the presence of inerts in the feed stream, pressure variation along the bed height and stoichiometric coefficient of reaction are studied with respect to conversion along the height of the bed, and conclusions are arrived at in this regard.

Chapter 6 deals with the experimental verification of the volume change model and the concept of catalyst dilution proposed earlier. The reaction chosen was ethanol dehydration to diethyl ether and ethylene. The reaction has the advantage of being a complex reaction at lower temperatures (< 340°C) and at higher temperatures intermediate ether formation is substantially lower so that the reaction becomes of the volume change type, wherein one mole of reactant is converted into two moles. Kinetic studies have been carried out in an integral reactor over commercial Flyk alumina catalyst and the data on product formation have been obtained at a lower (338°C) and higher (375°C) temperature. A 4" Ø fluidized bed reactor is utilized for the dehydration reaction. Runs are

carried out at 375°C with 95.6% w/w ethanol and varying amounts of nitrogen as inert, keeping the total number of moles entering the reactor constant. On the basis of the run with largest flow of inert nitrogen (so that the volume change effect is muted) the predictions of the KL and volume change model are extrapolated to the runs with larger ethanol flow rate in order to test the veracity of the latter model.

Runs are also carried out in the fluidized bed at 338°C, at which temperature ether formation is prevalent. Glass powder is employed as the inert catalyst diluent. The dilution ratio is varied while keeping the overall residence time in the bed unchanged. The effect of catalyst dilution on overall conversion and formation of intermediate ether is then experimentally obtained for the undiluted and diluted fluid beds, and is compared with the data obtained for the integral reactor at the same temperature by means of a modified selectivity-conversion plot. An increase in production of intermediate with dilution of catalyst is envisaged by the model, and the effect of catalyst dilution on intermediate formation at the bed exit is experimentally studied. An optimum catalyst dilution ratio is also sought to be obtained for the operating parameters employed in this system.

CHAPTER - 2

APPLICATION OF THE KL MODEL TO COMPLEX FIRST ORDER REACTION SCHEMES IN A FLUIDIZED BED

2. APPLICATION OF THE KL MODEL TO COMPLEX FIRST ORDER REACTION SCHEMES IN A FLUIDIZED BED

Some of the various models appearing in the literature have been the subject of a few extensions to complex reaction schemes. Thus the model of Partridge and Rowe[9] has been extended by Nashaie and Yates[30] to a complex parallel reaction of the type

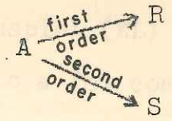

(2.1)

and their theoretical study based on this two phase model shows the influence of fluidized bed operation on the selectivity of competing first and second order reactions.

The compartment model of Kato and Wen[7] has been extended by Shaw et al.[31] to the hydrogenolysis of n-butane and a comparison between the observed results in terms of propane selectivity, methane selectivity and l-conversion are given with those predicted by the Kato and Wen model for the deep fluidized bed in which experiments were carried out.

The model proposed by Miyauchi[15,16] has been extended by Miyauchi and Furusaki[32] to cases such as

$$A \rightarrow R \rightarrow S, \quad A \begin{matrix} \nearrow R \\ \searrow S \end{matrix}, \quad A \rightarrow R \begin{matrix} \rightarrow T \\ \rightarrow U \end{matrix} \quad \text{etc.} \qquad (2.2)$$

Masao[33] has extended the Miyauchi model to successive first order isothermal reversible and successive reaction schemes and has obtained the general performance equations thereof.

The Kunii-Levenspiel (KL) model[2,3] has been the subject of extension to a few complex reaction schemes of the type

$$A \rightarrow R \rightleftharpoons S \qquad (2.3)$$

by Kunii and Levenspiel[34], and

$$A \rightarrow R \rightarrow S \qquad (2.4)$$

by Carberry[35]. Levenspiel et al.[36] recently applied it to the first order Denbigh reaction given by

$$A \longrightarrow R \begin{matrix} \longrightarrow S \\ \searrow U \end{matrix} \qquad (2.5)$$
$$\quad\; \searrow T$$

and obtained the performance equations thereof.

Considering the fact that the KL model has been reported to best represent the experimental data, the present

study was undertaken to extend this model to a variety of first order complex schemes and to present a unified development for both conversion and product distribution thereof. We first consider the rather general reaction scheme

$$A \underset{k_2}{\overset{k_1}{\rightleftharpoons}} R \underset{k_4}{\overset{k_3}{\rightleftharpoons}} S \qquad (2.6)$$

and the reversible parallel reaction scheme

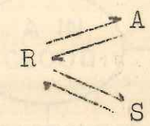

(2.7)

In addition we consider a complex reaction scheme of the type

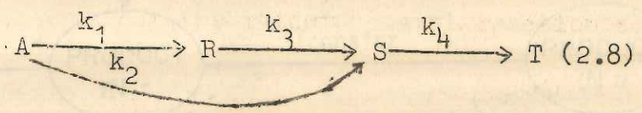

(2.8)

The above reaction schemes and their special cases together with the schemes considered earlier, serve to present a comprehensive picture of the various commonly encountered complex reaction schemes that can be analyzed by the KL model.

2.1 THE KL MODEL FOR A SIMPLE FIRST ORDER REACTION

Figure 2.1 outlines the main features of the KL model and shows that for a simple first order catalytic reaction

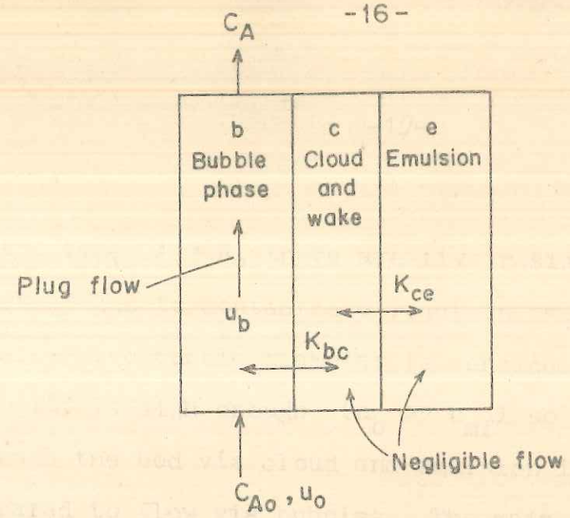

(a)

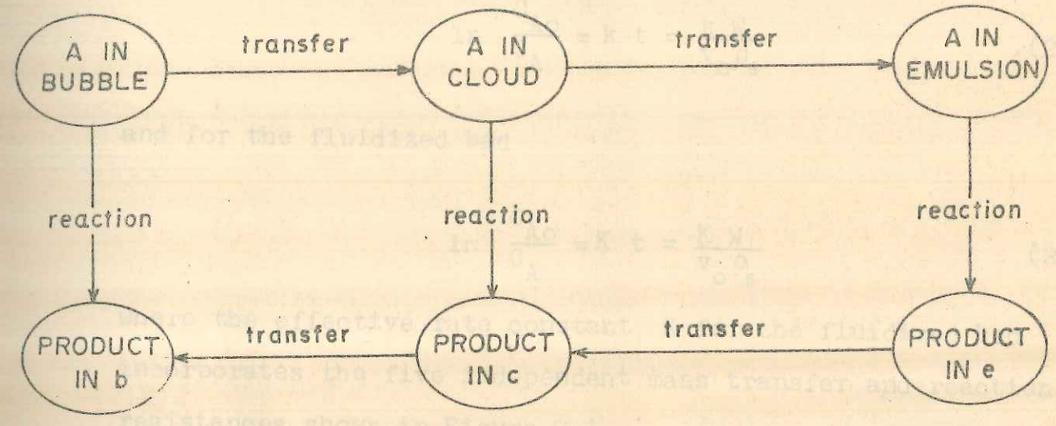

(b)

FIGURE 2·1. MAIN FEATURES OF THE SIMPLE KUNII-LEVENSPIEL FOR A BUBBLING BED ($u_b \gg u_{mf}$)

(a) THE MODEL USED FOR CHEMICAL CONVERSION CALCULATION

(b) THE FIVE MASS TRANSFER AND REACTION STEPS FOR THE REACTION A ⟶ R

of the type $A \rightarrow R$, there are five resistance steps for the reactant gas to contact and react on the surface of the solid. An effective bubble diameter is considered and the bubble velocity is high enough ($u_b >> u_{mf}$) so that gas flow through the bed via cloud and emulsion is negligible compared to flow via bubbles. The main parameters of the KL model are given in Table 2.1.

For $A \rightarrow R$, with $-r_A = kC_A$, we have for ideal plug flow

$$\ln \frac{C_{Ao}}{C_A} = k\,t = \frac{k\,W}{v_o \rho_s} \qquad (2.1)$$

and for the fluidized bed

$$\ln \frac{C_{Ao}}{C_A} = K\,t = \frac{K\,W}{v_o \rho_s} \qquad (2.2)$$

where the effective rate constant K for the fluidized bed incorporates the five independent mass transfer and reaction resistances shown in Figure 2.1.

$$K = k\,E = \frac{k\,u_o}{(1-\epsilon_{mf})u_{br}} \left[\gamma_b + \frac{1}{\frac{k}{K_{bc}} + \frac{1}{\gamma_c + \frac{1}{\frac{k}{k_{ce}} + \frac{1}{\gamma_e}}}} \right] \qquad (2.3)$$

and E is the efficiency of fluidized contacting, with $0 < E < 1$.

TABLE 2.1

PARAMETERS OF THE KUNII AND LEVENSPIEL MODEL

Parameter	Equation
Bubble diameter, d_b	Fitted
Bubble velocity with respect to emulsion, u_{br}	$0.711\ (g\ d_b)^{1/2}$
Bubble rise velocity, u_b	$u_o - u_{mf} + u_{br}$
Fraction of bed occupied by bubbles, δ	$\frac{u_o - u_{mf}}{u_b}$
Volume of solids in bubble/volume of bubbles, γ_b	0.01 ~ 0.001
Volume of solids in cloud/volume of bubbles, γ_c	$(1-\epsilon_{mf}) \left[\frac{3\ u_{mf}/\epsilon_{mf}}{u_{br} - u_{mf}/\epsilon_{mf}} + \alpha_w \right]$
Volume of solids in emulsion/volume of bubbles, γ_e	$(1-\epsilon_{mf}) \left(\frac{1-\delta}{\delta} \right) - (\gamma_b + \gamma_c)$
Bubble wake fraction, α_w	0.33
Bubble/cloud gas interchange coefficient, K_{bc}	$4.5 \left(\frac{u_{mf}}{d_b} \right) + 5.85 \left(\frac{D^{1/2}\ g^{1/4}}{d_b^{5/4}} \right)$
Cloud/emulsion gas interchange coefficient, K_{ce}	$6.78 \left[\frac{\epsilon_{mf}\ D_e\ u_b}{d_b^3} \right]^{1/2}$

2.2 FIRST ORDER REVERSIBLE REACTION SYSTEM

2.2.1 Successive Reversible Reactions

Consider the reaction scheme

$$A \underset{k_2}{\overset{k_1}{\rightleftharpoons}} R \underset{k_4}{\overset{k_3}{\rightleftharpoons}} S \qquad \ldots \text{ (all first order)}$$

For any differential bed height dl the following material balance equation for any species can be written

overall disappearance	=	reaction in bubble	+	transfer to cloud-wake	
transfer to cloud-wake	=	reaction in cloud-wake	+	transfer to emulsion	(2.4)
transfer to emulsion	$\simeq$	reaction in emulsion			

In writing the material balance equations, the transport coefficients K_{bc} (for bubble-cloud) and K_{ce} (for cloud-emulsion) can be assumed to be identical for all the species A, R and S[36] i.e. $D_A = D_R = D_S$. The conservation equations for the three species then become

$$- u_b \frac{dC_{Ab}}{dl} = \gamma_b k_1 (C_{Ab}-C_A^*) + \gamma_c k_1 (C_{Ac}-C_A^*) + \gamma_e k_1 (C_{Ae}-C_A^*)$$

$$K_{bc} (C_{Ab}-C_{Ac}) = \gamma_c k_1 (C_{Ac}-C_A^*) + K_{ce} (C_{Ac}-C_{Ae}) \qquad (2.5)$$

$$K_{ce} (C_{Ac}-C_{Ae}) = \gamma_e k_1 (C_{Ae}-C_A^*)$$

$$u_b \frac{dC_{Rb}}{dl} = \gamma_b k_1 (C_{Ab}-C_A^*) - \gamma_b k_3 (C_{Rb}-C_R^*) + K_{bc} (C_{Rc}-C_{Rb})$$

$$K_{bc} (C_{Rc}-C_{Rb}) = \gamma_c k_1 (C_{Ac}-C_A^*) - \gamma_c k_3 (C_{Rc}-C_R^*) + K_{ce} (C_{Re}-C_{Rc}) \qquad (2.6)$$

$$K_{ce} (C_{Re}-C_{Rc}) = \gamma_e k_1 (C_{Ae}-C_A^*) - \gamma_e k_3 (C_{Re}-C_R^*)$$

$$u_b \frac{dC_{Sb}}{dl} = \gamma_b k_3 (C_{Rb}-C_R^*) + K_{bc} (C_{Sc}-C_{Sb})$$

$$K_{bc} (C_{Sc}-C_{Sb}) = \gamma_c k_3 (C_{Rc}-C_R^*) + K_{ce} (C_{Se}-C_{Sc}) \qquad (2.7)$$

$$K_{ce} (C_{Se}-C_{Sc}) = \gamma_e k_3 (C_{Re}-C_R^*)$$

Neglecting the effect of solids dispersed in the bubbles ($\gamma_b = 0$), Equations (2.5), (2.6) and (2.7) can be simplified further. This assumption of γ_b equal to zero is reasonable for all but extremely fast reactions[34]. It should also be noted that the various rate constants appearing in Equations (2.5), (2.6) and (2.7) have the dimensions of

inverse time. Since, for solid catalyzed heterogeneous reactions the rate constants are usually expressed as cm^3/g catalyst-sec, they may be suitably modified by multiplying by the catalyst density.

Rearrangement of Equation (2.5) gives

$$C_{Ae} = \frac{\gamma_e k_1 C_A^* + K_{ce} C_{Ac}}{\gamma_e k_1 + K_{ce}} \tag{2.8}$$

$$C_{Ac} = \frac{K_{bc} C_{Ab} + \gamma_c k_1 C_A^* + K_{ce}\left(\frac{\gamma_e k_1 C_A^* + K_{ce} C_{Ac}}{\gamma_e k_1 + K_{ce}}\right)}{K_{bc} + K_{ce} + \gamma_c k_1} \tag{2.9}$$

or

$$C_{Ac} = \frac{K_{bc} C_{Ab} + \gamma_c k_1 C_A^* + \dfrac{K_{ce}\gamma_e k_1 C_A^*}{\gamma_e k_1 + K_{ce}}}{\left[1 - \dfrac{K_{ce}^2}{(\gamma_e k_1 + K_{ce})(K_{bc} + \gamma_c k_1 + K_{ce})}\right](K_{bc} + K_{ce} + \gamma_c k_1)} \tag{2.10}$$

Equation (2.5) may be rearranged to give

$$-u_b \frac{dC_{Ab}}{dl} = \gamma_c k_1 C_{Ac} + \gamma_e k_1 C_{Ae} - (\gamma_c + \gamma_e) k_1 C_A^* \tag{2.11}$$

Substituting for C_{Ae} and C_{Ac} from Equations (2.8) and (2.10) in Equation (2.11) results in

$$- u_b \frac{dC_{Ab}}{dl} = K_1 C_{Ab} + \left[K_1 \left(\gamma_c + \frac{K_{ce}\,\gamma_e}{\gamma_e k_1 + K_{ce}} \right) \frac{1}{K_{bc}} + \frac{\gamma_e^{\,2} k_1}{\gamma_e k_1 + K_{ce}} - \gamma_c - \gamma_e \right] k_1 C_A^{\,*} \tag{2.12}$$

where

$$K_i = \left[\frac{1}{\frac{k_i}{K_{bc}} + \frac{1}{\gamma_c + \frac{1}{\frac{k_i}{K_{ce}} + \frac{1}{\gamma_e}}}} \right] \quad i = 1,3 \text{ or } 4 \tag{2.13}$$

or rearranging

$$K_i = \left[\gamma_c k_i + \frac{\gamma_e k_i K_{ce}}{K_{ce} + \gamma_e k_i} \right] \left[\frac{K_{bc}(K_{ce} + \gamma_e k_i)}{(K_{ce} + \gamma_e k_i)(K_{bc} + \gamma_c k_i + K_{ce}) - K_{ce}^{\,2}} \right] \tag{2.14}$$

and substituting in Equation (2.12) for

$$\left[K_1 \left(\gamma_c + \frac{K_{ce}\,\gamma_e}{\gamma_e k_1 + K_{ce}} \right) \frac{1}{K_{bc}} + \frac{\gamma_e^{\,2} k_1}{\gamma_e k_1 + K_{ce}} - \gamma_c - \gamma_e \right] k_1 = K_1 \tag{2.15}$$

results in

$$- u_b \frac{dC_{Ab}}{dl} = K_1 C_{Ab} - K_1 C_A^{\,*} \tag{2.16}$$

Rearranging Equation (2.6) gives

$$u_b \frac{dC_{Rb}}{dl} = K_1(C_{Ab} - C_A^*) - (\gamma_c k_3 C_{Rc} + \gamma_e k_3 C_{Re}) + (\gamma_c + \gamma_e) k_3 C_R^* \qquad (2.17)$$

We also have

$$C_{Re} = \frac{K_{ce} C_{Rc} + \gamma_e k_1 (C_{Ae} - C_A^*) + \gamma_e k_3 C_R^*}{K_{ce} + \gamma_e k_3} \qquad (2.18)$$

and

$$C_{Rc} = \frac{K_{bc} C_{Rb} + \gamma_c k_1 (C_{Ac} - C_A^*) + \gamma_c k_3 C_R^* + \frac{\gamma_e K_{ce} [k_1 (C_{Ae} - C_A^*) + k_3 C_R^*]}{K_{ce} + \gamma_e k_3}}{\left[1 - \frac{K_{ce}^2}{(K_{ce} + \gamma_e k_3)(K_{bc} + K_{ce} + \gamma_c k_3)} \right] (K_{bc} + K_{ce} + \gamma_c k_3)} \qquad (2.19)$$

Substituting for C_{Re} and C_{Rc} in Equation (2.17) results in

$$u_b \frac{dC_{Rb}}{dl} = K_1(C_{Ab} - C_A^*) + (\gamma_c + \gamma_e) k_3 C_R^*$$

$$- \left[\left(\gamma_c k_3 + \frac{\gamma_e k_3 K_{ce}}{\gamma_e k_3 + K_{ce}} \right) \frac{K_{bc}(K_{ce} + \gamma_e k_3)}{(K_{ce} + \gamma_e k_3)(K_{bc} + K_{ce} + \gamma_c k_3) - K_{ce}^2} \right] C_{Rb}$$

$$+ \left(\gamma_c k_3 + \frac{\gamma_e k_3 K_{ce}}{\gamma_e k_3 + K_{ce}} \right) \left\{ \frac{\gamma_c k_1 (C_{Ac} - C_A^*) + \gamma_c k_3 C_R^* + \frac{\gamma_e K_{ce} [k_1 (C_{Ae} - C_A^*) + k_3 C_R^*]}{K_{ce} + \gamma_e k_3}}{(K_{ce} + K_{bc} + \gamma_c k_3) - \frac{K_{ce}^2}{K_{ce} + \gamma_e k_3}} \right\}$$

$$+ \gamma_e^2 k_3 \left\{ \frac{k_1 (C_{Ae} - C_A^*) + k_3 C_R^*}{\gamma_e k_3 + K_{ce}} \right\} \qquad (2.20)$$

and hence

$$u_b \frac{dC_{Rb}}{dl} = K_1(C_{Ab} - C_A^*) - K_3 C_{Rb} + \text{fn}\ (C_{Ac}, C_{Ae}, C_A^*, C_R^*) \qquad (2.21)$$

The coefficients of C_R^*, C_{Ae}, C_{Ac} and C_A^* are considered separately below :

Coefficient of C_R^*:

$$(\gamma_c+\gamma_e)k_3 - \frac{\left(\gamma_c k_3 + \frac{\gamma_e k_3 K_{ce}}{\gamma_e k_3+K_{ce}}\right)^2 (K_{ce}+\gamma_e k_3)}{(K_{ce}+\gamma_e k_3)(K_{bc}+K_{ce}+\gamma_c k_3) - K_{ce}^2} + \frac{\gamma_e^2 k_3^2}{K_{ce}+\gamma_e k_3}$$

$$= K_3 \qquad (2.22)$$

Coefficient of C_{Ae} :

$$\frac{\left(\gamma_c k_3 + \frac{\gamma_e k_3 K_{ce}}{K_{ce}+\gamma_e k_3}\right) K_{ce}\gamma_e k_1}{(K_{ce}+\gamma_e k_3)(K_{bc}+K_{ce}+\gamma_c k_3) - K_{ce}^2} + \frac{\gamma_e^2 k_1 k_3}{K_{ce}+\gamma_e k_3}$$

Coefficient of C_{Ac} :

$$\left(\gamma_c k_3 + \frac{\gamma_e k_3 K_{ce}}{\gamma_e k_3+K_{ce}}\right) \frac{\gamma_c k_1 (K_{ce}+\gamma_e k_3)}{(K_{ce}+\gamma_e k_3)(K_{bc}+K_{ce}+\gamma_c k_3) - K_{ce}^2}$$

The terms C_{Ae} and C_{Ac} are rewritten in terms of C_{Ab} and C_A^* [as given by Equations (2.8) and (2.9)] in Equation (2.20). The coefficients of the terms C_{Ab} and C_A^* are then obtained.

Coefficient of C_{Ab} :

$$K_1 - \left[\left(\gamma_c k_3 + \frac{\gamma_e k_3 K_{ce}}{\gamma_e k_3 + K_{ce}} \right) \left(\frac{\frac{\gamma_e k_1 K_{ce}^2}{\gamma_e k_1 + K_{ce}} + \gamma_c k_1 (\gamma_e k_3 + K_{ce})}{(K_{ce} + \gamma_e k_3)(K_{bc} + K_{ce} + \gamma_c k_3) - K_{ce}^2} \right) \right.$$

$$\left. + \frac{\gamma_e^2 k_1 k_3 K_{ce}}{(\gamma_e k_1 + K_{ce})(\gamma_e k_3 + K_{ce})} \right] \left[\frac{K_{bc}(K_{ce} + \gamma_e k_1)}{(K_{ce} + \gamma_e k_1)(K_{bc} + K_{ce} + \gamma_c k_1) - K_{ce}^2} \right]$$

Rearranging the above, the coefficient of C_{Ab} is obtained to be

$$K_1' = K_1 \left[1 - \frac{K_3}{K_1} \psi_1 \right] \qquad (2.23)$$

where

$$\psi_1 = \left[\left\{ \frac{\gamma_e k_1 K_{ce}}{\gamma_e k_1 + K_{ce}} + \frac{\gamma_c k_1 (K_{ce} + \gamma_e k_3)}{K_{ce}} \right\} \frac{K_{ce}}{K_{ce} + \gamma_e k_3} \right.$$

$$\left. + \frac{K_{bc}}{K_3} \frac{\gamma_e^2 k_1 k_3 K_{ce}}{(\gamma_e k_1 + K_{ce})(\gamma_e k_3 + K_{ce})} \right]$$

$$\times \left[\frac{K_{ce} + \gamma_e k_1}{(K_{ce} + \gamma_e k_1)(K_{bc} + K_{ce} + \gamma_c k_1) - K_{ce}^2} \right] \qquad (2.24)$$

Coefficient of C_A^* :

The coefficient of C_A^* is obtained from Equation (2.20) as

$$-\phi_1' = -(K_1 + \phi_2 - \phi_3) \tag{2.25}$$

where

$$\phi_2 = \left[\frac{K_1}{K_{bc}} \left\{ \left(\gamma_c k_3 + \frac{\gamma_e k_3 K_{ce}}{\gamma_e k_3 + K_{ce}} \right) \left(\frac{\frac{\gamma_e k_1 K_{ce}^2}{\gamma_e k_1 + K_{ce}} + \gamma_c k_1 (K_{ce} + \gamma_e k_3)}{(K_{ce} + \gamma_e k_3)(K_{bc} + K_{ce} + \gamma_c k_3) - K_{ce}^2} \right) \right. \right.$$

$$\left. \left. + \frac{\gamma_c \gamma_e k_1 k_3 K_{ce}}{(\gamma_e k_1 + K_{ce})(\gamma_e k_3 + K_{ce})} \right\} + \left\{ \frac{K_3 K_{ce}}{K_{bc}} + \gamma_e k_3 \right\} \frac{\gamma_e^2 k_1^2}{(\gamma_e k_1 + K_{ce})(\gamma_e k_3 + K_{ce})} \right] \tag{2.26}$$

and

$$\phi_3 = \frac{K_3}{K_{bc}} \left(\gamma_c k_1 + \frac{\gamma_e k_1 K_{ce}}{\gamma_e k_3 + K_{ce}} \right) + \frac{\gamma_e^2 k_1 k_3}{\gamma_e k_3 + K_{ce}} \tag{2.27}$$

Equation (2.17) can then be written as

$$u_b \frac{dC_{Rb}}{dl} = K_1' C_{Ab} - K_3 (C_{Fb} - C_R^*) - \phi_1' C_A^* \tag{2.28}$$

Equations (2.11) and (2.17) can be written in dimensionless form as

$$-\frac{d\bar{C}_{Ab}}{dz} = \left(K_{11}\,\bar{C}_{Ab} - K_{11}\,\bar{C}_A^*\right)\frac{W}{v_o\rho_s} \qquad (2.29)$$

$$\frac{d\bar{C}_{Rb}}{dz} = \left(K_{11}\,\bar{C}_{Ab} - K_{33}\,(\bar{C}_{Rb} - \bar{C}_R^*) - \phi_{11}'\,\bar{C}_A^*\right)\frac{W}{v_o\rho_s} \qquad (2.30)$$

where the overbar denotes the dimensionless parameter and z denotes the dimensionless height in the bed. The double subscripted letters are defined as

$$K_{ii} = K_i\,\frac{u_o}{(1-\varepsilon_{mf})u_{br}} \qquad (i = 1, 3 \text{ or } 4)$$

$$K_{jj}' = K_j'\,\frac{u_o}{(1-\varepsilon_{mf})u_{br}} \qquad (j = 1, 2) \qquad (2.31)$$

$$\phi_{11}' = \phi_1'\,\frac{u_o}{(1-\varepsilon_{mf})u_{br}}$$

The concentration profiles for the species A and R can now be obtained by integrating Equations (2.29) and (2.30) subject to the initial conditions

$$\bar{C}_{Ab} = 1; \quad \bar{C}_{Rb} = 0 \quad \text{at} \quad z = \frac{l}{L_f} = 0 \tag{2.32}$$

with the result

$$\bar{C}_{Ab} = (1 - \bar{C}_A^*) \exp(-K_{11} t) + \bar{C}_A^* \tag{2.33}$$

$$\bar{C}_{Rb} = \frac{K_1'}{K_3 - K_1} \left[\exp(-K_{11} t) - \exp(-K_{33} t) \right]$$

$$+ K_1' \left[\frac{1}{K_3} - \frac{\phi_1'}{K_3 K_1'} + \left(\frac{K_1}{K_3(K_3 - K_1)} + \frac{\phi_1'}{K_3 K_1'} \right) \exp(-K_{33} t) \right.$$

$$\left. - \frac{\exp(-K_{11} t)}{(K_3 - K_1)} \right] \bar{C}_A^* - \left[\exp(-K_{33} t) - 1 \right] \bar{C}_R^* \tag{2.34}$$

The concentration of the species S can be obtained from the material balance equation

$$\bar{C}_{Ab} + \bar{C}_{Rb} + \bar{C}_{Sb} = 1 \tag{2.35}$$

The distance at which maximum production of R occurs can be obtained by setting Equation (2.30) to zero. Using

the profiles given by Equations (2.33) and (2.34) this can be rearranged to give

$$t_{max} = \frac{\ln P}{K_{33} - K_{11}} = \frac{W}{v_o \rho_s} z_{max} \qquad (2.36)$$

where

$$P = \frac{K_1' K_3 - K_1' K_1 \bar{C}_A^* - [\phi_1' \bar{C}_A^* - K_3 \bar{C}_R^*] (K_3 - K_1)}{K_1' K_1 (1 - \bar{C}_A^*)} \qquad (2.37)$$

and

$$t = \frac{W}{v_o \rho_s} \cdot z \qquad (2.38)$$

The maximum concentration of R is then

$$\bar{C}_{R,max} = (PP_1 + P_2) \; P^{-\frac{K_3}{K_3 - K_1}} + P_3 \qquad (2.39)$$

where

$$P_1 = \frac{K_1'}{(K_3 - K_1)} (1 - \bar{C}_A^*) \qquad (2.40)$$

$$P_2 = \frac{K_1' K_1}{K_3 (K_3 - K_1)} \bar{C}_A^* - \frac{K_1'}{(K_3 - K_1)} + \frac{\phi_1' \bar{C}_A^* - K_3 \bar{C}_R^*}{K_3} \qquad (2.41)$$

and

$$P_3 = \frac{K_1'}{K_3}\,\bar{C}_A^* - \frac{\phi_1'\bar{C}_A^* - K_3\bar{C}_R^*}{K_3} \qquad (2.42)$$

Equations (2.36) and (2.39) represent expressions for a general reaction of the type $A \rightleftharpoons R \rightleftharpoons S$ and can be easily reduced to simplified cases by choosing appropriate values of the rate constants. The simplified cases are discussed in the next section.

2.3 SIMPLIFIED CASES OF REACTION SCHEME (2.6)

2.3.1 Consecutive Reaction Scheme (2.6.1)

$$A \xrightarrow{k_1} R \xrightarrow{k_3} S \qquad (2.6.1)$$

For this case of a consecutive reaction both $\bar{C}_A^*$ and $\bar{C}_R^*$ are zero and the various parameters in Equation (2.39) become

$$P = \frac{K_3}{K_1}\ ;\quad P_1 = \frac{K_1'}{(K_3 - K_1)} = -P_2\ ;\quad P_3 = 0 \qquad (2.43)$$

Substituting these in Equations (2.36) and (2.39) gives

$$t_{max} = \frac{W}{v_o \rho_s}\, z_{max} = \frac{\ln\left(\frac{K_3}{K_1}\right)}{(K_{33} - K_{11})} \qquad (2.44)$$

and

$$\bar{C}_{R,max} = \frac{K_1'}{K_1} \left(\frac{K_1}{K_3}\right)^{\frac{K_3}{K_3-K_1}} \tag{2.45}$$

which are the well known expressions for a consecutive reaction carried out in a fluidized bed reactor.

2.3.2 Reaction Scheme (2.6.2)

$$A \xrightarrow{k_1} R \underset{k_4}{\overset{k_3}{\rightleftharpoons}} S \tag{2.6.2}$$

For this scheme $\bar{C}_A^*$ is zero and the various parameters in Equation (2.39) become

$$P_1 = \frac{K_1'}{(K_3-K_1)} \quad ; \quad P_2 = -[P_1 + P_3] \quad ; \quad P_3 = \bar{C}_R^*$$

$$P = \frac{K_1' K_3 + K_3 \bar{C}_R^* [K_3 - K_1]}{K_1' K_1} \tag{2.46}$$

Substituting these in Equations (2.36) and (2.39) gives

$$t_{max} = \frac{\ln\left[\dfrac{K_1' K_3 + K_3 \bar{C}_R^* [K_3 - K_1]}{K_1' K_1}\right]}{[K_{33} - K_{11}]} \qquad (2.47)$$

and

$$\bar{C}_{R,max} - \bar{C}_R^* = \left[\frac{K_1'}{[K_3 - K_1]} \left[\frac{1}{K_1} - 1\right] + \bar{C}_R^* \left[\frac{K_3}{K_1} - 1\right]\right] P^{\frac{-K_3}{K_3 - K_1}} \qquad (2.48)$$

For the special case of $k_1 \to \infty$, from Equation (2.48) we get the corresponding expression for the reaction scheme $R \rightleftharpoons S$ as

$$C_{R,max} = C_{Ao}$$

or

$$\bar{C}_{R,max} = 1 \qquad (2.49)$$

2.3.3 Reaction Scheme (2.6.3):

$$A \underset{k_2}{\overset{k_1}{\rightleftharpoons}} R \xrightarrow{k_3} S \qquad (2.6.3)$$

For this scheme $\bar{C}_R^*$ is zero and the various parameters

in Equation (2.39) become

$$P_1 = \frac{K_1'}{[K_3 - K_1]}\,[1-\bar{C}_A^*] \;;\; P_2 = \frac{K_1' K_1}{K_3(K_3-K_1)}\,\bar{C}_A^* - \frac{K_1'}{(K_3-K_1)} + \frac{\phi_1'\bar{C}_A^*}{K_3}$$

$$P_3 = \frac{K_1'}{K_3}\,\bar{C}_A^* - \frac{\phi_1'\bar{C}_A^*}{K_3} \;;\; P = \frac{K_1'K_3 - K_1'K_1\bar{C}_A^* - \phi_1'\bar{C}_A^*\,(K_3-K_1)}{K_1'K_1(1-\bar{C}_A^*)} \qquad (2.50)$$

$$t_{max} = \frac{\ln\left[\dfrac{K_1'K_3 - K_1'K_1\bar{C}_A^* - \phi_1'\bar{C}_A^*(K_3-K_1)}{K_1'K_1(1-\bar{C}_A^*)}\right]}{[K_{33}-K_{11}]} \qquad (2.51)$$

$\bar{C}_{R,max}$ may be obtained by substituting for P_1, P_2, P_3 and P, as given above, in Equation (2.39).

2.4 REVERSIBLE PARALLEL REACTION SYSTEM

The reaction scheme (2.7), which is a reversible parallel scheme, can (for the purpose of analysis) be regarded as a variation of the consecutive reversible reaction scheme considered earlier, with A going to R going to S, while in fact R is the reactant species and A and S are

the products of the reaction. Following the procedure outlined in the earlier section, the following concentration profiles can be obtained

$$\bar{C}_{Rb}-\bar{C}_R^* = [1-\bar{C}_R^*] \exp(-K_{33}t) - \frac{K_1'\bar{C}_A^*}{(K_3-K_1)}\left[\exp(-K_{11}t) - \exp(-K_{33}t)\right]$$

$$+ \frac{[K_1' - \phi_1']\,\bar{C}_A^*}{K_3}\left[1 - \exp(-K_{33}t)\right] \qquad (2.52)$$

$$\bar{C}_{Ab} = \bar{C}_A^*\,[1 - \exp(-K_{11}t)] \qquad (2.53)$$

The concentration of the species S can be obtained from the material balance given by Equation (2.35). For maximum production of A, Equation (2.53) suggests a very long reactor with

$$\bar{C}_{A,max} = \bar{C}_A^* \qquad (2.54)$$

2.5 FIRST-ORDER IRREVERSIBLE REACTION SYSTEM

For the complex irreversible scheme of the type in Scheme (2.8), an analysis similar to that outlined in Section 2.2 is carried out, with the difference that $\bar{C}_A^*$ and $\bar{C}_R^*$ are

automatically precluded from the analysis. Figure 2.2 shows the 20 reaction and mass transfer steps representing the above reaction in a fluidized bed on the basis of the KL model. The equations given below incorporate these steps

$$- u_b \frac{dC_{Ab}}{dl} = \gamma_b(k_1 + k_2)C_{Ab} + K_{bc}(C_{Ab} - C_{Ac})$$

$$K_{bc}\,(C_{Ab} - C_{Ac}) = \gamma_c(k_1+k_2)C_{Ac} + K_{ce}(C_{Ac} - C_{Ae}) \qquad (2.55)$$

$$K_{ce}\,(C_{Ac} - C_{Ae}) = \gamma_e(k_1+k_2)C_{Ae}$$

$$u_b \frac{dC_{Rb}}{dl} = - \gamma_b k_3 C_{Rb} + K_{bc}\,(C_{Rc} - C_{Rb}) + \gamma_b k_1 C_{Ab}$$

$$K_{bc}\,(C_{Rc} - C_{Rb}) = - \gamma_c k_3 C_{Rc} + K_{ce}(C_{Re} - C_{Rc}) + \gamma_c k_1 C_{Ac} \qquad (2.56)$$

$$K_{ce}\,(C_{Re} - C_{Rc}) = \gamma_e k_1 C_{Ae} - \gamma_e k_3 C_{Re}$$

$$u_b \frac{dC_{Sb}}{dl} = \gamma_b k_2 C_{Ab} + \gamma_b k_3 C_{Rb} - \gamma_b k_4 C_{Sb} + K_{bc}\,(C_{Sc} - C_{Sb})$$

$$K_{bc}\,(C_{Sc} - C_{Sb}) = \gamma_e k_2 C_{Ac} + \gamma_c k_3 C_{Rc} - \gamma_c k_4 C_{Sc} + K_{ce}(C_{Se} - C_{Sc})$$

$$K_{ce}\,(C_{Se} - C_{Sc}) = \gamma_e k_2 C_{Ae} + \gamma_e k_3 C_{Re} - \gamma_e k_4 C_{Se} \qquad (2.57)$$

TANT A
RS HERE

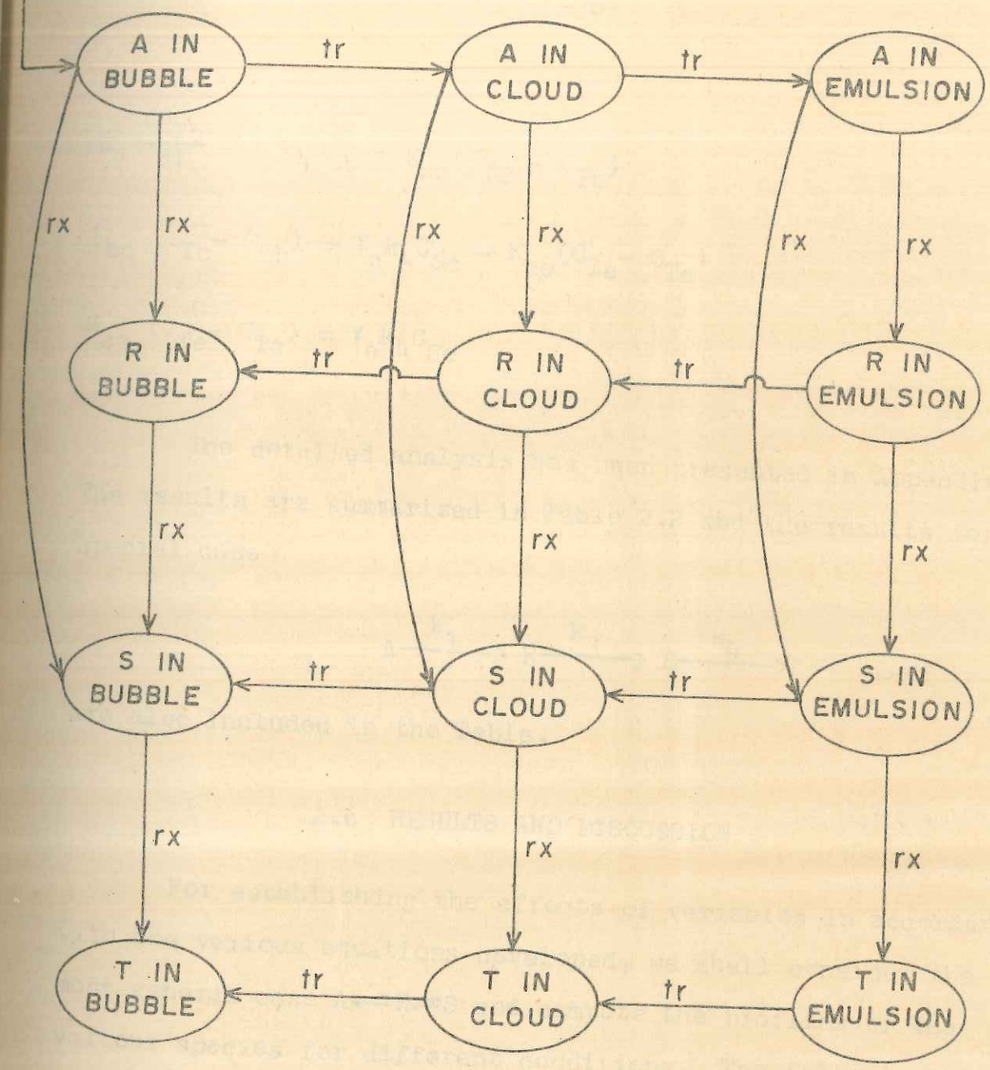

FIGURE 2·2. SKETCH SHOWING THE 20 REACTION AND MASS TRANSFER STEPS REPRESENTING THE REACTION A → R → S → T TAKING PLACE IN A FLUIDIZED BED

$$u_b \frac{dC_{Tb}}{dl} = \gamma_b k_4 C_{Sb} + K_{bc}(C_{Tc} - C_{Tb})$$

$$K_{bc}(C_{Tc} - C_{Tb}) = \gamma_c k_4 C_{Sc} - K_{ce}(C_{Te} - C_{Tc}) \qquad (2.58)$$

$$K_{ce}(C_{Te} - C_{Tc}) = \gamma_e k_4 C_{Se}$$

The detailed analysis has been presented in Appendix I. The results are summarized in Table 2.2 and the results for a special case

$$A \xrightarrow{k_1} R \xrightarrow{k_3} S \xrightarrow{k_4} T$$

are also included in the Table.

2.6 RESULTS AND DISCUSSION

For establishing the effects of variables in accordance with the various equations developed, we shall consider the most general case $A \rightleftharpoons R \rightleftharpoons S$ and compute the profiles of the various species for different conditions. The following data will be used : $k_1 = 10.0\ sec^{-1}$; $k_2 = 1.0\ sec^{-1}$; $k_3 = 1.0\ sec^{-1}$; $k_4 = 0.1\ sec^{-1}$; $\rho_s = 2.0\ g/cm^3$; $W/v_o = 12.0\ g\text{-}sec/cm^3$; $u_{mf} = 3\ cm/sec$; $u_o = 30\ cm/sec$; $\epsilon_{mf} = 0.4$; $D_e = D_A = 0.2\ cm^2/sec$; $V_w/V_b = 0.3$; $d_b = 8 - 30\ cm$.

The results of the computations are presented in Figures 2.3 - 2.5, while the computational procedure for an effective

TABLE 2.2

SUMMARY OF MODEL EQUATIONS FOR THE COMPLEX REACTION SCHEME (2.8) AND ITS SPECIAL CASE

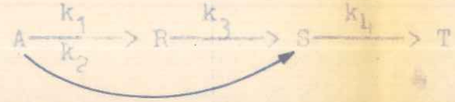

conservation Equations (and boundary conditions)	concentration profile
$-\frac{d\bar{C}_{Ab}}{dz} = K_{[1+2]_{1+2}} \frac{W}{v_o \rho_s} \bar{C}_{Ab}$ (at $z = 0$, $\bar{C}_{Ab} = 1$)	$\bar{C}_{Ab} = \exp\left(- K_{[1+2]_{1+2}} t\right)$
$\frac{d\bar{C}_{Rb}}{dz} = \left[K'_{[1+2]_{1+2}} \bar{C}_{Ab} - K_{33}\bar{C}_{Rb}\right] \frac{W}{v_o \rho_s}$ (at $z = 0$, $\bar{C}_{Rb} = 0$)	$\bar{C}_{Rb} = \frac{K'_{[1+2]}}{K_3 - K_{[1+2]}} \left[\exp\left(- K_{[1+2]_{1+2}} t\right) - \exp\left(- K_{33} t\right)\right]$
$\frac{d\bar{C}_{Sb}}{dz} = \left[K_{[12]_{12}} \bar{C}_{Ab} + K_{22} \bar{C}_{Rb} - K_{44}\bar{C}_{Sb}\right] \frac{W}{v_o \rho_s}$ (at $z = 0$, $\bar{C}_{Sb} = 0$)	$\bar{C}_{Sb} = \exp\left(-K_{[1+2]_{1+2}} t\right) \left[\frac{K_{[12]}}{(K_4 - K_{[1+2]})} + \frac{K_2' K'_{[1+2]}}{(K_3 - K_{[1+2]})(K_4 - K_{[1+2]})}\right]$ $+ \exp\left(- K_{33} t\right) \left[\frac{-K_2' K'_{[1+2]}}{(K_4 - K_3)(K_3 - K_{[1+2]})}\right]$ $+ \exp\left(-K_{44} t\right) \left[\frac{- K_2' K'_{[1+2]}}{(K_4 - K_3)(K_4 - K_{[1+2]})} + \frac{K_{[12]}}{(K_4 - K_{[1+2]})}\right]$ $\bar{C}_{Tb} = 1.0 - (\bar{C}_{Ab} + \bar{C}_{Rb} + \bar{C}_{Sb})$

where the following equations apply

$$K_{[1+2]} = [k_1+k_2]\left[\frac{1}{\frac{[k_1+k_2]}{K_{bc}} + \frac{1}{\gamma_c + \frac{1}{\frac{[k_1+k_2]}{K_{ce}} + \frac{1}{\gamma_e}}}}\right]$$

$$K_{[1+2]_{1+2}} = K_{[1+2]} \frac{\dot{u}_o}{(1-\varepsilon_{mf})u_{br}}$$

$$K'_{[1+2]} = K_{[1+2]} \Psi_{[1+2]} \; ; \; K'_{[1+2]_{1+2}} = K_{[1+2]} \Psi_{[1+2]} \frac{\dot{u}_o}{(1-\varepsilon_{mf})u_{br}}$$

$$\Psi_{[1+2]} = \frac{K_1}{K_{[1+2]}} - \left[\frac{\gamma_e^2 k_1 k_3 K_{ce}}{\gamma_e k_3 + K_{ce}} + \frac{K_3 k_1}{K_{bc}}\left(\gamma_c\left[K_{ce}+\gamma_e(k_1+k_2)\right] + \frac{K_{ce}^2 \gamma_e}{K_{ce}+\gamma_e k_3}\right)\right] \Bigg/ \left[\left(\gamma_c(k_1+k_2) + \frac{\gamma_e(k_1+k_2)K_{ce}}{\gamma_e(k_1+k_2)+K_{ce}}\right)\left(K_{ce}+\gamma_e(k_1+k_2)\right)\right]$$

$$K_{[12]_{12}} = K_{[1+2]} \Psi_3 \frac{\dot{u}_o}{(1-\varepsilon_{mf})u_{br}} \; ; \; K_{[12]} = K_{[1+2]} \Psi_3$$

$$\Psi_3 = \left\{\frac{K_{ce}}{\gamma_e(k_1+k_2)+K_{ce}}\left[\gamma_e k_2 + \frac{\gamma_e^2 k_1 k_3 K_{ce} K_4}{(K_{ce}+\gamma_e k_4)(K_{ce}+\gamma_e k_3)\left(\gamma_c k_4 + \frac{\gamma_e k_4 K_{ce}}{\gamma_e k_4 + K_{ce}}\right)} + \frac{\gamma_e k_1 K_{ce} \Psi_2 K_3 K_4}{K_{bc}(K_{ce}+\gamma_e k_3)} - \frac{\gamma_e k_2 k_4 K_{ce}(\gamma_c+\gamma_e K_{ce})K_4}{K_{bc}(K_{ce}+\gamma_e k_4)\left(\gamma_c k_4 + \frac{\gamma_c k_4 K_{ce}}{K_{ce}+\gamma_e k_4}\right)}\right.\right.$$

$$\left.\left. - \frac{\gamma_e^2 k_2 k_4}{(K_{ce}+\gamma_e k_4)}\right] + \left[\frac{\gamma_c k_1 \Psi_2 K_3 K_4}{K_{bc}} + \frac{\gamma_c k_2 K_4}{\left(\gamma_c k_4 + \frac{\gamma_e k_4 K_{ce}}{\gamma_e k_4 + K_{ce}}\right)}\right]\right\} \Bigg/ \left[\gamma_c(k_1+k_2) + \frac{\gamma_e(k_1+k_2)K_{ce}}{\gamma_e(k_1+k_2)+K_{ce}}\right]$$

where the following equations apply

$$K_{[1+2]} = [k_1+k_2]\left[\frac{1}{\frac{[k_1+k_2]}{K_{bc}} + \frac{1}{\gamma_c + \frac{1}{\frac{[k_1+k_2]}{K_{ce}} + \frac{1}{\gamma_e}}}}\right]$$

$$K_{[1+2]_{1+2}} = K_{[1+2]} \frac{u_o}{(1-\varepsilon_{mf})u_{br}}$$

$$K'_{[1+2]} = K_{[1+2]} \Psi_{[1+2]} \; ; \; K'_{[1+2]_{1+2}} = K_{[1+2]} \Psi_{[1+2]} \frac{u_o}{(1-\varepsilon_{mf})u_{br}}$$

$$\Psi_{[1+2]} = \frac{K_1}{K_{[1+2]}} - \left[\frac{\gamma_e^2 k_1 k_3 K_{ce}}{\gamma_e k_3 + K_{ce}} + \frac{K_3 k_1}{K_{bc}}\left(\gamma_c\left[K_{ce}+\gamma_e(k_1+k_2)\right] + \frac{K_{ce}^2 \gamma_e}{K_{ce}+\gamma_e k_3}\right)\right] \Bigg/ \left[\left(\gamma_c(k_1+k_2) + \frac{\gamma_e(k_1+k_2)K_{ce}}{\gamma_e(k_1+k_2)+K_{ce}}\right)\left(K_{ce}+\gamma_e(k_1+k_2)\right)\right]$$

$$K_{[12]_{12}} = K_{[1+2]} \Psi_3 \frac{u_o}{(1-\varepsilon_{mf})u_{br}} \; ; \; K_{[12]} = K_{[1+2]} \Psi_3$$

$$\Psi_3 = \left\{\frac{K_{ce}}{\gamma_e(k_1+k_2)+K_{ce}}\left[\gamma_e k_2 + \frac{\gamma_e^2 k_1 k_3 K_{ce} K_4}{(K_{ce}+\gamma_e k_4)(K_{ce}+\gamma_e k_3)\left(\gamma_c k_4 + \frac{\gamma_e k_4 K_{ce}}{\gamma_e k_4 + K_{ce}}\right)} + \frac{\gamma_e k_1 K_{ce} \Psi_2 K_3 K_4}{K_{bc}(K_{ce}+\gamma_e k_3)} - \frac{\gamma_e k_2 k_4 K_{ce}(\gamma_c+\gamma_e K_{ce})K_4}{K_{bc}(K_{ce}+\gamma_e k_4)\left(\gamma_c k_4 + \frac{\gamma_c k_4 K_{ce}}{K_{ce}+\gamma_e k_4}\right)}\right.\right.$$

$$\left.\left. - \frac{\gamma_e^2 k_2 k_4}{(K_{ce}+\gamma_e k_4)}\right] + \left[\frac{\gamma_c k_1 \Psi_2 K_3 K_4}{K_{bc}} + \frac{\gamma_c k_2 K_4}{\left(\gamma_c k_4 + \frac{\gamma_e k_4 K_{ce}}{\gamma_e k_4 + K_{ce}}\right)}\right]\right\} \Bigg/ \left[\gamma_c(k_1+k_2) + \frac{\gamma_e(k_1+k_2)K_{ce}}{\gamma_e(k_1+k_2)+K_{ce}}\right]$$

$$\Psi_2 = \frac{\left(\frac{K_{ce}^2 Y_e}{(K_{ce} + Y_e k_3)(K_{ce} + Y_e k_4)} + Y_c \right)}{\left(Y_c + \frac{Y_e K_{ce}}{K_{ce} + Y_e k_3} \right) \left(Y_c k_4 + \frac{K_{ce} Y_e k_4}{K_{ce} + Y_e k_4} \right)} ;$$

$$K_2^{'} = \Psi_2 K_3 K_4$$

We also obtain the expressions

$$\frac{W}{v_o \rho_s} z_{max} = t_{max} = \frac{\ln \left(\frac{K_3}{K_{[1+2]}} \right)}{\left(K_{33} - K_{[1+2]_{1+2}} \right)} ;$$

$$\bar{C}_{R,max} = \frac{K_{[1+2]}^{'}}{K_{[1+2]}} \left(\frac{K_{[1+2]}}{K_3} \right)^{K_3/(K_3 - K_{[1+2]})}$$

conservation Equations (and boundary conditions)	concentration profile

$$A \xrightarrow{k_1} R \xrightarrow{k_3} S \xrightarrow{k_4} T^a$$

$$-\frac{d\bar{C}_{Ab}}{dz} = K_{11}\frac{W}{v_o\rho_s}\bar{C}_{Ab} \qquad \bar{C}_{Ab} = \exp\ (-K_{11}\ t)$$

$$(\text{at } z = 0,\ \bar{C}_{Ab} = 1)$$

$$\frac{d\bar{C}_{Rb}}{dz} = [K_{11}'\bar{C}_{Ab} - K_{33}\bar{C}_{Rb}]\frac{W}{v_o\rho_s} \qquad \bar{C}_{Rb} = \frac{K_1'}{K_3-K_1}\left[\exp\ (-K_{11}\ t) - \exp\ (-K_{33}\ t)\right]$$

$$(\text{at } z = 0,\ \bar{C}_{Rb} = 0)$$

$$\frac{d\bar{C}_{Sb}}{dz} = [K_{11}''\bar{C}_{Ab} + K_{22}\bar{C}_{Rb} - K_{44}\bar{C}_{Sb}]\frac{W}{v_o\rho_s} \qquad \bar{C}_{Sb} = \exp\ (-K_{11}\ t)\left[\frac{K_1}{(K_4-K_1)} + \frac{K_2'K_1'}{(K_3-K_1)(K_4-K_3)}\right]$$

$$(\text{at } z = 0,\ \bar{C}_{Sb} = 0)$$

$$+ \exp\ (-K_{33}\ t)\left[\frac{-K_1'K_2'}{(K_4-K_3)(K_3-K_1)}\right]$$

$$+ \exp\ (-K_{44}\ t)\left[\frac{-K_2'K_1''}{(K_4-K_3)(K_4-K_1)} + \frac{K_1''}{(K_4-K_1)}\right]$$

$$\bar{C}_{Tb} = 1.0 - (\bar{C}_{Ab} + \bar{C}_{Rb} + \bar{C}_{Sb})$$

$$K_1'' = K_1\Psi_4;\quad K_{11}'' = K_1\Psi_4\ \frac{u_o}{(1-\varepsilon_{mf})u_{br}}$$

where

$$\Psi_4 = \left\{\frac{K_{ce}}{\gamma_e k_1 + K_{ce}}\left[\frac{\gamma_e^2 k_1 k_3 K_{ce} K_4}{(K_{ce}+\gamma_e k_3)(K_{ce}+\gamma_e k_4)\left(\gamma_c k_4 + \frac{\gamma_e k_4 K_{ce}}{K_{ce}+\gamma_e k_4}\right)} + \frac{\gamma_c k_1 K_{ce}\Psi_2 K_3 K_4}{K_{bc}(K_{ce}+\gamma_e k_3)}\right] + \frac{\gamma_c k_1 \Psi_2 K_3 K_4}{K_{bc}}\right\} \Bigg/ \left(\gamma_c k_1 + \frac{\gamma_e k_1 K_{ce}}{\gamma_e k_1 + K_{ce}}\right)$$

[a] This is a simplified case of Scheme (2·8)

representative bubble diameter (d_b = 15 cm) is presented in Appendix II.

Figure 2.3 shows the concentration profiles with varying bubble diameter. As a general observation it can be said that the conversion of A drops with increase in bubble diameter. This is quite consistent with the physical situation. Also, the fractional height of the fluidized bed at which the maximum concentration of R occurs in the reactor shifts to the right with increase in bubble diameter, as can be seen from Equation (2.36). It is noteworthy that in the case of a fluid bed reactor the extent of the maximum as well as its very presence can be controlled simply by changing the bubble diameter.

Figure 2.4 shows the variation of $\bar{C}_{R,max}$ with bubble diameter in the bed. The plug flow reactor (d_b = 0) represents the ideal case and corresponds to the highest value of $\bar{C}_{R,max}$ that is attainable. As can be seen from this figure, $\bar{C}_{R,max}$ decreases with increase in bubble diameter. This fact is consistent with the physical situation wherein a larger bubble diameter corresponds to a greater deviation from plug flow conditions.

The fluid bed performance is compared with that of a plug flow reactor (PFR) for k_1/k_3 = 10 in Figure 2.5, which shows the variation of selectivity with conversion for

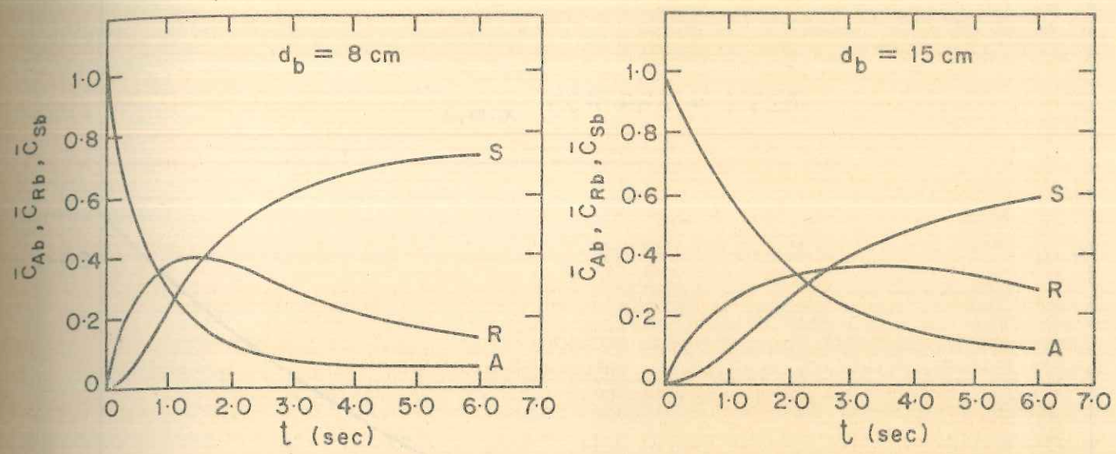

FIGURE 2·3. CONCENTRATION PROFILES WITH VARYING BUBBLE DIAMETERS FOR THE REACTION SCHEME $A \rightleftharpoons R \rightleftharpoons S$.

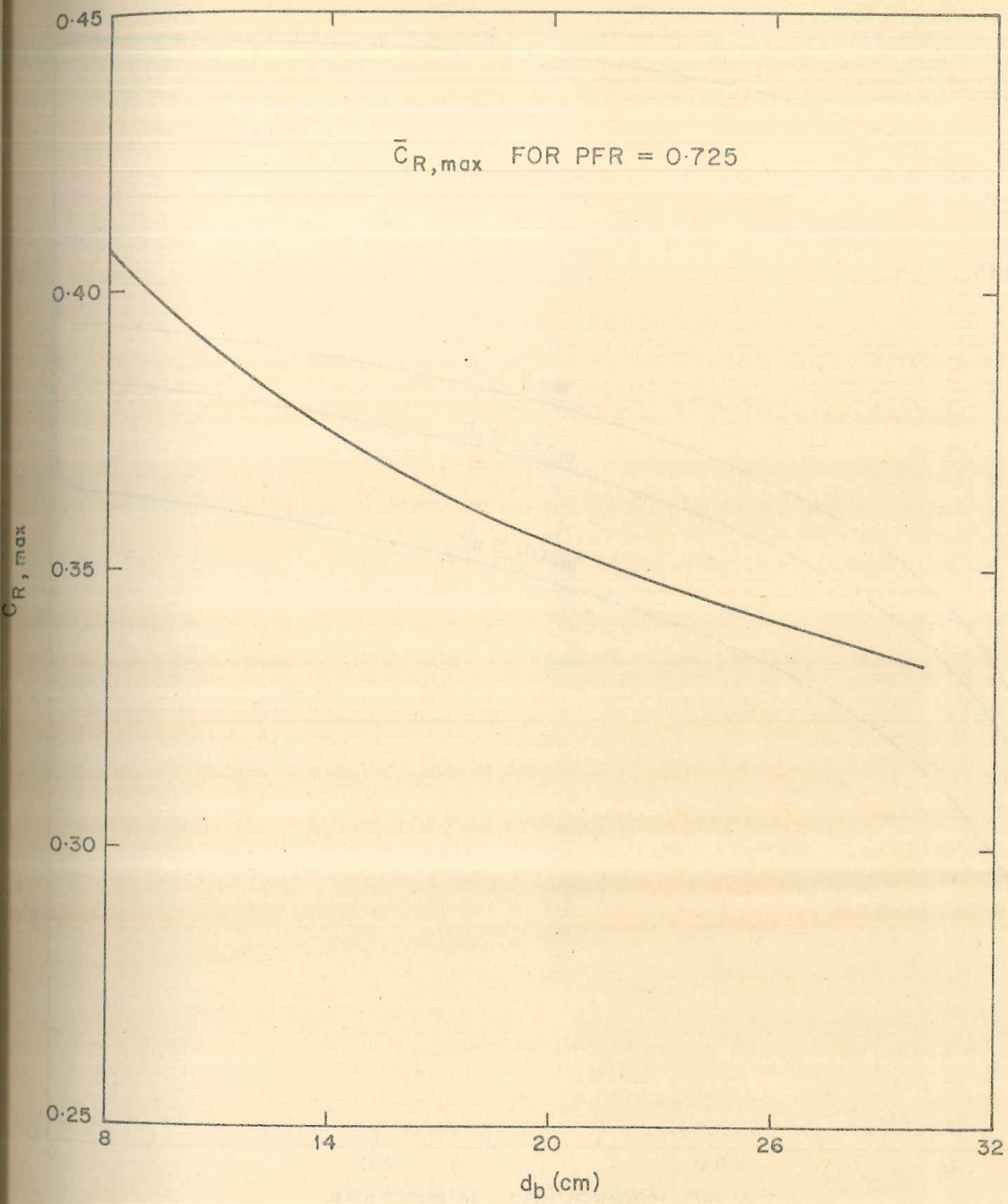

FIGURE 2·4. VARIATION IN $\bar{C}_{R,max}$ WITH BUBBLE DIAMETER FOR THE REACTION SCHEME $A \rightleftharpoons R \rightleftharpoons S$.

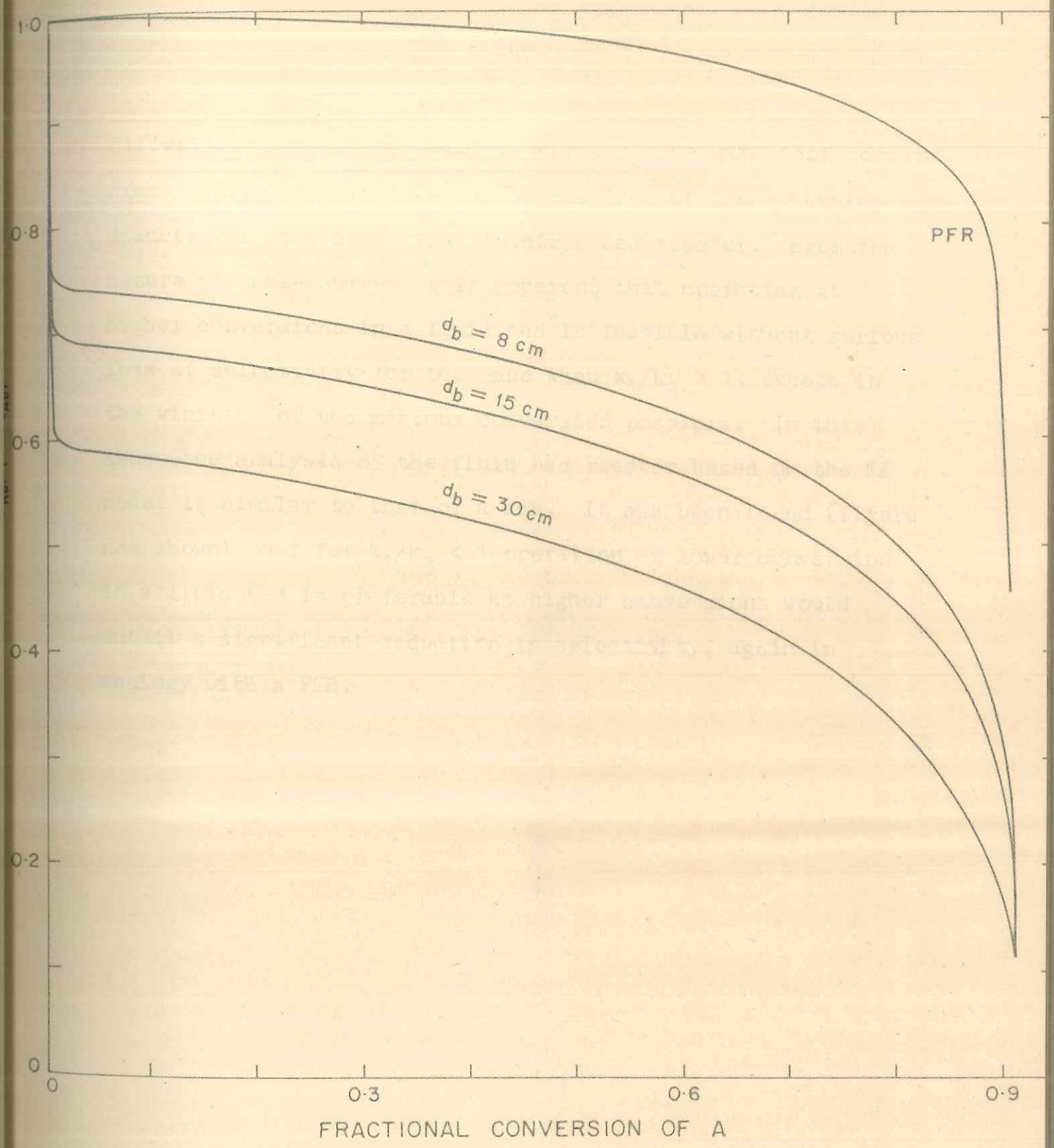

GURE 2·5. SELECTIVITY - CONVERSION PLOTS WITH VARYING BUBBLE DIAMETERS FOR THE REACTION SCHEME A ⇌ R ⇌ S.

different diameters of bubble. For the same extent of conversion higher selectivities can be realized at lower bubble diameters in the case of a fluidized bed reactor. From the nature of these curves it is apparent that operation at higher conversions in a fluid bed is feasible without serious loss of selectivity for the case when $k_1/k_3 > 1$, except in the vicinity of the maximum conversion possible. In this sense the analysis of the fluid bed reactor based on the KL model is similar to that of a PFR. It has been found (figure not shown) that for $k_1/k_3 < 1$ operation at lower conversion in a fluid bed is preferable as higher conversions would entail a significant reduction in selectivity, again in analogy with a PFR.

CHAPTER - 3

OPTIMAL PRODUCTION OF INTERMEDIATE FOR ZERO FIRST AND FIRST FIRST ORDER REACTION SEQUENCES IN THE FLUIDIZED BED

3. OPTIMAL PRODUCTION OF INTERMEDIATE FOR ZERO FIRST AND FIRST FIRST ORDER REACTION SEQUENCES IN THE FLUIDIZED BED

The bubbling bed model of Kunii and Levenspiel[2, 3] has been the subject of extension in Chapter 2 from a simple first order reaction to complex first order reaction schemes of the type

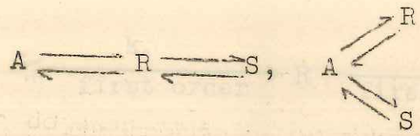

(3.1)

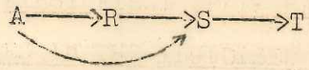

and the performance equations thereof have been developed.

The present chapter seeks to develop the performance equation of a fluidized bed reactor on the basis of the KL model for a zero first order reaction of the type.

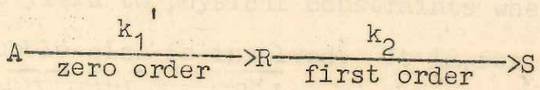

(3.2)

and analyze this reaction scheme with particular reference to optimization of the intermediate product. It is a well known fact that a zero order reaction is conceptually

different from a first or higher order reaction in that the rate of reaction is independent of the concentration of reactant **A.** Thus the concentration of reactant A drops to zero at some height in the bed, and from that height upwards the reaction becomes a simple first order reaction of the form

$$R \xrightarrow[\text{first order}]{k_2} S \qquad (3.3)$$

It is also proposed to analyze the reaction scheme

$$A \xrightarrow[\text{first order}]{k_1} R \xrightarrow[\text{first order}]{k_2} S \qquad (3.4)$$

where again optimization of the intermediate product R is sought.

The analysis in Chapter 2 has shown that operating with smaller bubble diameters in a fluidized bed is advantageous as it leads to a lesser deviation from the ideality of plug flow conditions. Whereas the desirability of operating with smaller bubble diameters is not in doubt, this often has to yield to physical constraints whereby a certain minium bubble size is involved. It is for this given bubble size that a technique is sought to be evolved for optimizing the production of intermediate at the bed exit for any given gas residence time.

3.1 ZERO FIRST ORDER REACTION SYSTEM

Consider the Reaction scheme (3.2). For any differential height in the bed dl

$$- u_b \frac{dC_{Ab}}{dl} = \gamma_b k_1' + K_{bc} (C_{Ab} - C_{Ac})$$

$$K_{bc}(C_{Ab} - C_{Ac}) = \gamma_c k_1' + K_{ce} (C_{Ac} - C_{Ae}) \qquad (3.1)$$

$$K_{ce}(C_{Ac} - C_{Ae}) = \gamma_e k_1'$$

and for a height in the bed at which the concentration of A is finite, i.e. $l < l_{cr}$,

$$- u_b \frac{dC_{Rb}}{dl} = - \gamma_b k_1' + \gamma_b k_2 C_{Rb} + K_{bc} (C_{Rb} - C_{Rc})$$

$$K_{bc}(C_{Rb} - C_{Rc}) = - \gamma_c k_1' + \gamma_c k_2 C_{Rc} + K_{ce}(C_{Rc} - C_{Re}) \qquad (3.2)$$

$$K_{ce}(C_{Rc} - C_{Re}) = - \gamma_e k_1' + \gamma_e k_2 C_{Re}$$

In writing the material balance equations the transport coefficients K_{bc} and K_{ce} are taken to be identical for the species A and R.

The interchange coefficients for A and R are identical, except for differing diffusion coefficients. Thus

$$K_{bc}^{j} = 4.50 \left(\frac{u_{mf}}{d_b}\right) + 5.85 \left(\frac{D_j^{1/2} g^{1/4}}{d_b^{5/4}}\right) \quad j = A, R$$

$$K_{ce}^{j} = 6.78 \left(\frac{\epsilon_{mf} D_j u_b}{d_b^3}\right)^{1/2} \tag{3.3}$$

The diffusion coefficients rarely differ greatly and affect the interchange coefficients at most by the 1/2 power. Thus the superscripts in the interchange terms can reasonably be deleted and the interchange coefficients can be taken to be identical for the species A and R.

Combining and expressing the cloud and emulsion phase concentrations C_{Ac}, C_{Ae}, C_{Rc}, C_{Re} in terms of the bubble phase concentrations C_{Ab} and C_{Rb}, Equations (3.1) and (3.2) can be solved with the initial conditions

$$\begin{aligned} l = 0, \ \bar{C}_{Ab} &= \frac{C_{Ab}}{C_{Ao}} = 1 \\ l = 0, \ \bar{C}_{Rb} &= \frac{C_{Rb}}{C_{Ao}} = 0 \end{aligned} \tag{3.4}$$

to give

$$\bar{C}_{Ab} = 1 - \lambda_1 t \tag{3.5}$$

where

$$t = \frac{W}{v_o \rho_s} z \tag{3.6}$$

and

$$\lambda_1 = (\gamma_b + \gamma_c + \gamma_e) \quad k_1' \frac{u_o}{(1-\varepsilon_{mf})\, u_{br}\, C_{Ao}} \tag{3.7}$$

The critical value of t, when A has been just depleted by the zero order step, results in the condition $\bar{C}_{Ab} = 0$ at $t = t_{cr}$. Using this condition in Equation (3.5) results in

$$t_{cr} = \frac{1}{\lambda_1} \tag{3.8}$$

For $t < t_{cr}$, the solution of Equation (3.2) is obtained as

$$\bar{C}_{Rb} = \frac{\lambda_1 - \lambda_2}{K_{22}} \left[1 - \exp(-K_{22}\, t) \right] \tag{3.9}$$

where

$$K_i = k_i \left[\gamma_b + \frac{1}{\frac{k_i}{K_{bc}} + \frac{1}{\gamma_c + \frac{1}{\frac{k_i}{K_{ce}} + \frac{1}{\gamma_e}}}} \right] \quad i = 1,2 \tag{3.10}$$

$$K_{ii} = K_i \frac{u_o}{(1-\varepsilon_{mf})\, u_{br}} \tag{3.11}$$

and

$$\lambda_2 = \left[\frac{\gamma_c^2 k_1' k_2 (K_{ce}+\gamma_e k_2) + 2\gamma_e\gamma_c k_1' k_2 K_{ce} + \dfrac{\gamma_e^2 k_1' k_2 K_{ce}^2}{(K_{ce}+\gamma_e k_2)}}{(K_{bc}+K_{ce}+\gamma_c k_2)(K_{ce}+\gamma_e k_2) - K_{ce}^2} + \frac{\gamma_e^2 k_1' k_2}{(K_{ce}+\gamma_e k_2)} \right] \frac{u_o}{(1-\varepsilon_{mf})\, u_{br} C_{Ao}} \tag{3.12}$$

and for $t \geq t_{cr}$, the concentration of intermediate is obtained to be

$$\bar{C}_{Rb} = \bar{C}_{Rb}\Big|_{t_{cr}} [\exp(-K_{22}(t - t_{cr}))] \tag{3.13}$$

It may be emphasized here that the existence of a critical value of t in the bed, where the concentration of A falls to zero, is not restricted only to the above case but also is observed in the case of a fractional order reaction, where the order of reaction is less than 1.

3.2 FIRST FIRST ORDER REACTION SYSTEM

The performance equations for the Reaction scheme (3.4) can be obtained as a simplification of the general equations developed in Chapter 2 and are summarized below for ease of reference

$$\bar{C}_{Ab} = \exp(-K_{11}\, t) \tag{3.14}$$

$$\bar{C}_{Rb} = \frac{K_1'}{K_2 - K_1}\left[\exp(-K_{11}\, t) - \exp(-K_{22}\, t)\right] \tag{3.15}$$

$$t \text{ at } \bar{C}_{R,max} = \frac{\ln\left(\frac{K_2}{K_1}\right)}{K_{22}-K_{11}} \tag{3.16}$$

where

$$K_1' = K_1\, \phi_1 \tag{3.17}$$

and

$$\phi_1 = \left[1 - \frac{K_2}{K_1}\left[\left\{\frac{\gamma_e k_1 K_{ce}}{\gamma_e k_1 + K_{ce}} + \frac{\gamma_c k_1 [K_{ce}+\gamma_e k_2]}{K_{ce}}\right\}\frac{K_{ce}}{\gamma_e k_2 + K_{ce}} + \frac{K_{bc}}{K_2}\,\frac{\gamma_e k_2 K_{ce}}{\gamma_e k_2 + K_{ce}}\,\frac{\gamma_e k_1}{\gamma_e k_1 + K_{ce}}\right] \times \left[\frac{K_{ce}+\gamma_e k_1}{(K_{ce}+\gamma_e k_1)(K_{bc}+K_{ce}+\gamma_c k_1) - K_{ce}^2}\right]\right] \tag{3.18}$$

3.3 RESULTS AND DISCUSSION

For establishing the effect of variables in accordance with the various equations developed above, the following data will be used :

$k_1' = 10^{-5}$ g mol/cm^3 sec (zero order); $k_1 = 10.0$ sec^{-1} (first order); $k_2 = 1.0$ sec^{-1}

$\rho_s = 2.0$ g/cm^3; $u_{mf} = 3$ cm/sec; $u_o = 30$ cm/sec; $\epsilon_{mf} = 0.4$;

$D_e = D_A = 0.2$ cm^2/sec; $\frac{W}{v_o} = 8.0$ g sec/cm^3; $\frac{V_w}{V_b} = 0.3$;

$C_{Ao} = 10^{-5}$ g mol/cm^3 $d_b = 8$-30 cm

The results of the calculations are presented in Figures 3.1-3.3.

Figure 3.1 shows the concentration profiles of reactant A and product R with varying bubble diameters for the Reaction scheme (3.2). As $\bar{C}_{Sb} = (1.0 - \bar{C}_{Ab} - \bar{C}_{Rb})$, the concentration profiles for S can be easily obtained. As can be seen from the figure, the concentration profile for A remains unchanged with bubble diameter and hence t_{cr} is independent of bubble diameter and has a constant value (in this case 0.9 sec). The value of residence time t at which $\bar{C}_{R,max}$ occurs corresponds to t_{cr}, as beyond this residence time in the bed only conversion of R to S by a first order reaction would occur, leading to depletion in the concentration of R.

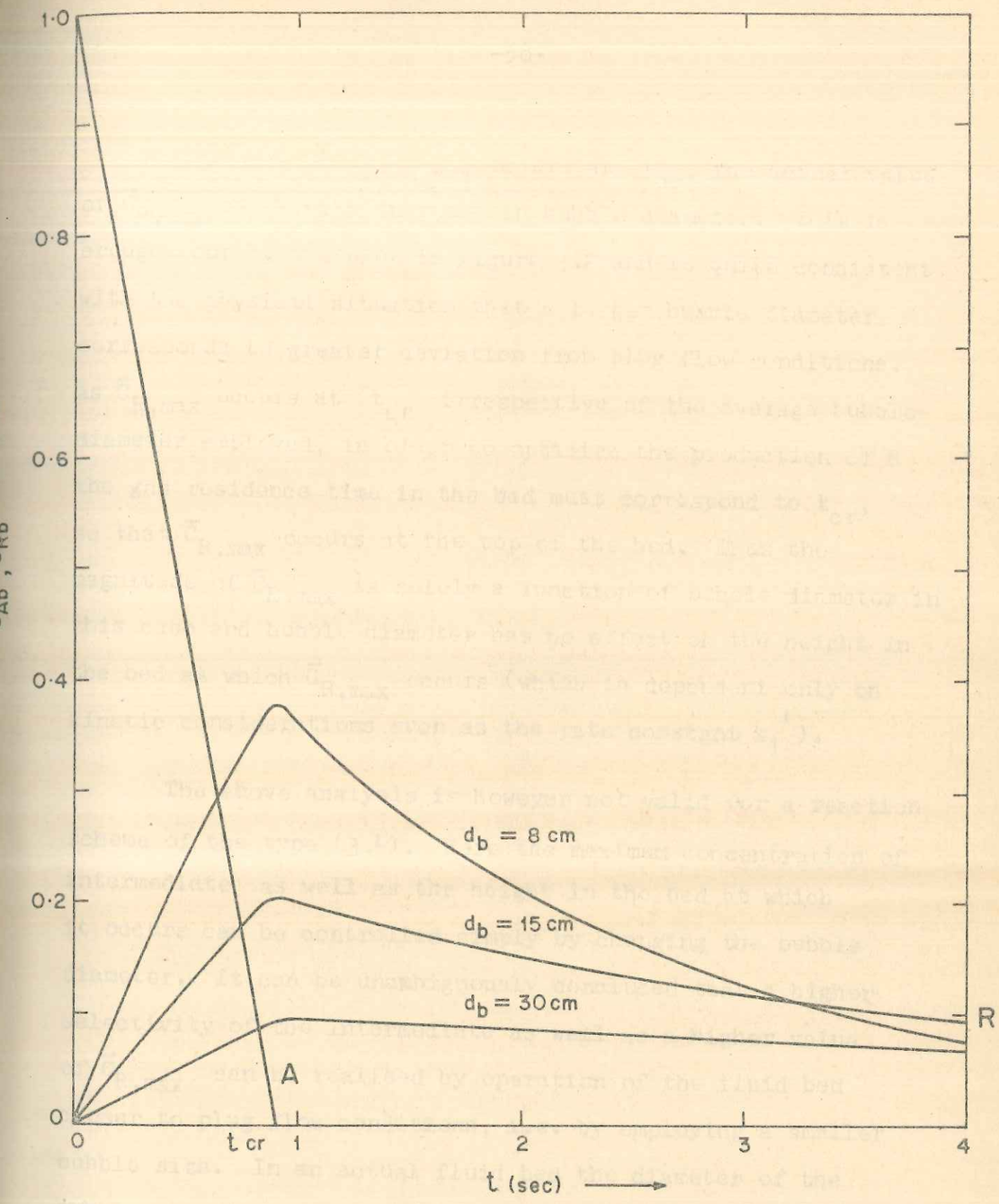

FIGURE 3·1. CONCENTRATION PROFILES WITH VARYING BUBBLE DIAMETERS FOR THE ZERO FIRST ORDER REACTION.

However, while $\bar{C}_{R,max}$ occurs at t_{cr}, the actual value of $\bar{C}_{R,max}$ falls with increase in bubble diameter. This is brought out by the plot in Figure 3.2 and is quite consistent with the physical situation that a larger bubble diameter corresponds to greater deviation from plug flow conditions. As $\bar{C}_{R,max}$ occurs at t_{cr} irrespective of the average bubble diameter employed, in order to optimize the production of R the gas residence time in the bed must correspond to t_{cr}, so that $\bar{C}_{R,max}$ occurs at the top of the bed. Thus the magnitude of $\bar{C}_{R,max}$ is solely a function of bubble diameter in this case and bubble diameter has no effect on the height in the bed at which $\bar{C}_{R,max}$ occurs (which is dependent only on kinetic considerations such as the rate constant k_1').

The above analysis is however not valid for a reaction scheme of the type (3.4). Here the maximum concentration of intermediate as well as the height in the bed at which it occurs can be controlled simply by changing the bubble diameter. It can be unambiguously concluded that a higher selectivity of the intermediate as well as a higher value of $\bar{C}_{R,max}$ can be realised by operation of the fluid bed closer to plug flow conditions, i.e. by employing a smaller bubble size. In an actual fluid bed the diameter of the bubble cannot, however, be restricted to very small sizes due to the phenomenon of bubble growth arising out of

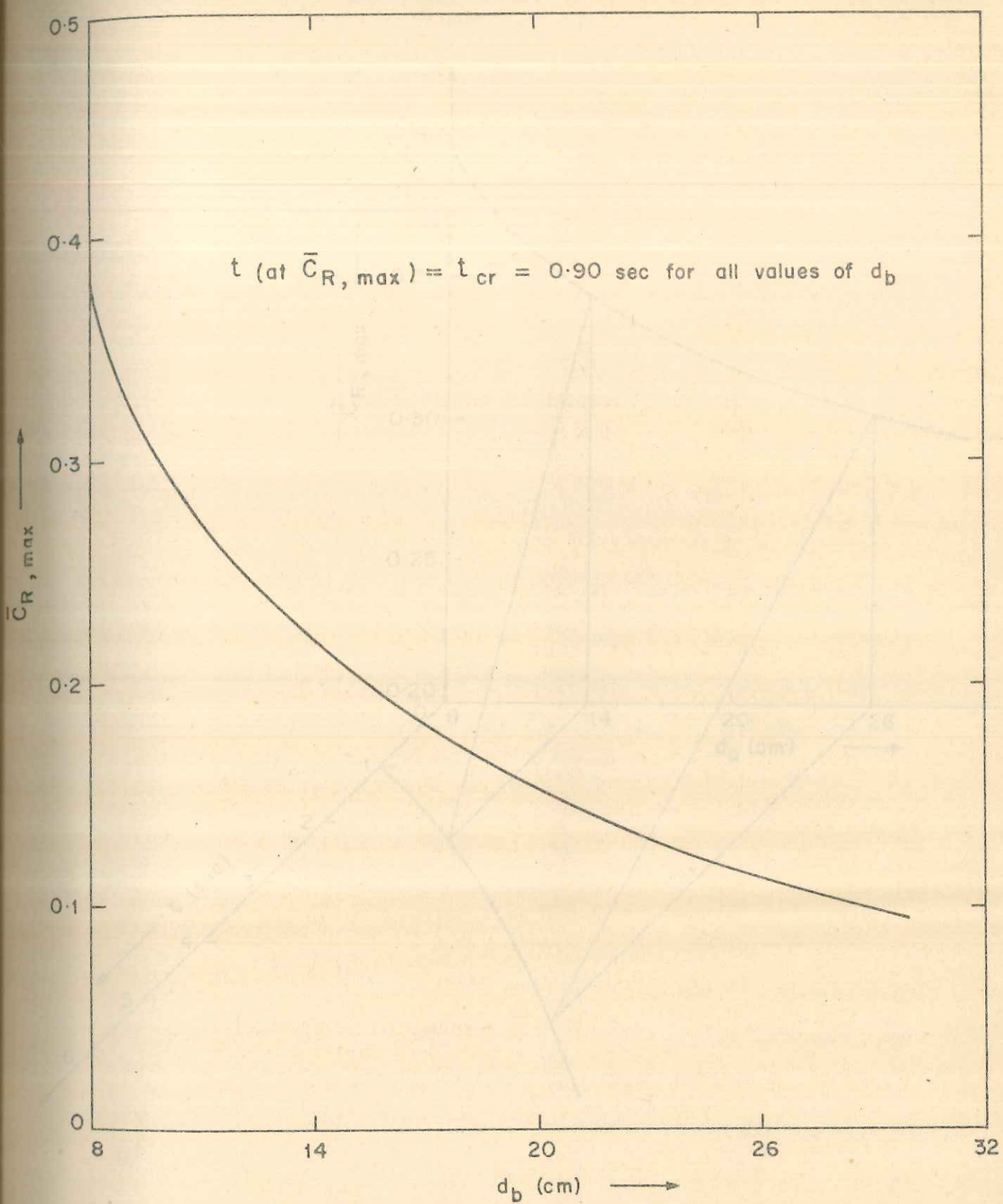

FIGURE 3·2 . VARIATION IN $\bar{C}_{R,max}$ WITH BUBBLE DIAMETER FOR THE ZERO FIRST ORDER REACTION.

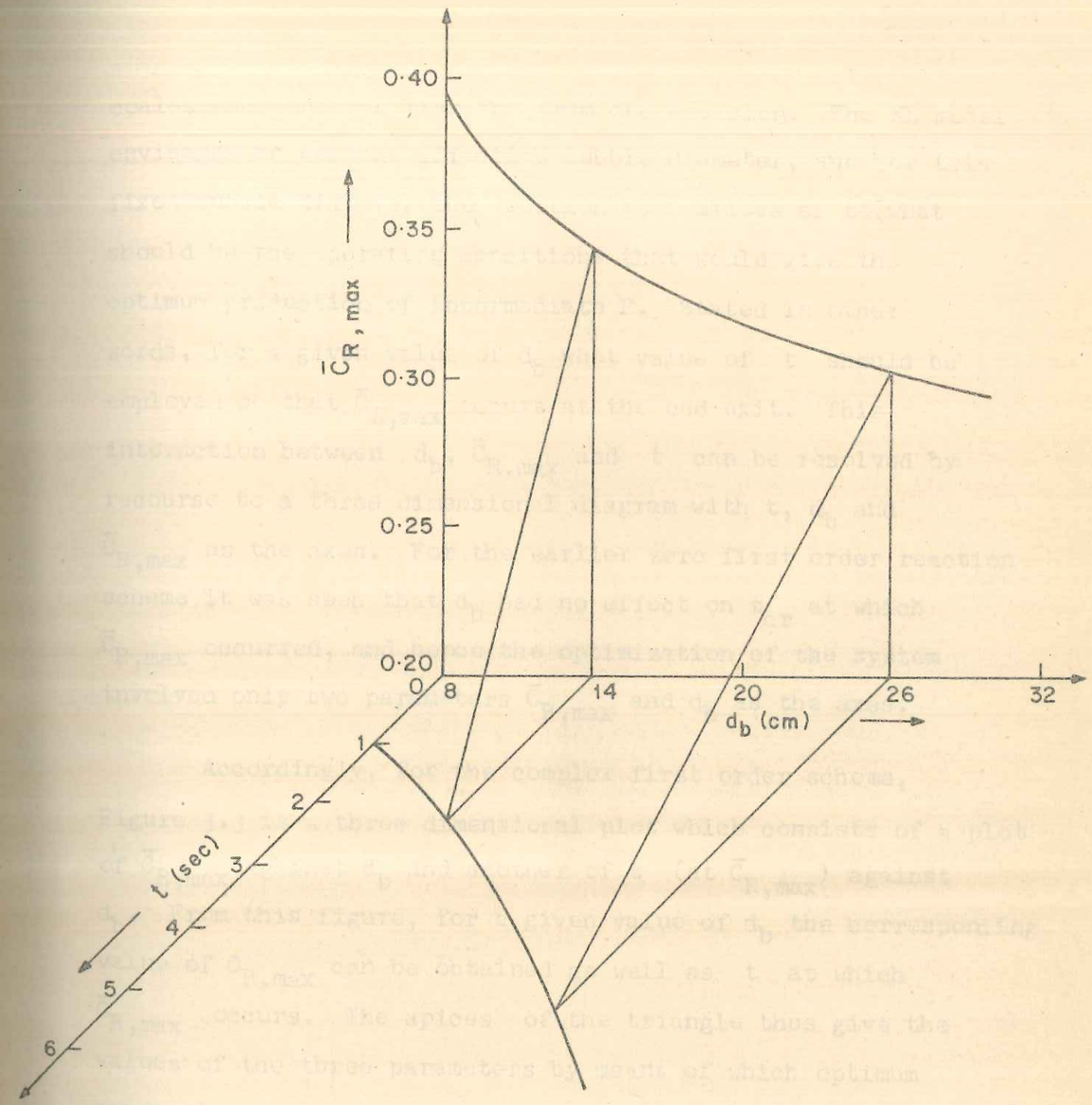

FIGURE 3·3 . GRAPH OF PARAMETER VALUES FOR OPTIMUM PRODUCTION OF R AT BED EXIT FOR THE FIRST FIRST ORDER REACTION.

coalescence and gas transfer from the emulsion. The KL model envisages an average effective bubble diameter, and for this fixed bubble diameter the question then arises as to what should be the operating conditions that would give the optimum production of intermediate R. Stated in other words, for a given value of d_b what value of t should be employed so that $\bar{C}_{R,max}$ occurs at the bed exit. This interaction between d_b, $\bar{C}_{R,max}$ and t can be resolved by recourse to a three dimensional diagram with t, d_b and $\bar{C}_{R,max}$ as the axes. For the earlier zero first order reaction scheme it was seen that d_b had no effect on t_{cr} at which $\bar{C}_{R,max}$ occurred, and hence the optimization of the system involved only two parameters $\bar{C}_{R,max}$ and d_b as the axes.

Accordingly, for the complex first order scheme, Figure 3.3 is a three dimensional plot which consists of a plot of $\bar{C}_{R,max}$ against d_b and another of t (at $\bar{C}_{R,max}$) against d_b. From this figure, for a given value of d_b the corresponding value of $C_{R,max}$ can be obtained as well as t at which $\bar{C}_{R,max}$ occurs. The apices of the triangle thus give the values of the three parameters by means of which optimum production of R at the top of the bed can be realised. This then is the procedure for optimizing the production of intermediate for a given bubble diameter in a complex first order reaction occurring in a fluid bed.

CHAPTER - 4

THE EFFECT OF CATALYST DILUTION ON FLUID BED REACTOR PERFORMANCE FOR COMPLEX FIRST ORDER REACTIONS

4. THE EFFECT OF CATALYST DILUTION ON FLUID BED REACTOR PERFORMANCE FOR COMPLEX FIRST ORDER REACTIONS

The concept of dilution of catalyst has previously been applied to exothermic reactions carried out in tubular reactors packed with catalyst. Here the rate of heat generation varies markedly along the length of the reactor, giving rise to undesirable temperature peaks. Thus a specific temperature profile can be established in a fixed bed by means of catalyst dilution and in certain cases this strategy can be employed to improve the reactor performance.

Gross catalyst dilution with inert has been employed to maintain near-isothermal conditions in kinetic studies in integral reactors as evidenced from the studies of Rihani et al.[37] and Gilliatt[38]. Caldwell and Calderbank[29] have also considered the case where a catalyst dilution profile is operating in the bed. This has special application in that category of reactions where a lower constraint exists on the temperature, which arises from the need to minimize reactor size for a given conversion, and a maximum constraint exists in order to prevent a temperature runaway or for considerations of selectivity. A small difference between these two constraints necessitates a quasi-isothermal mode of operation. Thus, by a combination of high temperature and high dilution, a diluted catalyst

fixed bed reactor can maintain the same productivity at the front end as a conventional reactor, whereas operation with a higher temperature and no dilution ensures a higher productivity at the tail end.

Narsimhan[39] has considered a reversible exothermic reaction taking place in a nonisothermal nonadiabatic plug flow reactor and has developed an analytical procedure for establishing an optimum catalyst dilution profile along the reactor length. The treatment has been extended to a sequence of ideal fluidized bed reactors which are treated as continuous stirred tank reactors for the purpose of analysis, and an optimum temperature progression for the sequence of well-mixed fluidized bed reactors has been obtained.

Temperature control poses no problem in a fluidized bed as near-isothermal conditions is one of the main features of this type of reactor. The drawback in a fluidized bed then is the reduced conversion for the same weight of catalyst employed, as compared to a tubular reactor. In complex reactions low selectivity is also an additional constraint on fluidized bed operation.

In Chapter 2 an analysis of reversible and irreversible complex first order reaction schemes was carried out on the basis of the KL model. The performance equations for both

conversion and product distribution were obtained and the effect of variation in the effective bubble size on conversion and selectivity was studied. In this chapter the concept of catalyst dilution has been combined with the characteristic features of the vigorously bubbling fluidized bed (as brought out in the performance equations derived earlier) with a view to studying the variation of concentration of the intermediate and its selectivity in a complex reaction taking place in the reactor.

4.1 THEORETICAL DEVELOPMENT

For solid catalyzed heterogeneous reactions the rate constants are usually expressed as

$$k' \text{ , } \frac{cm^3}{\text{g of active catalyst-sec}} \qquad (4.1)$$

If we define our catalyst dilution ratio as

$$R' = \frac{\text{total wt. of solids in the bed}}{\text{wt. of active catalyst in the bed}} \qquad (4.2)$$

then $R' \geq 1.0$ and the effective rate constant k_s based on total solids becomes

$$k_s = \frac{k'}{R'} \text{ , } \frac{cm^3}{\text{g of solid-sec}} \qquad (4.3)$$

If we replace a certain quantity of active catalyst from the bed by the same weight of an inert solid which has the same density as the active catalyst and comparable size distribution and fluidizing characteristics, then the residence time t of the reactant fluid in the bed, defined as

$$t = \frac{W}{v_o \rho_s} \qquad (4.4)$$

will remain unchanged. In the case of supported catalysts, dilution, satisfying these requirements, can be readily achieved by using unimpregnated support as diluent. Thus the hydrodynamics of the fluid bed has remained unaltered due to the dilution of catalyst and the gas-solid contacting pattern is also unchanged, whereas the rate constant for the catalyst needs to be replaced by an effective rate constant outlined earlier, based on solids in the bed.

The rate constant may be suitably modified by multiplying by the catalyst density so that it has the units of inverse time. Thus

$$\frac{k}{R'} = \frac{k' \rho_s}{R'} \ , \ \text{sec}^{-1} \qquad (4.5)$$

Considering now a fluid bed reactor, the effective

rate constant in the KL model for a simple first order reaction can be modified to incorporate catalyst dilution by writing it in the form

$$(K)_{dil} = \frac{k\, u_o}{R'(1-\varepsilon_{mf})u_{br}} \left[\frac{1}{\frac{k}{R'K_{bc}} + \frac{1}{\gamma_c + \frac{1}{\frac{k}{R'K_{ce}} + \frac{1}{\gamma_e}}}} \right] \qquad (4.6)$$

By definition γ_e and γ_c represent the volume of solids in the emulsion and cloud, respectively, per unit volume of bubbles in the bed. Thus catalyst dilution will have no effect on the value of γ_e and γ_c and hence they would not be modified in any way. As γ_b (which represents the volume of solids in the bubbles per unit volume of bubbles) $\simeq 0.01 \backsim 0.001$, it has been neglected in the analysis, which is reasonable for all but extemely fast reactions.

Equation (4.6) can be written in the form

$$(K)_{dil} = \frac{k}{R'} E \qquad (4.7)$$

where E is the efficiency of fluidized contacting, with $0 < E < 1$. Thus from Equations (4.6) and (4.7) it is seen that

$$E = \frac{u_o}{(1-\epsilon_{mf})u_{br}} \left[\frac{1}{\frac{k}{R'K_{bc}} + \frac{1}{\gamma_c + \frac{1}{\frac{k}{R'K_{ce}} + \frac{1}{\gamma_e}}}} \right] \qquad (4.8)$$

An increase in catalyst dilution will result in a decrease in k/R', but as can be seen from Equation (4.6), this decrease is partially offset by a resultant improvement in the contacting efficiency E.

For a simple first order reaction

$$A \xrightarrow{k} R$$

the KL model predicts that catalyst dilution will only result in a decreasing conversion of A if the same residence time t is maintained in the bed. This is in consonance with the physical situation. As

$$\ln \frac{C_{Ao}}{C_A} = K\,t \qquad (4.9)$$

and K decreases with decreasing k (Figure 4.1), the conversion of A is seen to decrease in a fluid bed in a simple first order

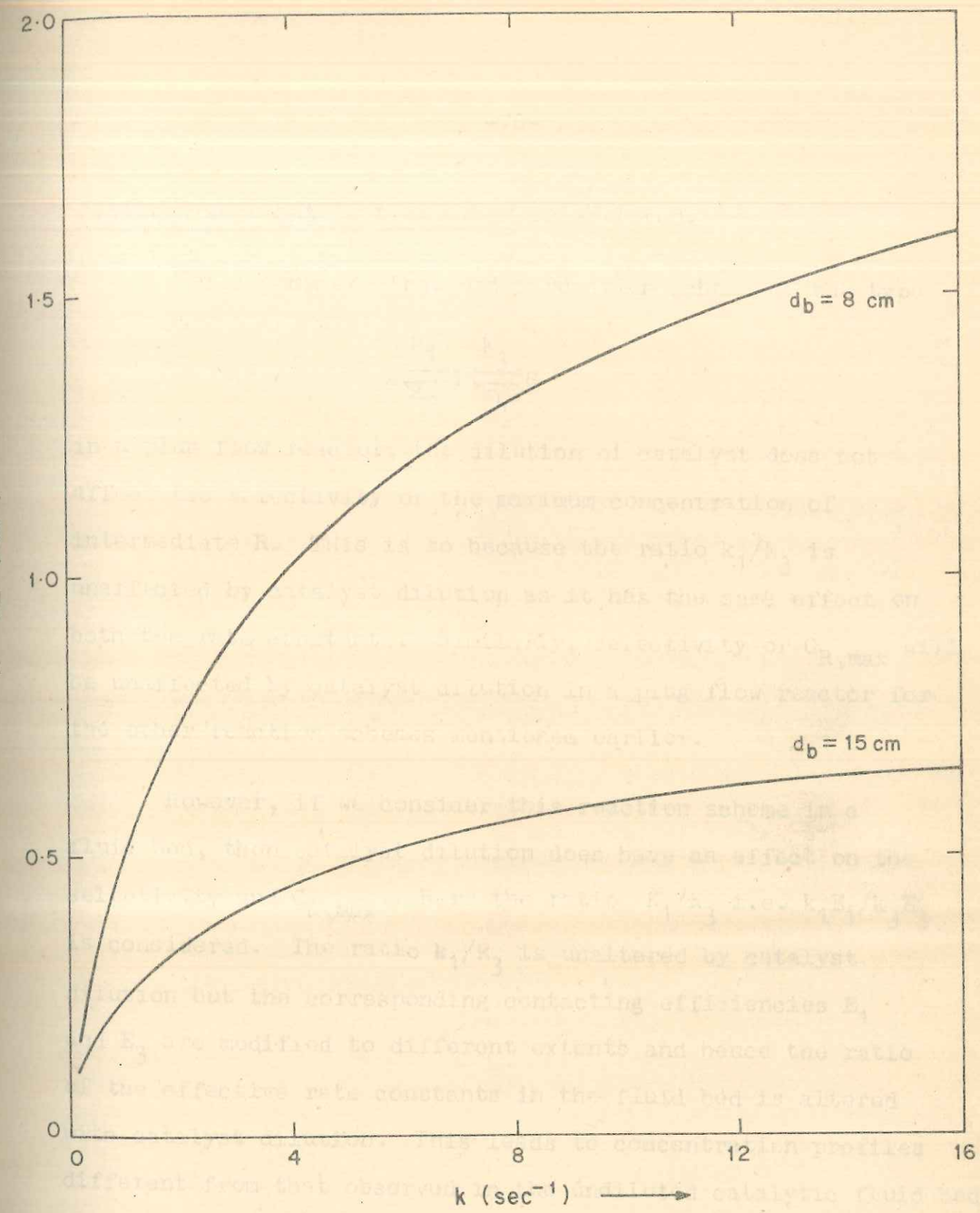

FIGURE 4·1. VARIATION OF EFFECTIVE RATE CONSTANT FOR A FLUID BED WITH FIXED BED RATE CONSTANT.

reaction when catalyst dilution is employed.

For a complex first order reaction scheme of the type

$$A \underset{k_2}{\overset{k_1}{\rightleftharpoons}} R \underset{k_4}{\overset{k_3}{\rightleftharpoons}} S$$

in a plug flow reactor, the dilution of catalyst does not affect the selectivity or the maximum concentration of intermediate R. This is so because the ratio k_1/k_3 is unaffected by catalyst dilution as it has the same effect on both the rate constants. Similarly, selectivity or $C_{R,max}$ will be unaffected by catalyst dilution in a plug flow reactor for the other reaction schemes mentioned earlier.

However, if we consider this reaction scheme in a fluid bed, then catalyst dilution does have an effect on the selectivity and $C_{R,max}$. Here the ratio K_1/K_3 i.e. k_1E_1/k_3E_3 is considered. The ratio k_1/k_3 is unaltered by catalyst dilution but the corresponding contacting efficiencies E_1 and E_3 are modified to different extents and hence the ratio of the effective rate constants in the fluid bed is altered with catalyst dilution. This leads to concentration profiles different from that observed in the undiluted catalytic fluid bed.

For establishing the effect of catalyst dilution in a fluid bed in accordance with the theory developed above, we shall consider the most general case

$$A \underset{k_2}{\overset{k_1}{\rightleftharpoons}} R \underset{k_4}{\overset{k_3}{\rightleftharpoons}} S$$

and compute the concentration profiles of the various species and also the selectivity and maximum concentration of intermediate R for different conditions.

The theoretical derivations for calculating the contacting efficiencies for the various steps, and expressions for calculating the concentration profiles of the various species, together with selectivity of the intermediate, have been presented earlier in Chapter 2. The following data will be used :

$k_1 = 10\ sec^{-1}$; $k_2 = 1.0\ sec^{-1}$; $k_3 = 1.0\ sec^{-1}$; $k_4 = 0.1\ sec^{-1}$

$\rho_s = 2.0\ g/cm^3$; $W/v_o = 8.0\ g\ sec/cm^3$; $u_{mf} = 3\ cm/sec$; $u_o = 30\ cm/sec$

$\varepsilon_{mf} = 0.4$; $D_e = D_A = 0.2\ cm^2/sec$; $V_w/V_b = 0.3$; $d_b = 8{,}15\ cm.$

The results are presented in Figures 4.1-4.7.

4.2 RESULTS AND DISCUSSION

Figure 4.1 shows the variation of the effective rate constant K in a fluid bed for varying values of the rate constant k in a fixed bed for a simple first order reaction. An interesting conclusion can be drawn from this figure. If the bed is considered to be half diluted with inerts, then the fixed bed rate constant k is reduced to half its original value, whereas the corresponding effective rate constant K in the fluid bed is reduced to a far lesser extent. This is due to the fact that the reduction in the fixed bed rate constant is partially offset by an improvement in the efficiency of fluidized bed contacting. In general, then, fluid bed operation is more insensitive (with respect to conversion) to catalyst dilution as compared to fixed bed operation for a simple first order reaction.

This conclusion can be easily extended to more complex first order reactions occurring in a fluid bed. Figure 4.2 shows the influence of catalyst dilution on the concentration profiles of the different species in a complex reaction $A \rightleftharpoons R \rightleftharpoons S$. It can be seen here that in fluid bed operation the overall conversion is not affected significantly whereas the selectivity of intermediate is modified to a considerable extent with catalyst dilution. Figure 4.3 represents the

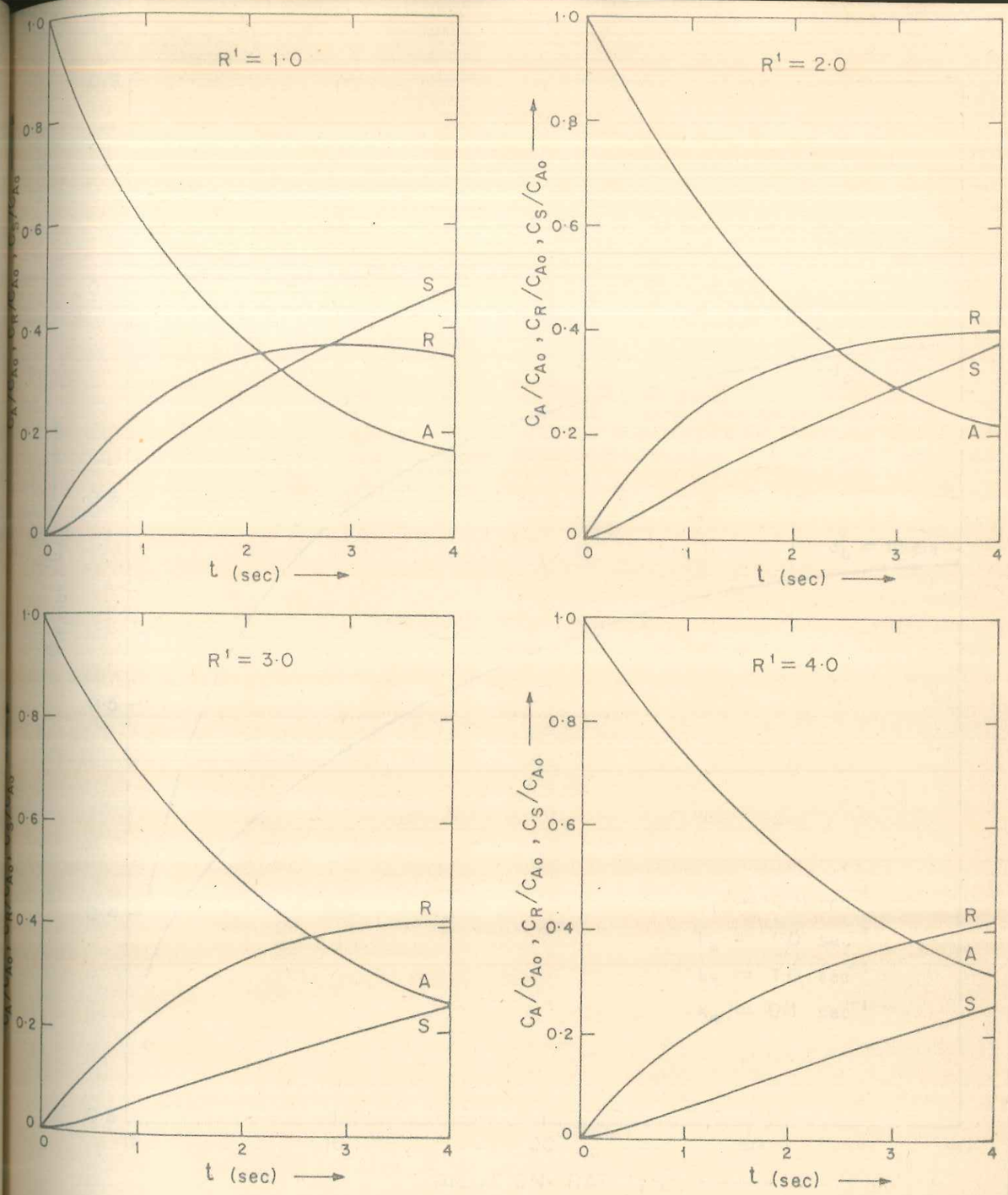

$k_1 = 10{\cdot}0\ sec^{-1}$ $k_2 = 1{\cdot}0\ sec^{-1}$

$k_3 = 1{\cdot}0\ sec^{-1}$ $k_4 = 0{\cdot}1\ sec^{-1}$

$d_b = 15$ cm

GURE 4·2. CONCENTRATION PROFILES IN A FLUID BED WITH VARYING CATALYST DILUTION RATIOS FOR THE REACTION SCHEME $A \rightleftharpoons R \rightleftharpoons S$.

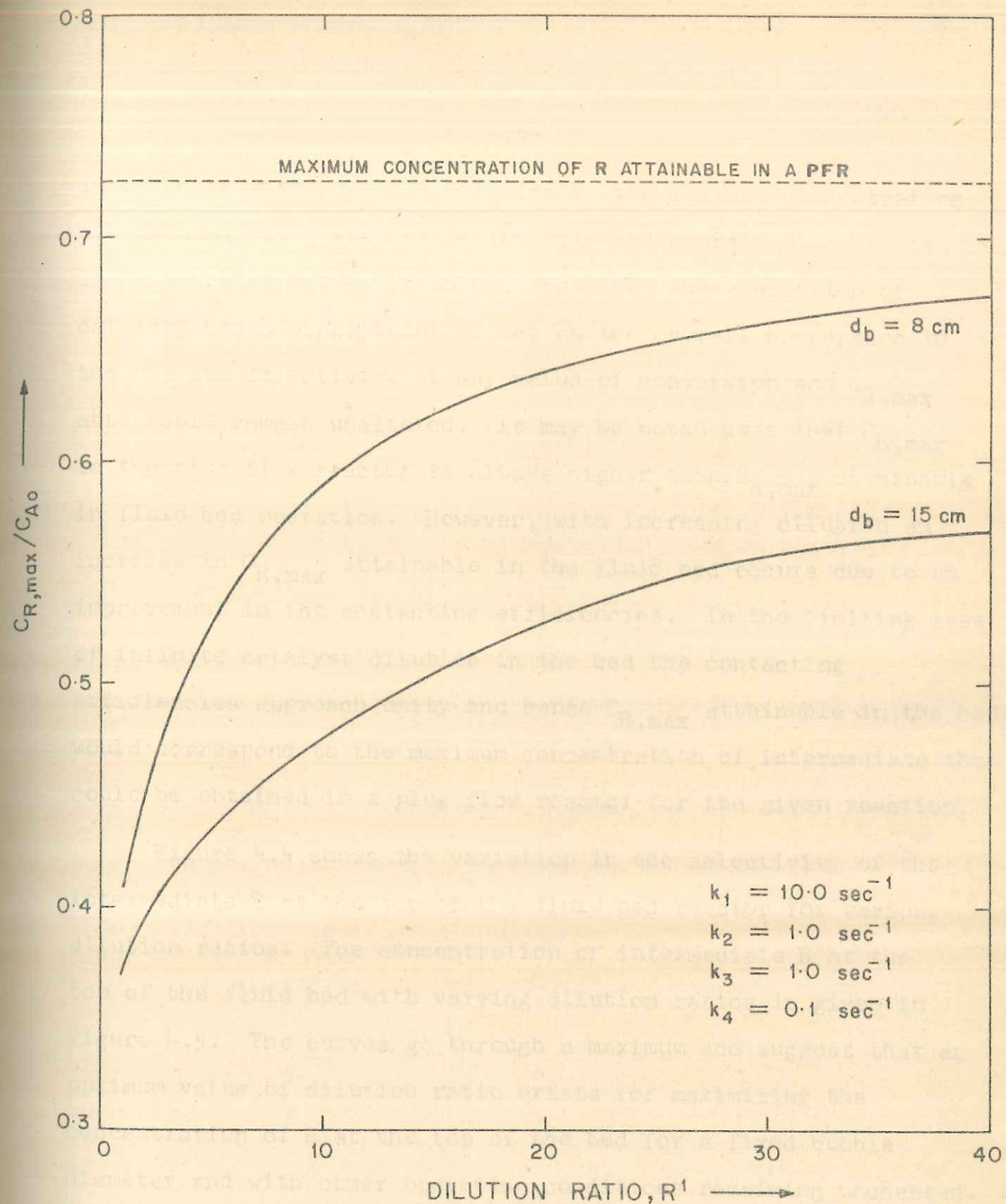

FIGURE 4·3. MAXIMUM CONCENTRATION OF INTERMEDIATE R ATTAINABLE IN THE FLUID BED CORRESPONDING TO VARYING CATALYST DILUTION RATIOS FOR THE REACTION SCHEME $A \rightleftharpoons R \rightleftharpoons S$.

improvement with catalyst dilution in the maximum concentration of intermediate R attainable in fluid bed operation. This is in direct contrast to fixed bed operation where dilution of catalyst has a significant effect on the overall conversion in the bed but selectivity at any value of conversion and $C_{R,max}$ attainable remain unaltered. It may be noted here that $C_{R,max}$ in the plug flow reactor is always higher than $C_{R,max}$ attainable in fluid bed operation. However, with increasing dilution an increase in $C_{R,max}$ attainable in the fluid bed occurs due to an improvement in the contacting efficiencies. In the limiting case of infinite catalyst dilution in the bed the contacting efficiencies approach unity and hence $C_{R,max}$ attainable in the bed would correspond to the maximum concentration of intermediate that could be obtained in a plug flow reactor for the given reaction.

Figure 4.4 shows the variation in the selectivity of the intermediate R at the top of the fluid bed reactor for various dilution ratios. The concentration of intermediate R at the top of the fluid bed with varying dilution ratios is given in Figure 4.5. The curves go through a maximum and suggest that an optimum value of dilution ratio exists for maximizing the concentration of R at the top of the bed for a fixed bubble diameter and with other operating conditions remaining unchanged. Figure 4.5 correspond to the concentration of R obtained at the top of the reactor. This is different from the maximum concentration of R attainable in a fluid bed which is denoted by $C_{R,max}$

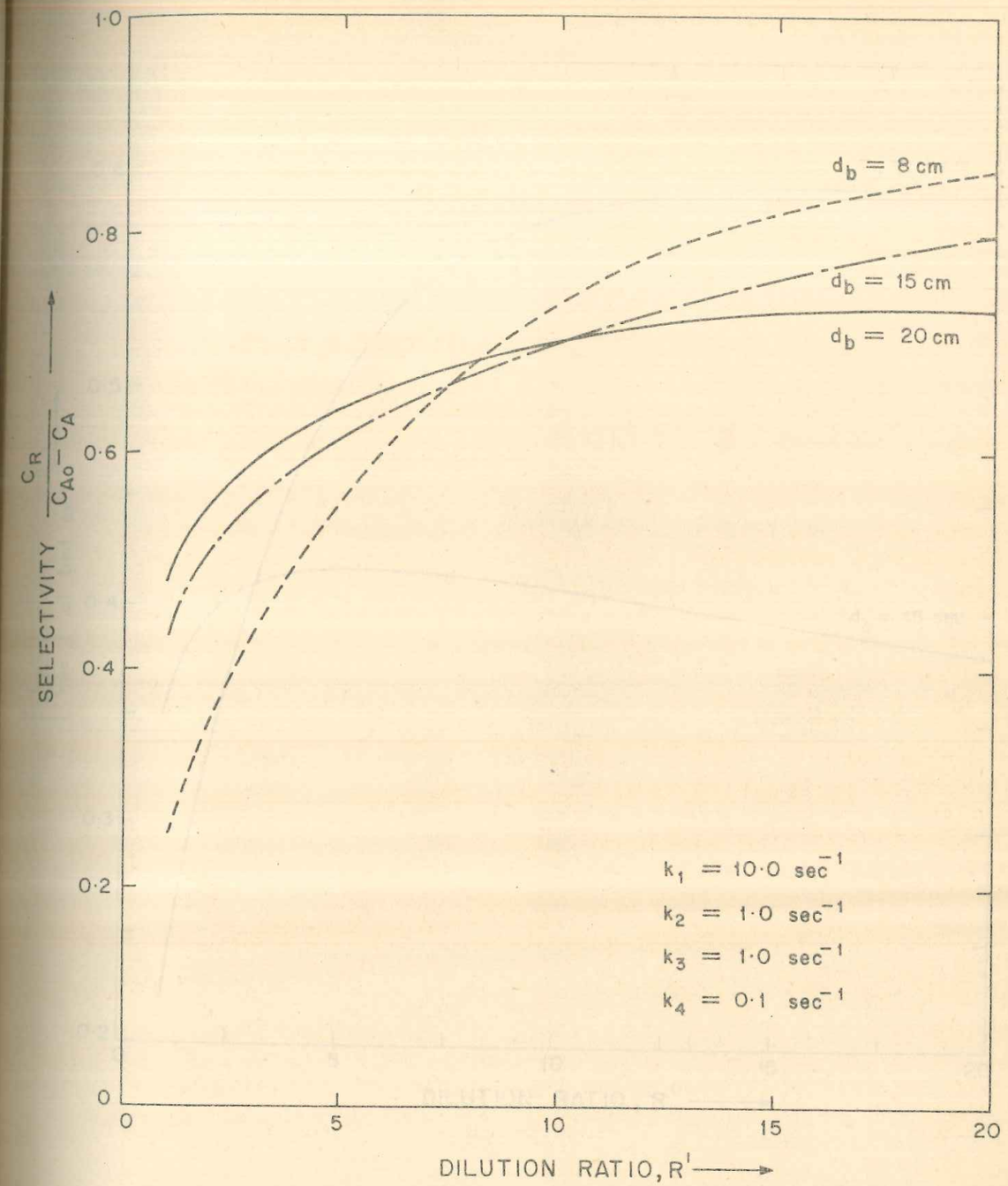

FIGURE 4·4. SELECTIVITY AT THE TOP OF THE BED WITH VARYING CATALYST DILUTION RATIOS FOR THE REACTION SCHEME A ⇌ R ⇌ S

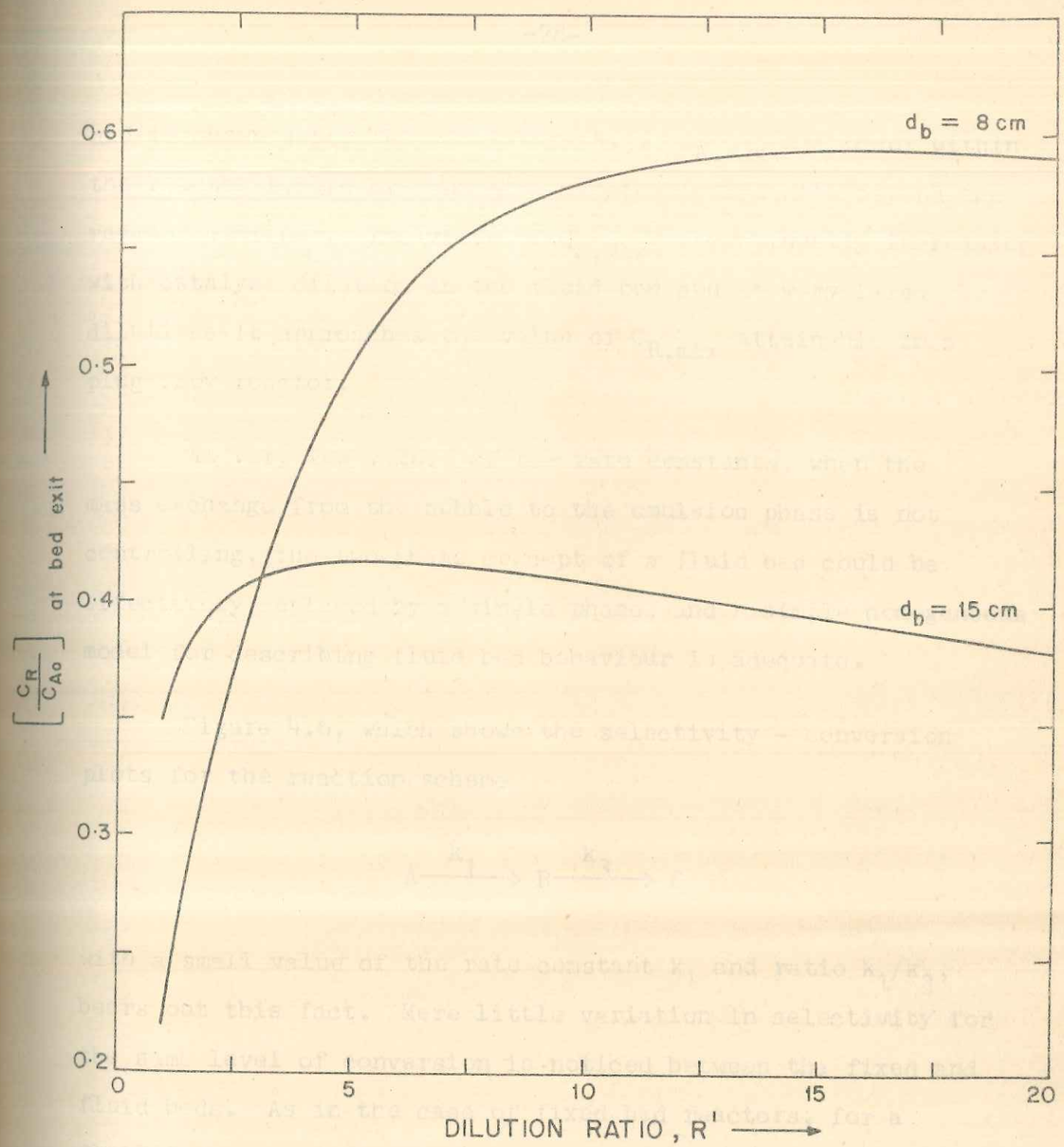

FIGURE 4·5. CONCENTRATION OF INTERMEDIATE R AT THE TOP OF THE BED CORRESPONDING TO VARYING DILUTION RATIOS FOR THE REACTION SCHEME $A \rightleftharpoons R \rightleftharpoons S$.

and is shown separately in Figure 4.3. $C_{R,max}$ may occur within the reactor length or even at a hypothetical length beyond the reactor confines. The value of $C_{R,max}$ is continually increasing with catalyst dilution in the fluid bed and at very large dilutions it approaches the value of $C_{R,max}$ attainable in a plug flow reactor.

At very low values of the rate constants, when the mass exchange from the bubble to the emulsion phase is not controlling, the two phase concept of a fluid bed could be effectively replaced by a single phase, and a simple homogeneous model for describing fluid bed behaviour is adequate.

Figure 4.6, which shows the selectivity - conversion plots for the reaction scheme

$$A \xrightarrow{k_1} R \xrightarrow{k_3} S$$

with a small value of the rate constant k_1 and ratio k_1/k_3, bears out this fact. Here little variation in selectivity for the same level of conversion is noticed between the fixed and fluid beds. As in the case of fixed bed reactors, for a fluid bed operating under conditions where the reaction is very slow and $k_1/k_3 \ll 1$, higher selectivities can be realized only at lower conversion levels.

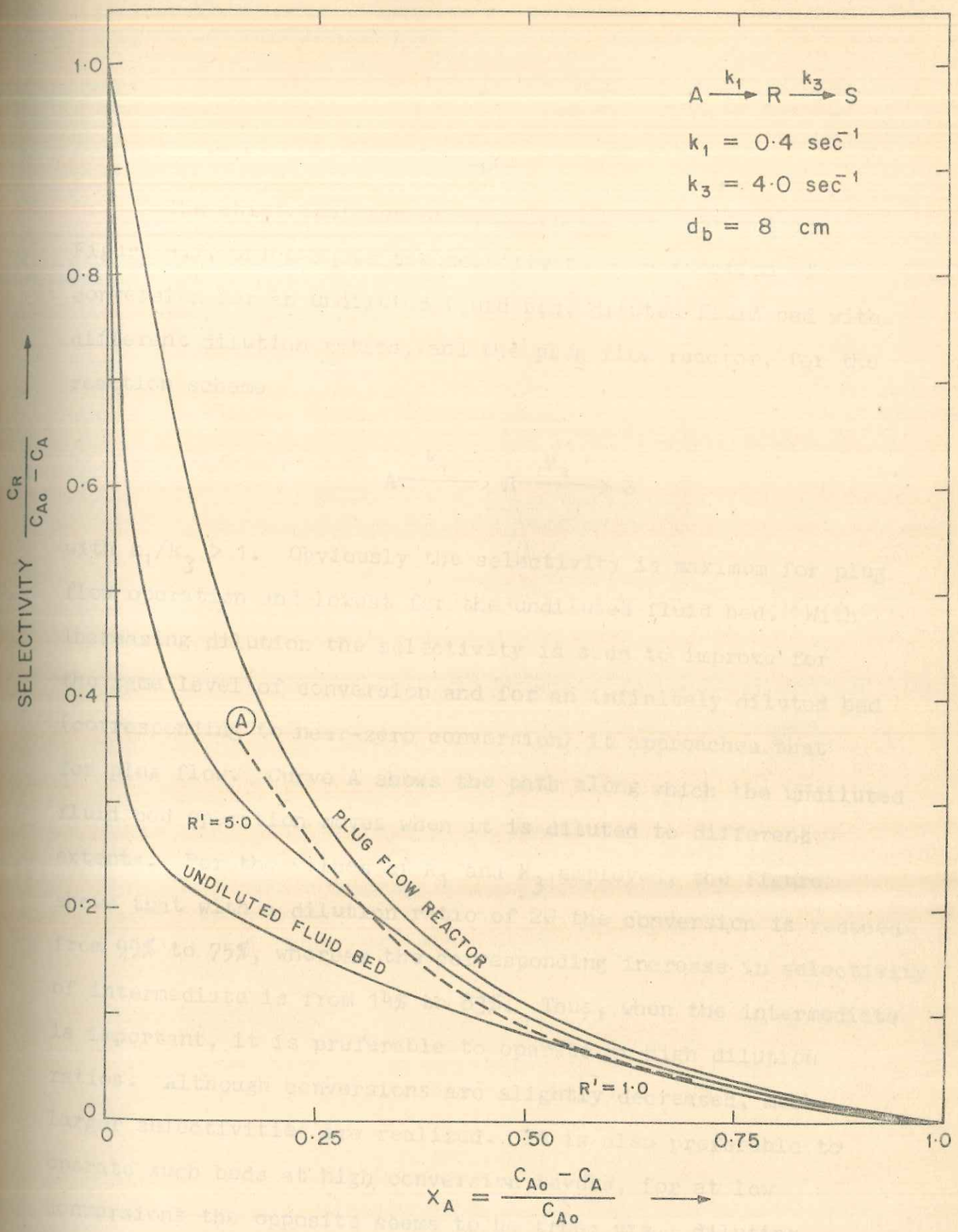

FIGURE 4·6 . SELECTIVITY - CONVERSION PLOTS FOR THE PLUG FLOW, UNDILUTED AND DILUTED FLUID BED REACTORS.

The chief features of dilution are brought out in Figure 4.7, which shows the selectivity as a function of conversion for an undiluted fluid bed, diluted fluid bed with different dilution ratios, and the plug flow reactor, for the reaction scheme

$$A \xrightarrow{k_1} R \xrightarrow{k_3} S$$

with $k_1/k_3 > 1$. Obviously the selectivity is maximum for plug flow operation and lowest for the undiluted fluid bed. With increasing dilution the selectivity is seen to improve for the same level of conversion and for an infinitely diluted bed (corresponding to near-zero conversion) it approaches that for plug flow. Curve A shows the path along which the undiluted fluid bed operation moves when it is diluted to different extents. For the values of k_1 and k_3 employed, the figure shows that with a dilution ratio of 20 the conversion is reduced from 99% to 75%, whereas the corresponding increase in selectivity of intermediate is from 14% to 83%. Thus, when the intermediate is important, it is preferable to operate at high dilution ratios. Although conversions are slightly decreased, much larger selectivities are realized. It is also preferable to operate such beds at high conversion levels, for at low conversions the opposite seems to be true; viz., diluting

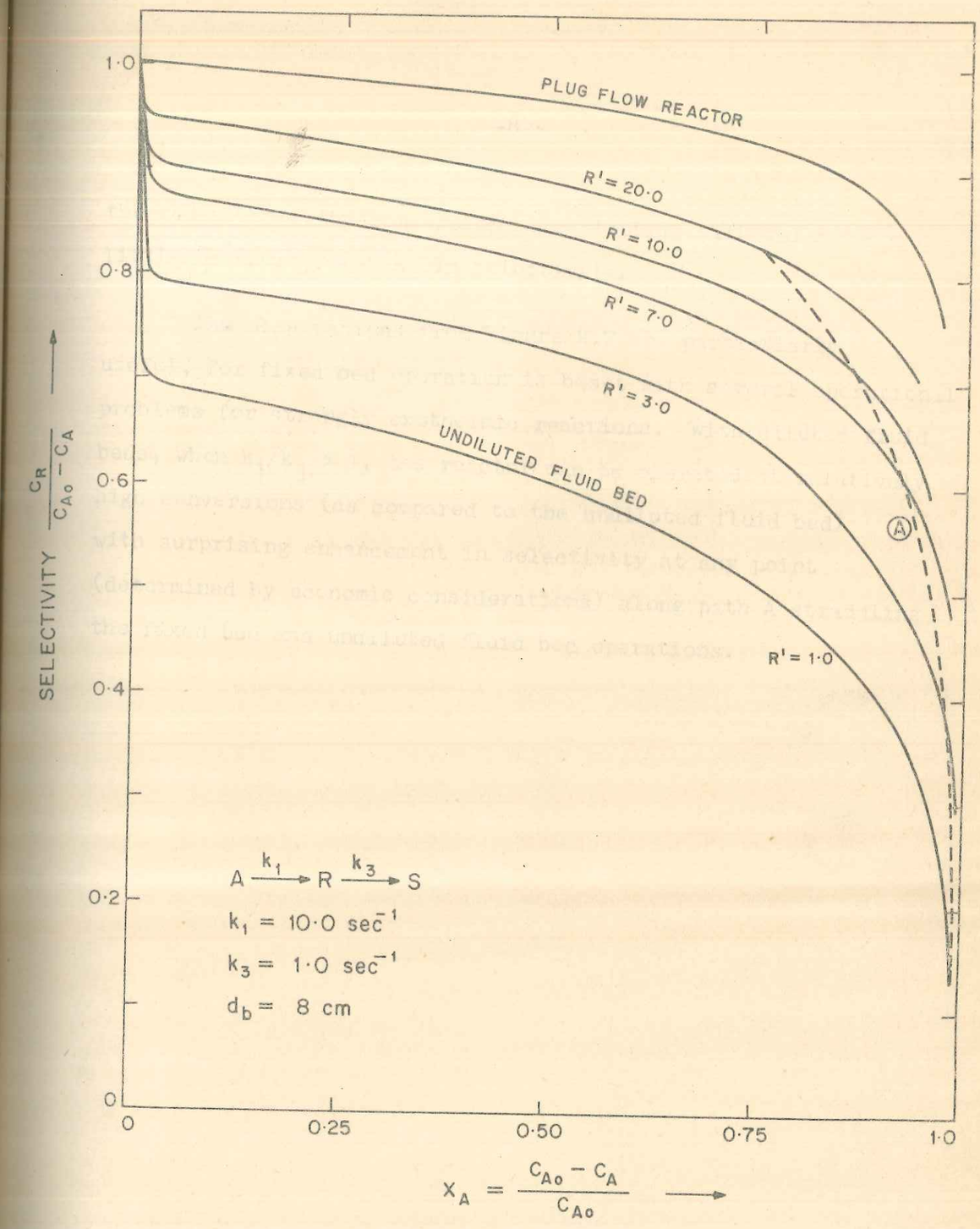

FIGURE 4·7. SELECTIVITY-CONVERSION PLOTS FOR THE PLUG FLOW, UNDILUTED AND DILUTED FLUID BED REACTORS.

the bed affects the conversion more strongly with relatively little or no improvement in selectivity.

The observations from Figure 4.7 are particularly useful, for fixed bed operation is beset with several operational problems for strongly exothermic reactions. With diluted fluid beds, when $k_1/k_3 > 1$, the reactor can be operated at relatively high conversions (as compared to the undiluted fluid bed) with surprising enhancement in selectivity at any point (determined by economic considerations) along path A straddling the fixed bed and undiluted fluid bed operations.

CHAPTER - 5

ANALYSIS OF FLUID BED REACTORS FOR REACTIONS INVOLVING A CHANGE IN NUMBER OF MOLES

5. ANALYSIS OF FLUID BED REACTORS FOR REACTIONS INVOLVING A CHANGE IN NUMBER OF MOLES

A large number of parameters are known to affect the performance of a fluid bed reactor. Additionally the interdependence of these parameters on each other makes the design of such units a very cumbersome and involved task. Accurate design and scale-up of fluid bed reactors thus presents a multiparameter problem. A more serious problem concerns the reliable estimation of these parameters. Parameters such as volume fraction of the phases and the interphase transport coefficients are known to be influenced by the type of gas distributor design and geometry of the reactor and as such cannot be estimated with any reliance. Many models which attempt to predict these parameters have been published in the literature and have been recently reviewed[40, 41]. The application of these models to reactor design is demonstrated, almost always, by considering a simple first order chemical reaction. Caram and Amundson[42] have recently carried out a parametric study of the steam-oxygen-char gasification reaction on the basis of the Davidson-Harrison[1] and Kunii-Levenspiel[2,3] models. Under certain conditions of operation such as high oxygen content, the reactions with volume change in their stoichiometry become dominant; thus volume change is indirectly accounted for. Many other industrially important systems

involve a change in volume of the gas phase due to reaction as typified by systems like dehydration of alcohol, catalytic cracking, oxidation of hydrocarbons, hydrogenation of nitrobenzene, ammoxidation of propylene, manufacture of high density polyethylene, absorption of sulphur dioxide in lime, etc. The equations available for predicting the conversion for a simple first order system are inapplicable for these cases and no model that takes into account the volume change due to reaction has as yet been published. It is the objective of the present chapter to propose such a model.

5.1 THEORETICAL MODEL

5.1.1 Choice of Basic Model

In the present chapter we consider the scheme

$$A \rightarrow \beta B \qquad (5.1)$$

which involves a change in number of moles, and develop the performance equations for calculating the conversion in the bed on the basis of the KL model. The KL model has been chosen mainly on the basis of the experimental results of Chavarie and Grace[17] which clearly showed that this model best characterizes the performance of a fluid bed reactor for simple first order reactions. Note, however, that the subsequent

experimental findings of Chavarie and Grace[43] indicate that the KL model underpredicts the rate of interphase mass transfer. Also, Mori and Wen[8] have compared the simpler models in general [e.g. the KL model] with the more sophisticated models and shown that the former are less acceptable for fast reactions. Lehmann and Schügerl[44] also suggest modification of the basic KL model to estimate the parameters of the fluid bed. Despite these findings the KL model has been used in the present analysis, chiefly because of its simplicity, to illustrate the importance of volume change.

In essence the KL model says that the behaviour of the bed can be completely characterized if the conditions at minimum fluidization (u_{mf}, ϵ_{mf}), the effective diameter of the bubble d_b, and the superficial velocity u_o in the bed are known[34]. All other parameters are then described in terms of this effective diameter and have been summarized in Table 2.1 for convenience of reference.

The model for a simple first order reaction gives the concentration C_A in the bubble phase as a function of height (and correspondingly gas residence time) in the bed by the equation

$$\ln \frac{C_{Ao}}{C_A} = Kt \qquad (5.1)$$

where $K = k\,E$, E being the efficiency of contact defined as

$$E = \left[\gamma_b + \cfrac{1}{\cfrac{k}{K_{bc}} + \cfrac{1}{\gamma_c + \cfrac{1}{\cfrac{k}{K_{ce}} + \cfrac{1}{\gamma_e}}}} \right] \frac{u_o}{(1 - \epsilon_{mf})\, u_{br}}$$

and

$$e = E\ (1 - \epsilon_{mf}) u_{br}/u_o \qquad (5.2)$$

The various quantities appearing in Equation (5.2) have been defined in Table 2.1. As can be seen from this table, the parameters K_{ce} and γ_e depend on the parameter u_b. For reactions involving a change in number of moles, there can occur a substantial change in the volume of the gas phase, altering the superficial velocity u_o in the bed.

5.1.2 Physical Aspect of Change in Moles Reaction

Most industrial reactions involve a change in number of moles and this change can manifest itself either as an increase in the volume of each of the bubbles or in the

number of bubbles. Creation of new bubbles in preference to augmenting the ones which are already present seems somewhat unlikely. However, no experimental data to settle this point is available as yet, and in the present analysis it is assumed that the extra gas generated in the fluid bed goes to form new bubbles. In the KL model the reaction takes place predominantly in the cloud and emulsion phases. If the extra gas generated in these phases is assumed to foster growth in the bubble size then it implies bulk flow from one phase to the other, thus influencing the interphase transport coefficients. In the present analysis, however, since it is assumed that the extra gas generated goes to form new bubbles, there is no additional bulk movement of gas between the phases. It is therefore reasonable to assume that the interphase transport coefficients remain unaffected as a result of volume change.

5.1.3 Development of Model

The constitutive equation that describes the concentration of the species A in Reaction scheme (5.1) can be written as

$$-\frac{d}{dl}\left(u_b C_{Ab}\right) = k\, e(l)\, C_{Ab} \qquad (5.3)$$

with the initial condition

$$C_{Ab} = C_{Ao} \quad \text{at} \quad l = 0 \qquad (5.4)$$

The solution of Equation (5.3) requires a knowledge of the variation of u_b and e with height in the bed, which is difficult to obtain. A simplification however seems possible if we take a look at the order of magnitude of the variation of e in the bed. For a range of parameter values (u_o = 10 to 30 cm/sec) and given values of k and d_b, the term e(l) was calculated and found to vary but little with height, suggesting that Equation (5.3) can be rearranged as

$$-\frac{d}{dl}\,(u_b\, C_{Ab}) = K\, C_{Ab} \qquad (5.5)$$

without any serious loss of accuracy.

Assuming the ideal gas law to be valid Equation (5.5) can be written in terms of the mole fraction as

$$-\frac{d}{dl}\,(u_b\, P'\, y_A) = K\, P'\, y_A \qquad (5.6)$$

Also, if inerts are present in the feed, a balance on inerts leads to

$$-\frac{d}{dl}\,(u_b\, P'\, y_j) = 0 \qquad (5.7)$$

Equation (5.7) can be readily integrated to obtain

$$(u_b P' y_j)_{l=1} = (u_b P' y_j)_{l=o} = \text{constant} \tag{5.8}$$

Rewriting Equation (5.6) as

$$- \frac{d}{dl} (u_b P' y_j \frac{y_A}{y_j}) = K P' y_A \tag{5.9}$$

and incorporating the result obtained in Equation (5.8) we have

$$- (u_b P' y_j)_{l=0} \frac{d}{dl} (\frac{y_A}{y_j}) = K P' y_A \tag{5.10}$$

The mole fraction of inert (y_j) in the system varies as a result of the variation in y_A. The relation between y_A and y_j can be obtained from the following considerations:

Let the feed to the reactor consist of N_{Ao} moles of species A along with N_j moles of inert per unit time. At a certain distance l in the reactor let N_A be the moles of species A remaining. The total moles at distance l can then be calculated from reaction stoichiometry as

$$\underset{\text{(moles of A)}}{N_A} + \underset{\text{(moles of B)}}{\beta\,(N_{Ao} - N_A)} + \underset{\text{(moles of inert)}}{N_j} = \underset{\text{(total moles)}}{\beta N_{Ao} + (1-\beta)N_A + N_j} \qquad (5.11)$$

or, in terms of the mole fraction, as

$$y_A = \frac{N_A}{\beta\, N_{Ao} + (1 - \beta)\, N_A + N_j} \qquad (5.12)$$

$$y_B = \frac{\beta\,(N_{Ao} - N_A)}{\beta\, N_{Ao} + (1 - \beta)\, N_A + N_j} \qquad (5.13)$$

$$y_j = \frac{N_j}{\beta\, N_{Ao} + (1 - \beta)\, N_A + N_j} \qquad (5.14)$$

The moles of species A, (N_A), remaining at any distance l in the bed can be expressed in terms of mole fraction y_A from Equation (5.12) as

$$N_A = \frac{y_A(\beta\, N_{Ao} + N_j)}{1 - (1 - \beta)\, y_A} \qquad (5.15)$$

Using this definition of N_A in Equation (5.14) the mole fraction y_j can now be expressed in terms of y_A as

$$y_j = 1 - (1 - \beta)y_A - \frac{\beta N_{Ao}}{\beta N_{Ao} + \dfrac{(1 - \beta)(\beta N_{Ao} + N_j)\, y_A}{[1 - (1 - \beta)\, y_A]}} + N_j \qquad (5.16)$$

Incorporating Equation (5.16) in (5.10) we finally obtain

$$-(u_b P' y_j)_{l=0} \frac{d}{dl} \left[\frac{y_A}{1-(1-\beta)y_A - \dfrac{\beta N_{Ao}}{\beta N_{Ao} + \dfrac{(1-\beta)(\beta N_{Ao} + N_j)y_A}{[1-(1-\beta)y_A]}} + N_j} \right] = K P' y_A \qquad (5.17)$$

which after some algebraic manipulations leads to

$$-(u_b P' y_j)_{l=o} \quad \frac{(\beta N_{Ao} + N_j)}{N_j} \quad \frac{d}{dl} \left[\frac{y_A}{1-(1-\beta)y_A} \right] = K P' y_A \qquad (5.18)$$

Equation (5.18) allows the pressure variations in the bed to be taken into account. The pressure at any distance l in the bed can be written as the sum of the pressure at the top of the bed and the hydrostatic head :

$$P'(l) = P_T + (1-\delta)\, \rho_s g (L_f - l) \qquad (5.19)$$

Incorporating Equation (5.19) in (5.18) and using the transformation

$$\frac{l}{L_f} = z \qquad (5.20)$$

gives

$$\frac{P'(z)}{P_T} = 1 + \frac{(1-\delta)\, \rho_s g\, L_f (1-z)}{P_T} \qquad (5.21)$$

or

$$\frac{P'(z)}{P_T} = 1 + \alpha\,(1-z) \qquad (5.22)$$

where

$$\alpha = \frac{(1-\delta)\, \rho_s g\, L_f}{P_T} \qquad (5.23)$$

Therefore

$$\frac{P'|_{z=0}}{P_T} = 1 + \alpha \qquad (5.24)$$

Equation (5.20) results in

$$dl = L_f \, dz \tag{5.25}$$

Incorporating the above in Equation (5.18) gives

$$-\frac{1}{P_T}(u_b P' y_j)_{z=o}\left[\frac{\beta N_{Ao}+N_j}{N_j}\right]\frac{1}{L_f}\frac{d}{dz}\left[\frac{y_A}{1-(1-\beta)y_A}\right] = K\,\frac{P'}{P_T}\,y_A \tag{5.26}$$

Rearranging the above

$$-\frac{P'|_{z=o}}{P_T}(u_b y_j)_{z=o}\left[\frac{\beta N_{Ao}+N_j}{N_j}\right]\frac{1}{K L_f}\frac{d}{dz}\left[\frac{y_A}{1-(1-\beta)y_A}\right] = [1+\alpha(1-z)]y_A \tag{5.27}$$

Now

$$y_j\Big|_{z=o} = \frac{N_j}{N_{Ao}+N_j} \tag{5.28}$$

Thus Equation (5.27) becomes

$$-(1+\alpha)\frac{u_b}{KL_f}\left[\frac{\beta N_{Ao}+N_j}{N_{Ao}+N_j}\right]\frac{d}{dz}\left[\frac{y_A}{1-(1-\beta)y_A}\right] = [1+\alpha(1-z)]y_A \tag{5.29}$$

which may be rewritten as

$$-a \frac{d}{dz}\left[\frac{y_A}{1-(1-\beta)y_A}\right] = [1+\alpha(1-z)]y_A \qquad (5.30)$$

where

$$a = \frac{u_b}{KL_f}\left(\frac{\beta N_{Ao} + N_j}{N_{Ao} + N_j}\right)[1+\alpha] \qquad (5.31)$$

The solution to Equation (5.30) can be obtained subject to the initial condition

$$y_A = y_{Ao} \quad \text{at} \quad z = 0 \qquad (5.32)$$

as

$$-a\left[\frac{(1-\beta)(y_A - y_{Ao})}{[1-(1-\beta)y_A][1-(1-\beta)y_{Ao}]} + \ln \frac{y_A[1-(1-\beta)y_{Ao}]}{y_{Ao}[1-(1-\beta)y_A]}\right]$$

$$= (1+\alpha)z - \frac{\alpha z^2}{2} \qquad (5.33)$$

Equation (5.33) is quadratic in z and can be solved to obtain

$$z = \frac{(1+\alpha)}{\alpha} \pm \left[\frac{(1+\alpha)^2 + 2\alpha\gamma}{\alpha^2}\right]^{1/2} \qquad (5.34)$$

where

$$Y = a \left[\frac{(1-\beta)(y_A - y_{Ao})}{[1-(1-\beta)y_A][1-(1-\beta)y_{Ao}]} + \ln \frac{y_A[1-(1-\beta)y_{Ao}]}{y_{Ao}[1-(1-\beta)y_A]} \right] \qquad (5.35)$$

Equation (5.33) or (5.34) accounts for the volume change of the gas phase (through β), allows for the presence of inerts in the feed stream (through y_{Ao}), takes into account the pressure variations in the bed (through α), and as such represents the general solution that relates the mole fraction of the species A to the dimensionless height z in the bed.

For a given set of parameter values Equation (5.33) can be solved to get the mole fraction of A remaining unconverted at any distance z in the reactor. A quantity of greater interest than the mole fraction is, however, the conversion in the reactor. The value of y_A obtained from Equation (5.33) is then used in Equation (5.15) to get the moles of A, (N_A) remaining unconverted at any distance z in the reactor. The conversion can then be calculated using Equation (5.36) :

$$\text{conversion} = \frac{N_{Ao} - N_A}{N_{Ao}} \qquad (5.36)$$

5.2 SIMPLIFIED CASES

5.2.1 Exclusion of Volume Change and Pressure Variation Effects

It is instructive to check the validity of Equation (5.33) by reducing it to some of the simplified cases. Thus, for the case of no pressure variation in the bed ($\alpha = 0$) and for a reaction with no volume change ($\beta = 1$), the above general solution reduces to

$$\ln \frac{y_A}{y_{Ao}} = -\frac{z}{a} = -\frac{L_f}{u_b} K z \qquad (5.37)$$

which is the KL model solution for a simple first-order reaction.

5.2.2 Exclusion of Pressure Variation Effect

A simplification of the general solution can be obtained by neglecting the pressure variation along the height of the bed, i.e. by taking $\alpha = 0$. Then Equation (5.33) is reduced to the following simplified solution

$$-a\left[\frac{(1-\beta)(y_A-y_{Ao})}{[1-(1-\beta)y_A][1-(1-\beta)y_{Ao}]} + \ln \frac{y_A[1-(1-\beta)y_{Ao}]}{y_{Ao}[1-(1-\beta)y_A]}\right] = z \qquad (5.38)$$

5.3 RESULTS AND DISCUSSIONS

5.3.1 Data for Analysis of the Model

For establishing the effects of the stoichiometric coefficient β, molar percentage of inerts in feed and pressure variation along the height of the bed, in accordance with Equation (5.33) developed above, we shall consider the first order reaction

$$A \xrightarrow{k} \beta B$$

and use the following data for fluid bed reaction :

k = 10 sec^{-1}; u_{mf} = 3 cm/sec; ρ_s = 2.0 g/cm^3.

y_{Ao} = 0.98 , 0.5 ; d_b = 8 cm; $\epsilon_{mf} = \epsilon_{packed}$ = 0.5.

D_e = 0.2 cm^2/sec; α_w = 0.33; L_f = 100 cm.

D_t = 100 cm; P_T = 1.0 atm; Reaction temperature = 250°C.

ϵ_e = 0.5; β = 0,1,2,3; $u_o\big|_{z=0}$ = 30 cm/sec.

The results of the calculations are presented in Figures 5.1 - 5.3. The influence on the overall conversion in the bed for varying amounts of inert in the feed stream,

different stoichiometric coefficients β for the change in volume reaction, and pressure variations in the bed, are sought to be analyzed on the basis of the volume change model.

5.3.2 Effect of Stoichiometric Coefficient

As can be seen from Figure 5.1, the conversion for a reaction with change in number of moles ($\beta > 1$) for a given fluid bed is always less than that for a reaction with no volume change. The result is not unexpected as the presence of extra moles of product dilutes the reactant species A in the reactor, thereby decreasing the conversion. This effect would be muted with an increasing quantity of inert being employed in the feed and would be most discernible in the case of pure feed A. The predictions of the KL model are represented by the case $\beta = 1$, as the model equations developed reduce to the KL model for this special case.

For $\beta < 1$, however, the conversion is always higher in a fluid bed than that which would be obtained if the reaction were considered with no attendant volume change. This is consequent to the physical situation wherein the superficial gas velocity u_o decreases with increasing conversion along the height of the bed for the case $\beta < 1$.

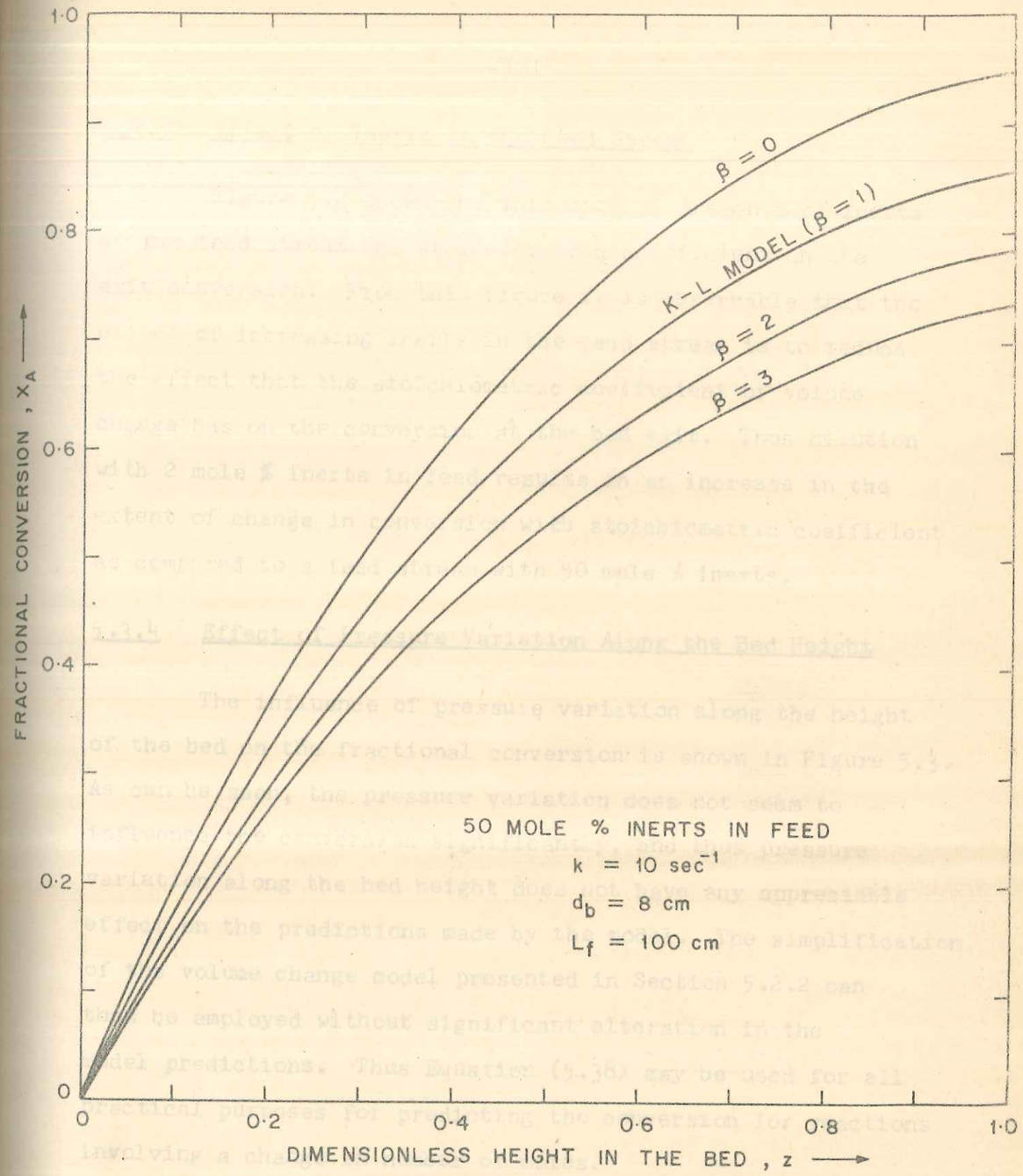

FIGURE 5·1 . INFLUENCE OF STOICHIOMETRIC COEFFICIENT ON THE CONVERSION PROFILE ALONG THE BED HEIGHT.

5.3.3 Effect of Inerts in the Feed Stream

Figure 5.2 shows the influence of presence of inerts in the feed stream and stoichiometric coefficient on the exit conversion. From this figure it is observable that the effect of increasing inerts in the feed stream is to reduce the effect that the stoichiometric coefficient of volume change has on the conversion at the bed exit. Thus dilution with 2 mole % inerts in feed results in an increase in the extent of change in conversion with stoichiometric coefficient as compared to a feed stream with 50 mole % inerts.

5.3.4 Effect of Pressure Variation Along the Bed Height

The influence of pressure variation along the height of the bed on the fractional conversion is shown in Figure 5.3. As can be seen, the pressure variation does not seem to influence the conversion significantly, and thus pressure variation along the bed height does not have any appreciable effect on the predictions made by the model. The simplification of the volume change model presented in Section 5.2.2 can thus be employed without significant alteration in the model predictions. Thus Equation (5.38) may be used for all practical purposes for predicting the conversion for reactions involving a change in number of moles.

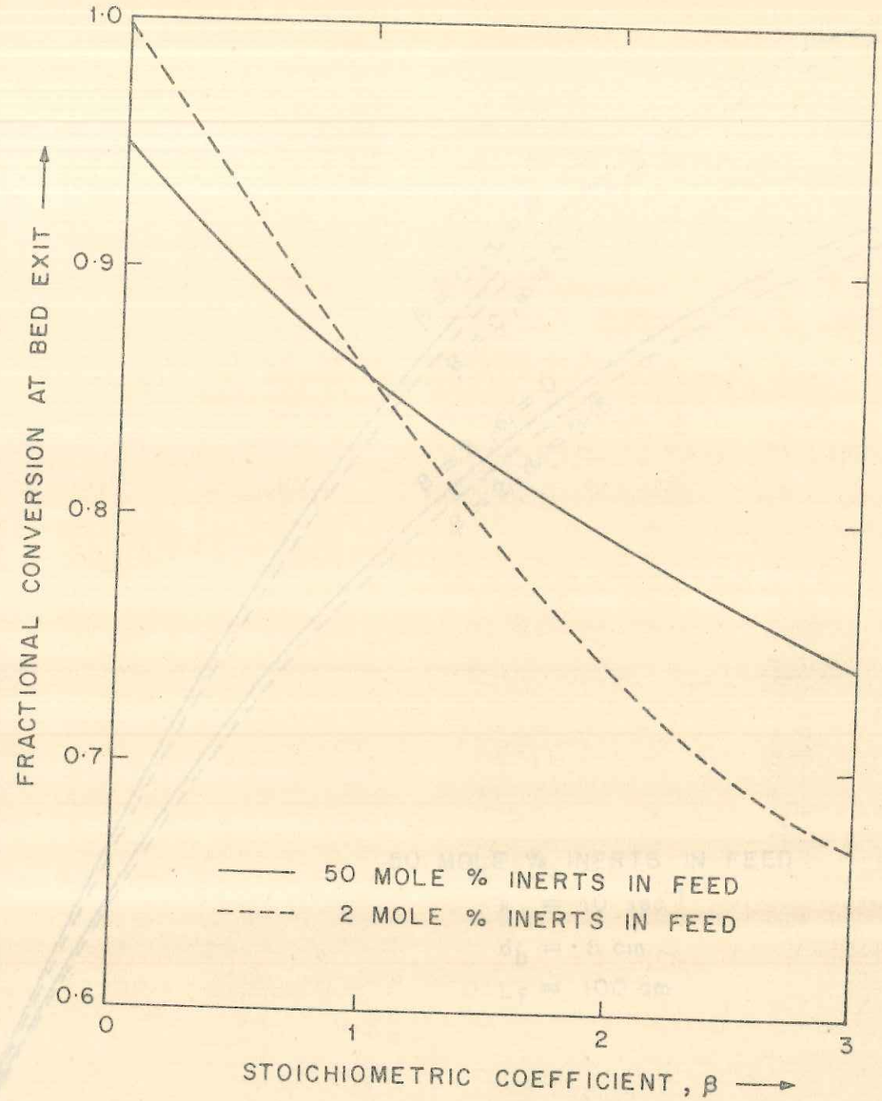

FIGURE 5·2. INFLUENCE OF STOICHIOMETRIC COEFFICIENT AND PRESENCE OF INERTS IN THE FEED STREAM ON THE EXIT CONVERSION IN THE BED.

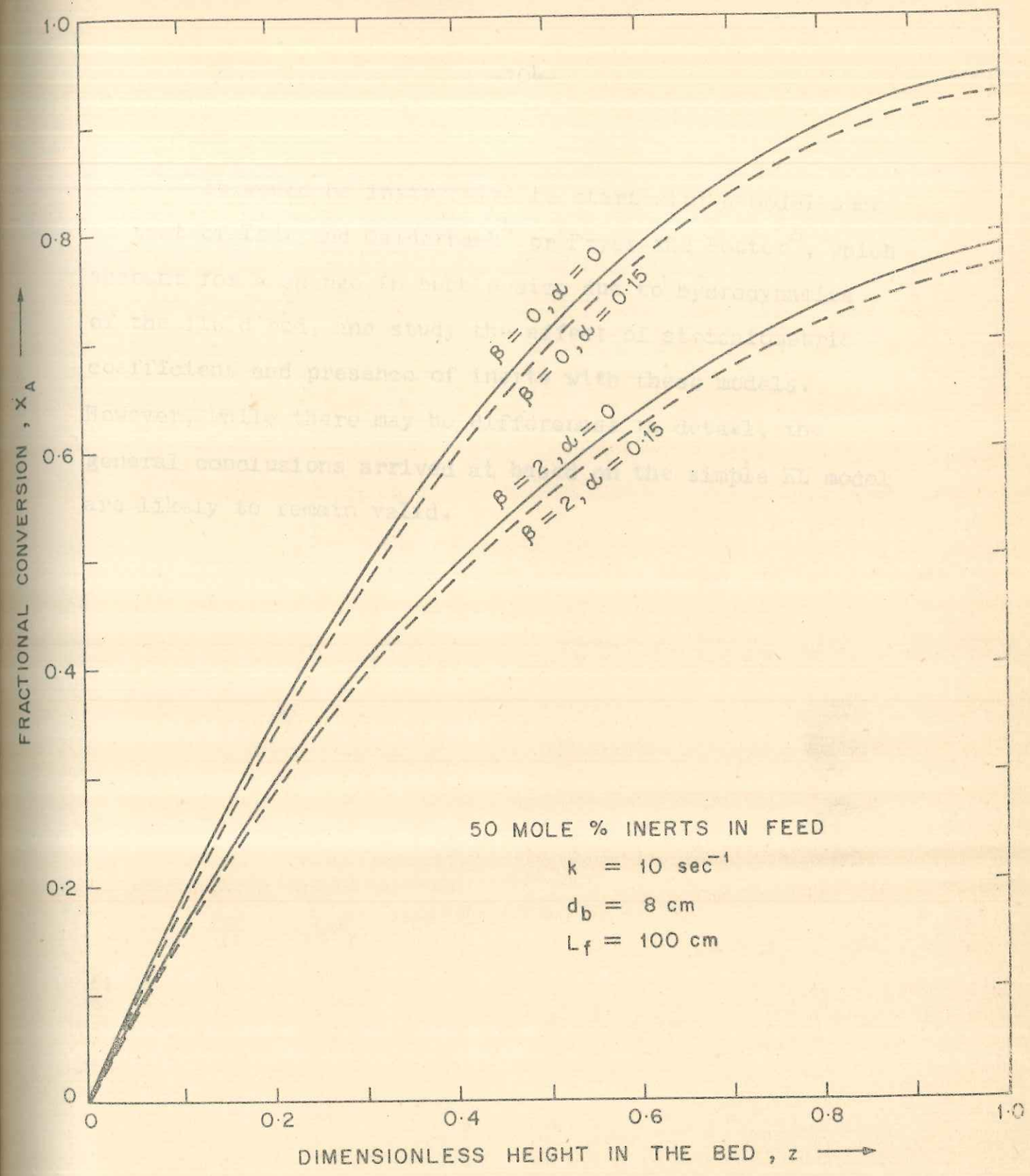

FIGURE 5·3 . INFLUENCE OF PRESSURE VARIATION ALONG THE BED ON THE EXTENT OF CONVERSION.

It would be instructive to start with a model such as that of Toor and Calderbank[4] or Fryer and Potter[6], which account for a change in bubble size due to hydrodynamics of the fluid bed, and study the effect of stoichiometric coefficient and presence of inerts with these models. However, while there may be differences in detail, the general conclusions arrived at based on the simple KL model are likely to remain valid.

CHAPTER - 6

VERIFICATION OF THE CATALYST DILUTION CONCEPT AND VOLUME CHANGE MODEL: DEHYDRATION OF ETHANOL

6. VERIFICATION OF THE CATALYST DILUTION CONCEPT AND VOLUME CHANGE MODEL : DEHYDRATION OF ETHANOL

The concept of dilution of catalyst has previously been applied to exothermic reactions carried out in tubular reactors packed with catalyst[29,37]. Thus a specific temperature profile can be established in a fixed bed by means of catalyst dilution. Temperature control poses no problems in a fluidized bed as near isothermal conditions is one of the main features of this type of reactor. The drawback in a fluidized bed is the reduced conversion for the same mass of catalyst employed, in relation to a tubular reactor, and also the lower selectivity for complex reactions carried out in this type of reactor.

The concept of catalyst dilution in a fluidized bed has been applied in Chapter 4 to simple and complex first order reaction schemes on the basis of the KL model. Dilution of catalyst is seen to result in an improvement in the efficiency of fluidized contacting. This partially offsets the reduction in rate constant which has now to be based on total solids in the bed. Thus the fluidized bed is relatively insensitive (with respect to overall conversion) to catalyst dilution as compared to fixed bed operation. With total mass of solids in the bed remaining unchanged it has been shown on the

basis of the above model that in certain cases a diluted fluid bed displays an improvement in performance for complex reaction schemes over the corresponding undiluted fluid bed. At very high dilution the selectivity of intermediate approaches that obtainable in the corresponding plug flow reactor, for the same level of conversion.

It is the object of the present work to experimentally verify the above conclusions and the reaction chosen was the dehydration of ethanol to ethylene with diethyl ether formed principally as an intermediate. Experimental runs were conducted in an integral reactor (free of pore diffusion, temperature and external mass transfer effects), undiluted fluid bed reactor and diluted fluid bed reactor. At the temperature of operation (338^{o}C) diethyl ether formation was appreciable and the effect of dilution of catalyst, keeping the residence time in the bed unchanged, on the selectivity of formation of ether and overall conversion of ethanol was obtained and compared with the corresponding integral reactor. For the parameters employed in the fluid bed an optimum catalyst dilution ratio R' was sought to be obtained so that the production of intermediate diethyl ether at the bed exit was maximized.

6.1 REACTION SYSTEM

The reaction employed in the present study is the dehydration of ethanol to ethylene over alumina catalyst, with diethyl ether formed principally as an intermediate. The reaction besides being of industrial importance and finding increasing application in fluidized bed operation, has the additional advantage of being a pseudo first order reaction involving a change in number of moles at higher temperatures (> 360°C) where ether formation is low. Thus the experimental set up was also employed to verify the volume change model proposed in Chapter 5, in experiments at a later stage.

The catalytic dehydration of ethanol on an alumina catalyst was first reported at the end of the Eighteenth century[45]. The first systematic study of ethanol dehydration was done by Ipatieff[46, 47]. Kinetic studies of ethanol dehydration over alumina have been carried out by Clark et al.[48] and Alvarado[49]. The studies of Pease and Yung[50] show that ether formation is in the temperature range of 200-350°C and at higher temperatures ether formation is negligible. A review of the literature shows that the reaction appears to be a stepwise reaction with diethyl ether as an intermediate and the overall reaction appears to be of first order[51-62].

The dehydration of ethanol in a fluidized bed has been the subject of a few studies[21,22,63,64] and the effect of hydrodynamic process parameters on the conversion have been reported by Topchieva and Zenkovich[65-68]. A more detailed description of these studies is presented in Section 6.7.1.

6.2 EXPERIMENTAL ASSEMBLY AND PROCEDURE FOR THE INTEGRAL REACTOR

6.2.1 Integral Reactor Assembly

The apparatus used in the kinetic experiments is shown schematically in Figure 6.1 and a photograph of the assembly is presented in Figure 6.2. The integral reactor employed was provided with a thermocouple well which extended from the top of the reactor to just above the wire mesh support for the catalyst. A metering pump was used for feeding the reactant to the reactor. The capacity of the pump could be varied by adjusting the stroke adjustment micrometer. A direct check on the quantity of ethanol fed to the reactor could also be maintained from the calibrated feed bottle. The s.s. tube containing the catalyst was of 3/4" i.d. and 13" in length. The temperature of the catalyst bed was maintained at the required constant level by careful control of the rate of fluidizing air on the external jacket and electrical power input. A chromel-alumel thermocouple was used for the temperatu

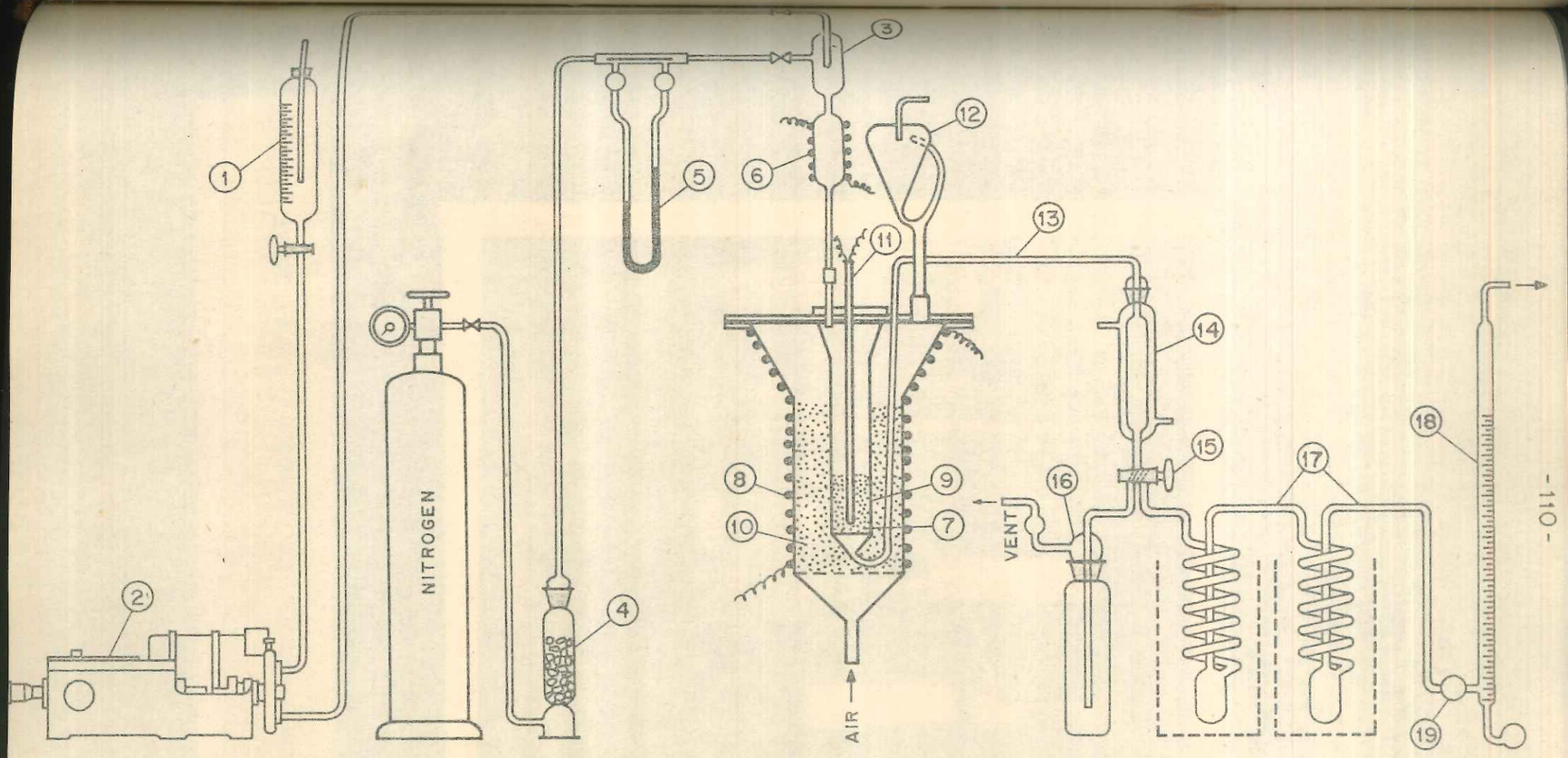

1 CALIBRATED ETHANOL FEED BOTTLE
2 MICRO PUMP
3 FEED INLET
4 SILICA GEL TRAP
5 CAPILLARY FLOW METER
6 PREHEATER
7 CATALYST AND SUPPORT
8 OUTER HEATING JACKET
9 TUBULAR REACTOR
10 FLUIDIZED HEATING BED
11 THERMOWELL
12 CYCLONE
13 PRODUCT OUTLET
14 WATER CONDENSER
15 THREE WAY STOP COCK
16 VENT
17 LOW TEMPERATURE TRAPS
18 SOAP BUBBLE FLOW METER
19 GAS SAMPLER

FIGURE 6·1. EXPERIMENTAL SET-UP (INTEGRAL REACTOR ASSEMBLY)

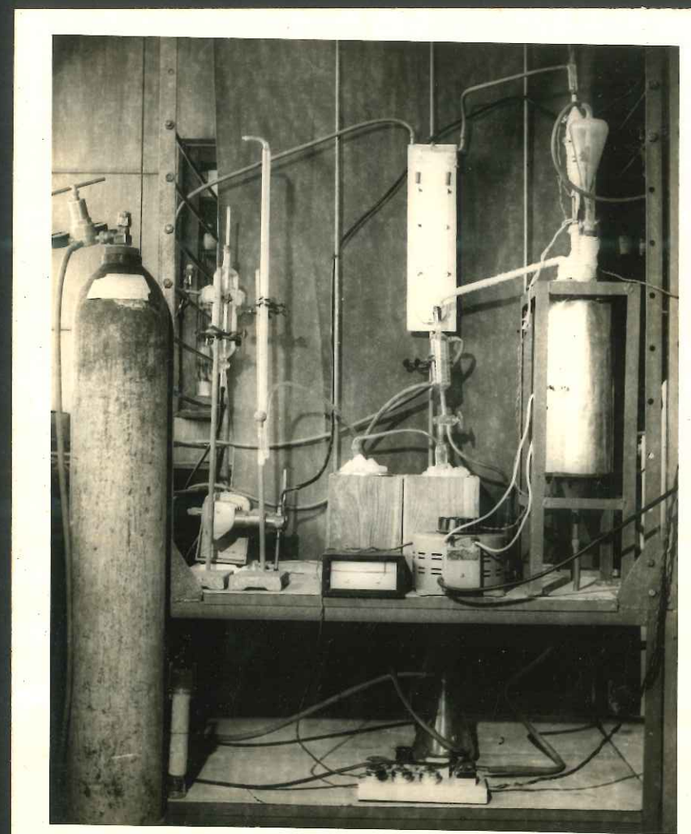

FIGURE 6.2. PHOTOGRAPH OF THE EXPERIMENTAL SET-UP
(INTEGRAL REACTOR ASSEMBLY)

measurement. The thermocouple was calibrated against a thermometer which had a least count of 0.5°C.

6.2.2 Description of Catalyst

The catalyst employed was commercial Flyk alumina (-70 to +80 mesh) supplied by the Associated Cement Companies Ltd., and reported to have a surface area of 240-260 m^2/g and minimum Al_2O_3 content of 99.5%.

6.2.3 Method of operation

The catalyst was maintained at 400°C for 2 hours in a nitrogen atmosphere before use. After attaining the required temperature of operation the catalyst was kept in a nitrogen atmosphere for $\frac{1}{2}$ hour. The first part of the reaction products was discarded while the system was reaching a steady state. Runs were carried out employing different flow rates of the 95.6% w/w ethanol and 4.4% w/w water feed. An electrically heated preheater was employed for the feed. The condensible reaction products were condensed in traps cooled in a calcium chloride-ice mixture and an MK-70 cooling unit in series.

6.2.4 Techniques of Analysis

In the present study an N.C.L.-AIMIL GC MKII Gas

Chromatograph was used. Preliminary analysis was made with pure compounds and synthetic mixtures for determing the peak heights and retention times. The separation of the condensible products was effected on the following column : $\frac{1}{4}$" Ø, 6 ft length 10% Carbowax 1500 on Chromosorb W. The hydrogen carrier gas flow rate was 50 cm^3/min and Injector, Column and T.C.D. temperatures were 130°C, 85°C, and 170°C respectively. Preliminary runs established that these conditions gave the best separation of components. The olefin composition was investigated on a $\frac{1}{4}$" Ø, 12 ft length column of silver nitrate in ethylene glycol, after freezing out the condensible products. The Column and T.C.D. were maintained at room temperature and 90°C respectively. The uncondensed ethylene gas was also measured by means of a soap bubble flow meter.

6.2.5 Elimination of External and Pore Diffusion Effects

Preliminary runs without catalyst exhibited negligible conversion and thus the possibility of homogeneous reaction was precluded. Runs with three different catalyst sizes (-70 to +80, -80 to +100, -100 to +120 mesh) under identical conditions yielded only marginal differences in overall conversion and thus it was established that for the particle size (-70 to +80 mesh) employed in the kinetic runs pore

diffusion effects were not prevalent. The method of Ford and Perlmutter [68] was employed to check the partial pressure gradient $\Delta P/P_g$ and establish that for the runs in the present study $\Delta P/P_g$ was not appreciable, thus showing the absence of external mass transfer effects.

6.3 DATA FROM INTEGRAL REACTOR EXPERIMENTS

The results of the kinetic runs in the integral reactor are presented in Table 6.1 in terms of formation of the principal products diethyl ether and ethylene.

6.4 EXPERIMENTAL SET-UP AND PROCEDURE FOR THE FLUIDIZED BED

6.4.1 Reactor Assembly

The experimental assembly consists of heating the liquid 95.6% w/w ethanol feed to a temperature of 215°C in three stages consisting of preheater, vaporizer and superheater prior to the ethanol vapours entering the fluid bed reactor. The ethanol is fed from a storage vessel by means of a calibrated feed pump into the preheater and vaporizer assembly which are heated by means of Nichrome electrical resistance wiring. The entire assembly is suitably lagged in order to prevent heat losses. Heating control is by means of variacs. The flow of nitrogen gas is maintained over the catalyst prior to ethanol flow to the reactor and is stopped once the

TABLE 6.1

RESULTS OF THE KINETIC RUNS IN THE INTEGRAL REACTOR

Catalyst size = -70 to +80 mesh

Catalyst mass = 12.0 g

Feed = 95.6% w/w ethanol (A) + 4.4% w/w water

Temperature = 330°C

Reading No.	F_{Ao} g mole /hr	W/F_{Ao} g cat-hr/g mole	Moles ether formed/mole of ethanol fed to the reactor	Moles ethylene formed/mole of ethanol fed to the reactor
1.	0.955	12.56	0.20	0.09
2.	0.755	15.90	0.22	0.12
3.	0.666	18.02	0.25	0.15
4.	0.535	22.44	0.26	0.17
5.	0.432	27.78	0.25	0.21
6.	0.327	36.70	0.23	0.27
7.	0.282	42.55	0.21	0.32
8.	0.232	51.72	0.19	0.39

ethanol flow is begun. Thermowells exist in the vaporizer, superheater and fluid bed in order to maintain a constant check on the respective temperatures and thus avoid local superheating. A bypass condenser is fitted at the superheater exit in case it becomes necessary to divert the flow of ethanol from the reactor. A schematic sketch of the assembly has been presented in Figure 6.3 and photograph in Figure 6.4.

The fluidized bed is a 4" Ø 3' in length m.s. reactor heated externally by two electrical resistance circuits for ease of temperature control. A disengaging section and metallic cyclone exist above the reactor in order to prevent elutriation which may be caused by attrition. For the fluidized bed experiments alumina catalyst of the size -70 to + 120 mesh was employed, as for the operating feed flow rates elutriation occurred to a significant extent with finer mesh size of particles.

The thermowell in the reactor has a chromel-alumel thermocouple in a moveable s.s. sheath which can be moved on a pulley so that axial temperatures can be read in the bed and the absence of any axial temperature gradients ensures that the quality of fluidization is good. The reaction products pass through a cooling water condenser and therefrom to low temperature traps employing a calcium chloride-ice mixture and MK-70 cooling unit. Thereafter the noncondensible

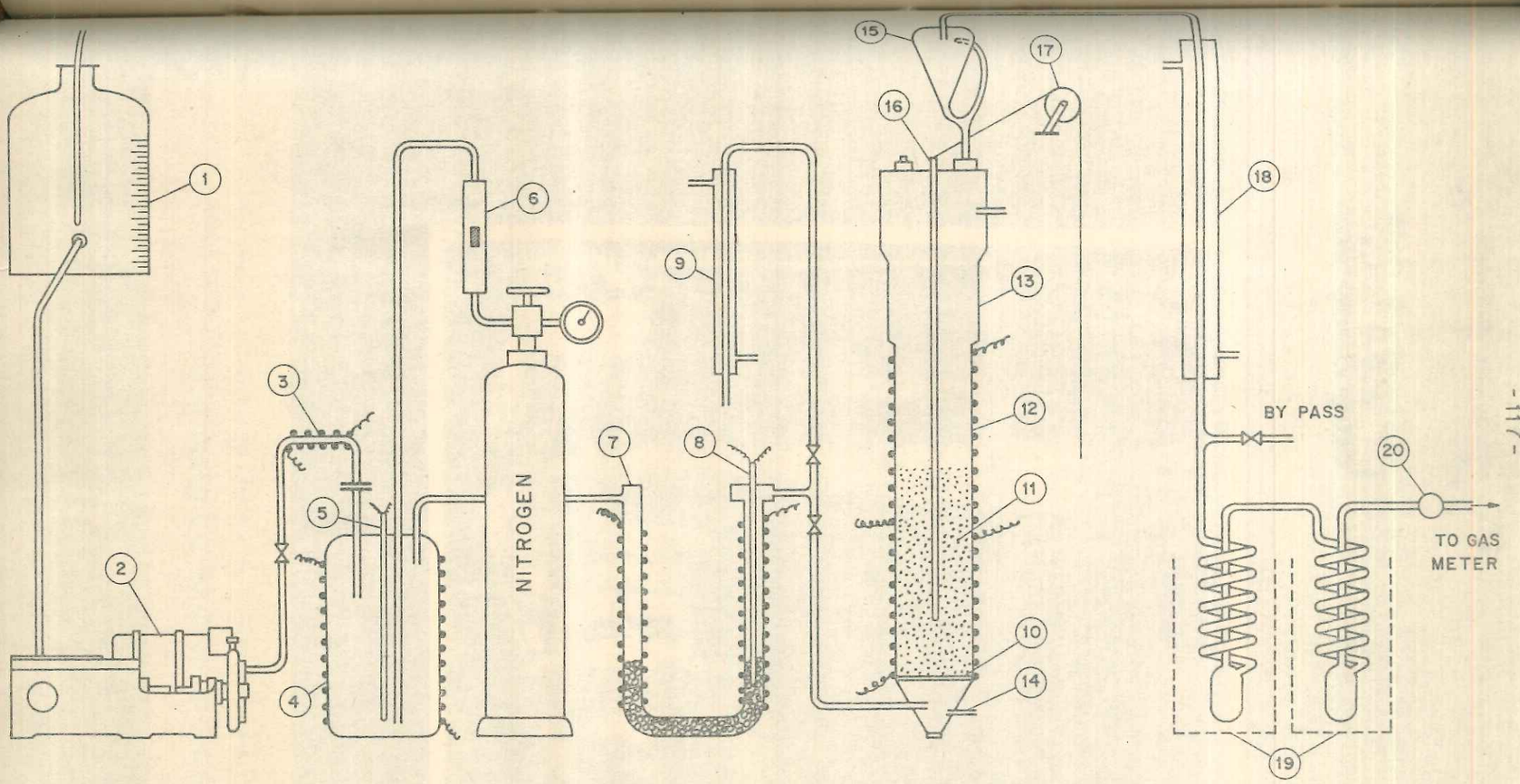

1	CALIBRATED ETHANOL FEED VESSEL	8	SUPERHEATER THERMOWELL	15	CYCLONE
2	PUMP	9	BYPASS CONDENSER	16	THERMOCOUPLE IN MOVEABLE S.S. SHEATH
3	PREHEATER	10	PERFORATED GRID PLATE	17	PULLEY
4	VAPORIZER	11	ALUMINA CATALYST BED	18	CONDENSER
5	THERMOWELL	12	4"ø m.s. FLUID BED REACTOR	19	LOW TEMPERATURE TRAPS
6	GAS ROTAMETER FOR N_2 FEED	13	DISENGAGING SECTION	20	UNCONDENSED GAS SAMPLER
7	SUPERHEATER WITH PACKING	14	PRESSURE TAP		

FIGURE 6·3. EXPERIMENTAL SET-UP (FLUIDIZED BED REACTORS ASSEMBLY).

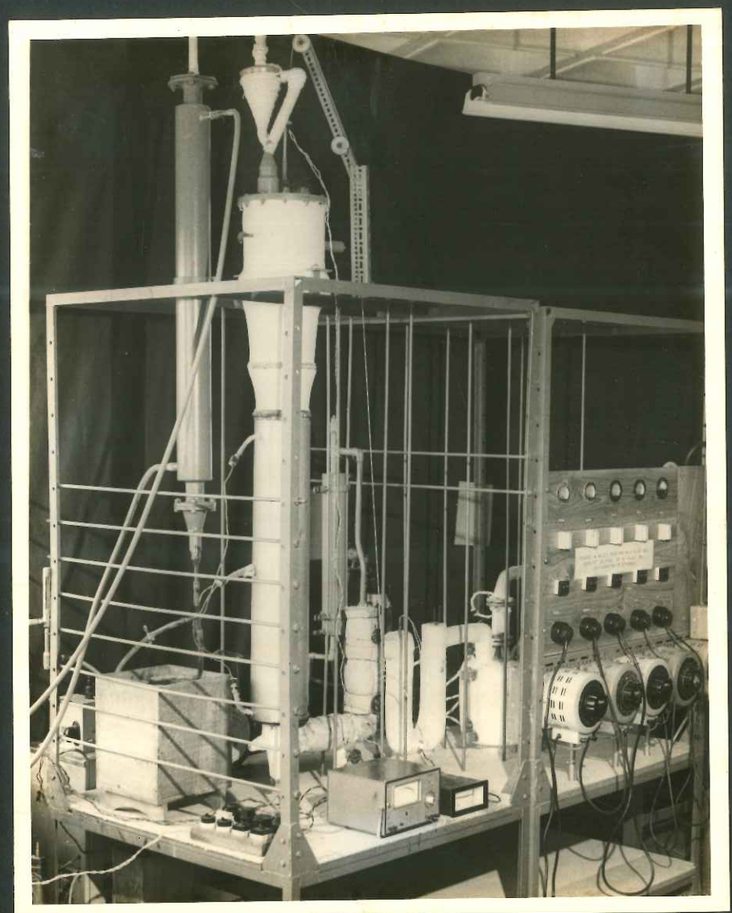

FIGURE 6.4. PHOTOGRAPH OF THE EXPERIMENTAL SET-UP
(FLUIDIZED BED REACTOR ASSEMBLY)

gas is sampled and metered separately.

6.4.2 Method of operation

The method of operation of the reactor is as follows : The catalyst is maintained at 400°C for 2 hours in a nitrogen atmosphere before use. After attaining the required temperature of operation the catalyst is kept in a flow of nitrogen gas for $\frac{1}{2}$ hour. Thereafter the ethanol flow is begun and the flow of nitrogen is stopped. Runs are taken once steady state conditions of temperature and operation have been achieved. The cooling follows a similar pattern.

Initial runs were carried out to adjust the ethanol feed rate so that appreciable elutriation did not occur and the quality of fluidization was good. A feed rate of 1.9 l/hr was fixed upon and kept constant throughout the runs so that the hydrodynamics of the bed remained unaltered in terms of the initial feed rate. A catalyst mass of 2.2 kg was employed in the undiluted bed. The catalyst was commercial Flyk alumina (-70 to +120 mesh) and the catalyst specifications have been presented in Section 6.2.2.

6.4.3 Dilution of the Fluid Bed

A variety of solid inert diluents were tested for bulk density and fluidization characteristics similar to the

alumina catalyst employed, as well as inertness to the reaction. These included pure silicon, sea sand, pumice, silica gel, glass etc. Whereas some of the materials (e.g. pumice, silicon) showed slight activity and were not totally inert at the temperature of operation, others, such as silica gel, possessed a bulk density at great variance with that of the catalyst. Washed and dried glass power (-120 to +200 mesh) was found to be relatively inert and also have a bulk density (ρ_g = 1.10g/cm^3) in closer agreement with alumina (ρ_a= 0.94 g/cm^3) than some of the other inerts. In order to eliminate segregation of catalyst and inert in the bed, glass powder of a finer size (-120 to +200 mesh) was employed as inert along with the alumina catalyst in the fluid bed. The small difference in bulk densities was compensated for by keeping the residence time in the bed unchanged. Thus, in the case of the undiluted bed

$$t = \frac{W}{v_o \rho_a} \qquad (6.1)$$

In the case of the diluted bed, a weighted mean of the bulk densities ρ_a and ρ_g was considered in the denominator of Equation (6.1) and thus the total mass of solids in the bed was taken such that the residence time t was unaltered with dilution of catalyst in the bed.

The catalyst dilution ration R' was considered to be

$$R' = \frac{\text{mass of catalyst in the undiluted bed}}{\text{mass of catalyst in the diluted bed}} \qquad (6.2)$$

and runs were taken employing different catalyst dilution ratios and maintaining the temperature in the fluidized bed at 338°C.

6.5 RESULTS OF EXPERIMENTAL RUNS IN THE FLUIDIZED BED

The results of the experimental runs have been given in Table 6.2.

6.6 DISCUSSION OF RESULTS

The experimental results obtained in the integral reactor are plotted in Figure 6.5 in terms of the moles of principal products ether and ethylene formed per mole of ethanol fed to the reactor, as a function of the time factor W/F_{Ao}. Figure 6.6 then shows a modified comparative selectivity-conversion plot for formation of the intermediate diethyl ether for the integral and fluid bed reactors. The integral reactor corresponds to plug flow conditions and hence at any given level of conversion the corresponding selectivity of ether formation will always be higher than for the fluid bed. Here selectivity of ether formation is represented in terms of moles of

TABLE 6.2

RESULTS OF THE UNDILUTED AND DILUTED FLUID BED RUNS

Catalyst size = -70 to +120 mesh

Catalyst mass for undiluted bed = 2200 g

Feed = 95.6% w/w ethanol + 4.4% w/w water

Temperature = 338°C

Reading No.	Ethanol feed l/hr	Catalyst dilution ratio R'	Moles converted to ether/mole of ethanol fed to the reactor	Mole ethylene formed/mole of ethanol fed to the reactor
1.	1.9	1.0	0.07	0.61
2.	1.9	1.40	0.09	0.53
3.	1.9	1.83	0.10	0.46
4.	1.9	2.20	0.12	0.40
5.	1.9	2.51	0.13	0.35
6.	1.9	3.03	0.15	0.27
7.	1.9	3.67	0.16	0.22
8.	1.9	4.19	0.15	0.20
9.	1.9	4.63	0.14	0.18

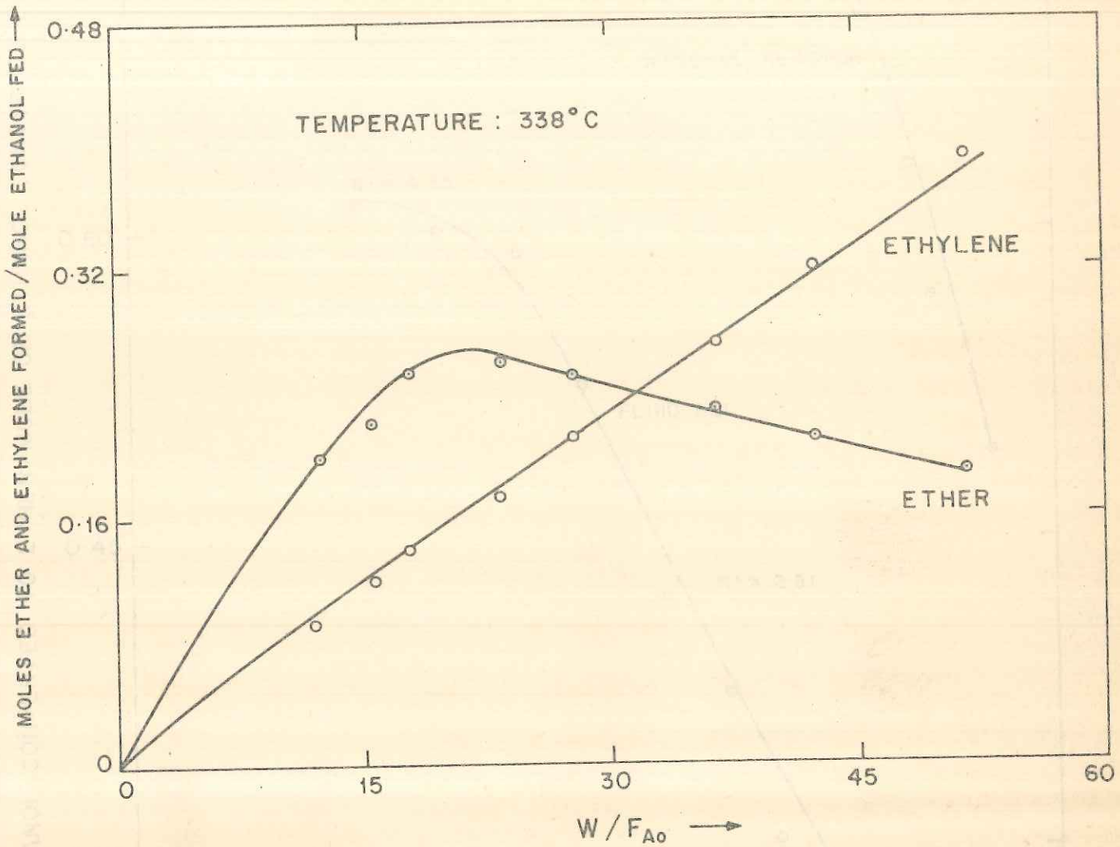

FIGURE 6·5. CONVERSION OF ETHANOL TO ETHYLENE AND ETHER IN THE INTEGRAL REACTOR.

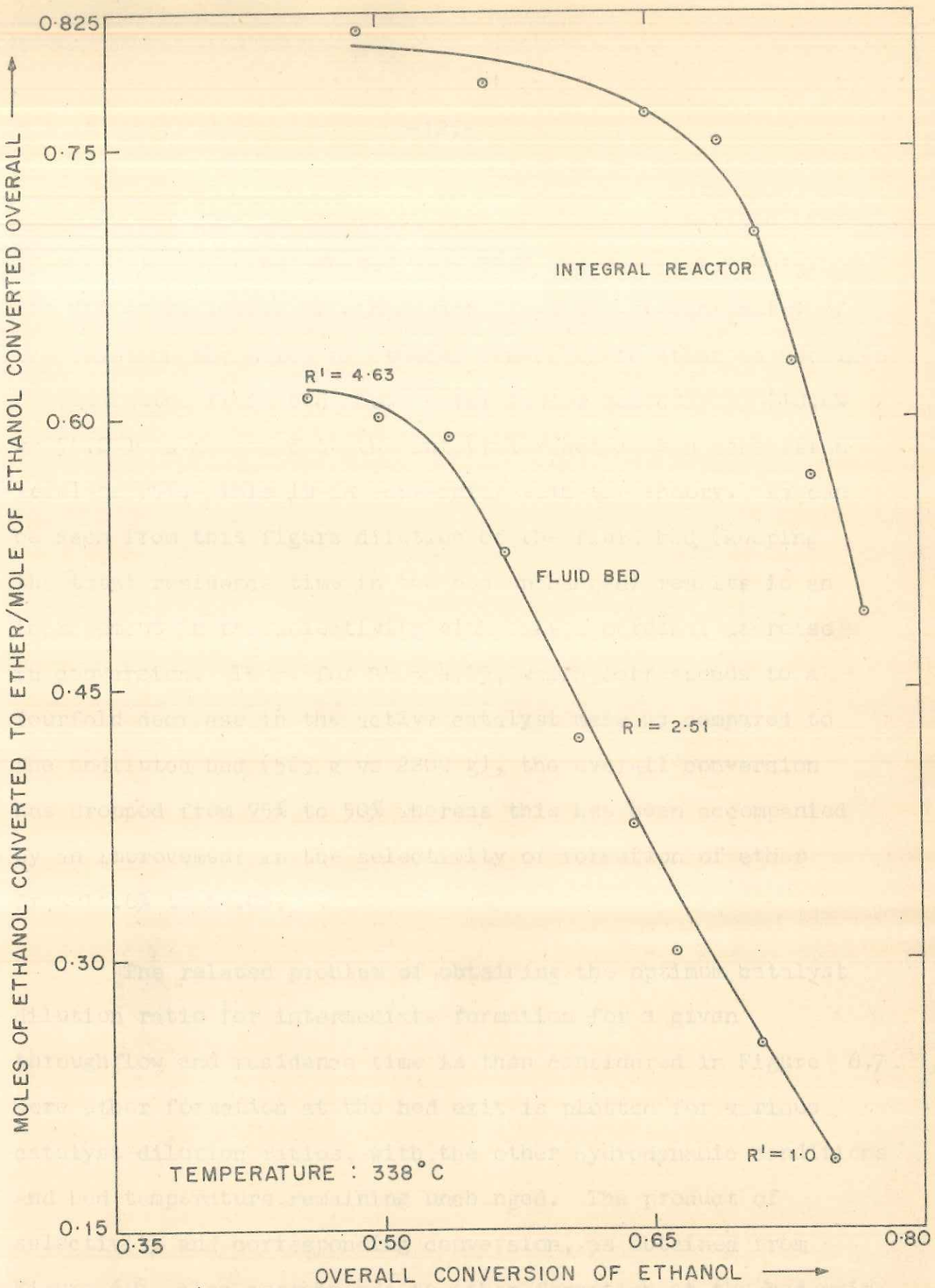

FIGURE 6·6. SELECTIVITY OF ETHANOL CONVERSION TO ETHER-OVERALL ETHANOL CONVERSION PLOTS FOR THE INTEGRAL REACTOR, UNDILUTED AND DILUTED FLUID BEDS.

ethanol converted to ether per mole of ethanol converted overall. As the moles of ether formed have been experimentally obtained for different levels of conversion, from the stoichiometry of the reaction the moles of ethanol converted to ether is obtained. The undiluted fluid bed shows a far lesser selectivity (18.6% vs 54.0%) as compared to the integral reactor at a conversion level of 75%. This is in conformity with the theory. As can be seen from this figure dilution of the fluid bed (keeping the total residence time in the bed unchanged) results in an improvement in the selectivity with only a marginal decrease in conversion. Thus, for R' = 4.19, which corresponds to a fourfold decrease in the active catalyst mass as compared to the undiluted bed (525 g vs 2200 g), the overall conversion has dropped from 75% to 50% whereas this has been accompanied by an improvement in the selectivity of formation of ether from 18.6% to 60.0%.

The related problem of obtaining the optimum catalyst dilution ratio for intermediate formation for a given throughflow and residence time is then considered in Figure 6.7. Here ether formation at the bed exit is plotted for various catalyst dilution ratios, with the other hydrodynamic conditions and bed temperature remaining unchanged. The product of selectivity and corresponding conversion, as obtained from Figure 6.6, also corresponds to ether formation at the bed exit.

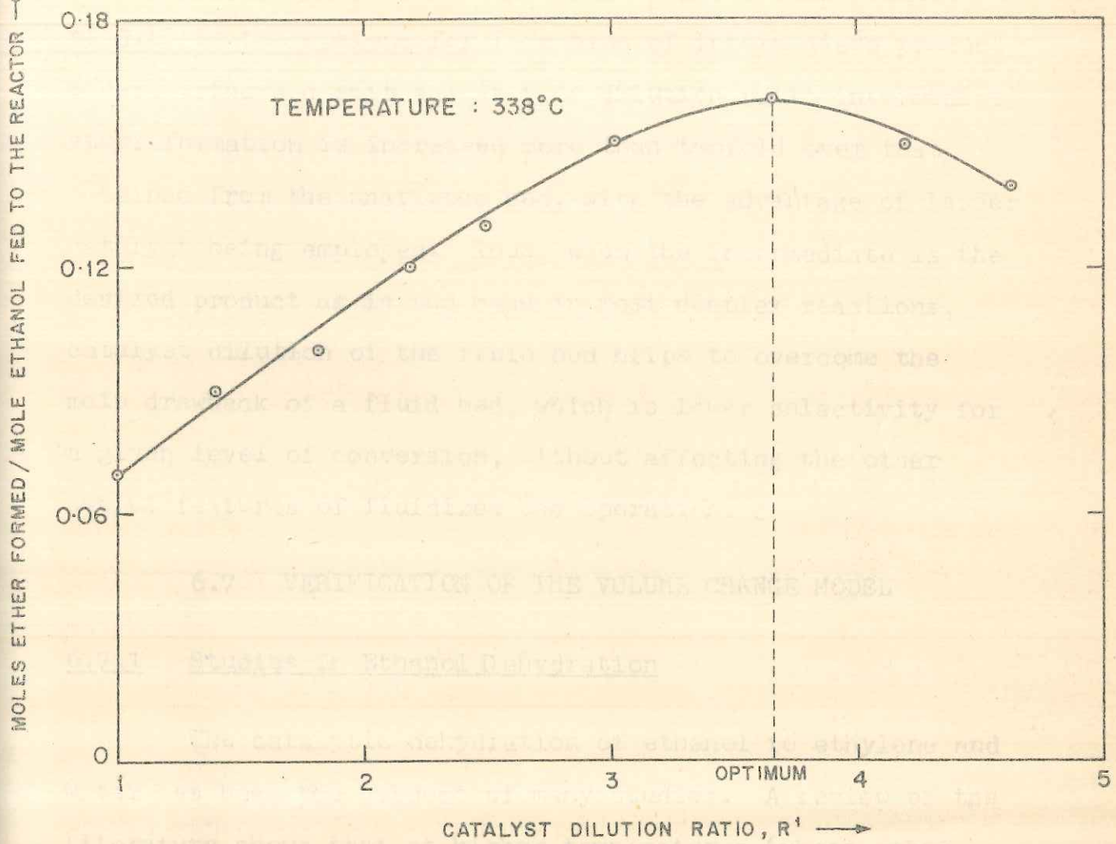

FIGURE 6·7. EFFECT OF CATALYST DILUTION ON INTERMEDIATE ETHER FORMATION AT BED EXIT.

From the figure it is seen that a catalyst dilution ratio of 3.67 is the optimum for formation of intermediate product ether at the bed exit and at this dilution ratio intermediate ether formation is increased more than twofold over that obtained from the undiluted bed, with the advantage of lesser catalyst being employed. Thus, when the intermediate is the desired product as is the case in most complex reactions, catalyst dilution of the fluid bed helps to overcome the main drawback of a fluid bed, which is lower selectivity for a given level of conversion, without affecting the other useful features of fluidized bed operation.

6.7 VERIFICATION OF THE VOLUME CHANGE MODEL

6.7.1 Studies in Ethanol Dehydration

The catalytic dehydration of ethanol to ethylene and water has been the subject of many studies. A review of the literature shows that at higher temperatures (where ether formation is not substantial) the reaction can be represented by pseudo first order kinetics. Antipina and Frost [69-71] have proposed a pseudo first order rate equation for the reaction and the experimental results of Roy and Bose[72,73] conform to this rate equation. The reaction is also one in which a single mole of reactant gives two moles of products, and is hence a reaction involving a change in number of moles.

The dehydration of ethanol to ethylene in a fluidized bed has been the subject of a few studies. Bleloch[22] has given a detailed description of an industrial process in which ethylene was produced by introducing ethanol vapours at circa 220°C into a reaction chamber heated by low frequency induction heating. The catalyst used was alumina of a size range from -1" to -240 mesh and the bed temperature was varied from 330-380°C. From the description of the process it appears that the top part of the bed was in a fluidized condition. The use of bauxite in a fluid bed has also been reported for ethanol dehydration by Wu Lian Yuan[63] and Deshpande et al.[64] The latter process employes a height to diameter ratio not exceeding 6:1 and the catalyst bed is heated by means of electric resistors fitted on the outside of the reactor. The temperature of the fluidized bed is in the range 370-380°C. Recently a series of papers by Topchieva and Zenkovich[65-67] have considered the above dehydration reaction in a fluidized bed and the effect of hydrodynamic process parameters on the conversion thereof. A new fluidized bed process described by Winter and Eng[21] shows that a higher ethylene yield can be obtained therefrom as compared with a fixed bed system. High yields are accomplished by means of close temperature control in the fluid bed as well as by keeping catalyst at high activity at all times. This is accomplished by circulating

the catalyst through a regenerator and by replacing catalyst losses due to attrition and consequent elutriation.

6.7.2 Scope of Present Work

The reaction

$$C_2H_5OH \rightarrow C_2H_4 + H_2O \qquad (6.1)$$

is a reaction in which a change in number of moles occurs. The reaction also has relevance to fluid beds due to its endothermic nature. As a preliminary study kinetic runs free from pore diffusion, temperature and external mass transfer effects were carried out at 375°C in an integral reactor in order to ascertain the applicability of a first order kinetic equation for the specific operating parameters and catalyst employed, as a step to modelling of the fluid bed. Runs were conducted in the fluid bed with varying amounts of inert nitrogen with the 95.6% ethanol feed. It was our purpose to compare observed conversions in the fluidized bed on the basis of the KL model, as also the volume change model outlined in Chapter 5, which takes into account the change in number of moles due to reaction and the presence of inerts in the bed.

6.7.3 Integral Reactor Set up and Method of Operation

The apparatus used in the kinetic experiments has been shown schematically in Figure 6.1 and a description of the apparatus has been presented in Section 6.2. The integral reactor experiments were carried out at 375°C at which temperature, for high values of the time factor W/F_{Ao}, ethylene formation is the predominant reaction. The method of operation of the reactor has been described in Section 6.2.3. Experiments were carried out using varying flow rates of the 95.6% w/w ethanol + 4.4% w/w water feed and separate runs were also conducted with nitrogen gas flow as inert. The nitrogen gas flow rate was measured by means of a calibrated capillary flow meter. The method of analysis of the condensible products and uncondensed gases remained the same as that employed in the experiments at the lower temperature of 338°C. Runs were conducted with varying amounts of nitrogen gas as inert in order to determine the effect that the introduction of nitrogen gas had on the reaction rate.

6.7.4 Elimination of External and Pore Diffusion Effects

Preliminary runs without catalyst exhibited negligible conversion and thus the possibility of homogeneous reaction was precluded. Runs with three different catalyst sizes (-70 to + 80 mesh, -80 to + 100 mesh, -100 to + 120 mesh)

under identical conditions yielded only marginal differences in conversion and thus it was established that for the particle size (-70 to + 80 mesh) employed in the kinetic runs pore diffusion effects were not prevalent.

The external mass transfer effect was evaluated by the method of Ford and Perlmutter[68] who equated the rate of mass transfer and chemical reaction under steady state conditions and derived the equation

$$\frac{\Delta P}{P_g} = \frac{d \ln r'/d \ln G}{b} \qquad (6.3)$$

where b equals 0.59 for $N'_{Re} > 350$ and 0.49 for $N'_{Re} < 350$. In the present study $N'_{Re} < 350$ and hence b equals 0.49. The rate (r) calculated in the present study has the units of g mole/hr-g cat., and is converted into the dimensions of r' in Equation (6.3) by multiplying by the molecular weight of the feed, the particle density and radius of the catalyst particles.

Plots in ln r' vs ln G (where G is the total mass flow rate) show that for the flow rates employed for the kinetic runs, the value of $\Delta P/P_g$ approaches zero, thus showing the absence of external mass transfer effects. The kinetic runs taken thus give the intrinsic kinetics of the reaction, free from the limitations of external and pore diffusion effects.

6.8 RESULTS OF THE INTEGRAL REACTOR EXPERIMENTS

The data from the experiments in the integral reactor runs are presented in Tables 6.3 and 6.4. Table 6.3 presents the data for 95.6% ethanol feed. For lower values of the time factor W/F_{Ao}, there is a drop in conversion and an attendant increase in the level of ether formation. The runs with substantial ether formation are not considered for fitting the rate equation.

Runs are also carried out with nitrogen flow as inert and the effect on conversion of ethanol is presented in Table 6.4. Here the initial value of time factor W/F_{Ao} employed is high, so that ether formation is not of a significant level in these runs.

6.8.1 Interpretation of Kinetic Data

Several workers[58,74] have already presented detailed kinetic models of the reaction based on Langmuir-Hinshelwood kinetics. It was the objective of the present work to study the ethanol dehydration reaction in a fluidized bed and for this purpose experimental runs free of external and pore diffusion were carried out in an integral reactor and a pseudo first order equation was tested for a reasonable fit to the kinetic data obtained. The adsorption parameters K_A and K_W

TABLE 6.3

RESULTS OF KINETIC RUNS IN THE INTEGRAL REACTOR

Catalyst size = -70 to +80 mesh

Catalyst mass = 12.0 g

Feed = 95.6% w/w ethanol (A) + 4.4% w/w water

Temperature = 375°C

Reading No.	F_{Ao} g mole /hr	W/F_{Ao} g cat-hr/ g mole	Moles converted to ethylene(and ether)/mole of ethanol fed to the reactor	Moles ether formed/mole of ethanol fed to the reactor
1.	0.201	59.70	0.88	-
2.	0.232	51.72	0.84	0.01
3.	0.257	46.69	0.83	0.01
4.	0.282	42.55	0.78	0.01
5.	0.327	36.70	0.76	0.02
6.	0.379	31.66	0.75	0.04
7.	0.432	27.78	0.74	0.05
8.	0.535	22.44	0.72	0.08

TABLE 6.4

RESULTS OF KINETIC RUNS IN THE INTEGRAL REACTOR
(WITH NITROGEN FLOW)

Catalyst size = -70 to +80 mesh

Catalyst mass = 12.0 g

Feed = 95.6% w/w ethanol (A) + 4.4% w/w water + inert nitrogen

Temperature = 375°C

Reading No.	Nitrogen flow rate ml/min	F_{Ao} g mole/hr	F_{Ao} g cat-hr/ g mole	Fractional conversion at bed exit
1.	12	0.232	51.72	0.81
2.	25	0.232	51.72	0.79
3.	40	0.232	51.72	0.78
4.	55	0.232	51.72	0.76
5.	65	0.232	51.72	0.75
6.	75	0.232	51.72	0.73

for ethanol and water respectively (which decrease with increasing temperature) were incorporated in the kinetic rate constant k to provide an effective value for use in fitting the experimental data.

For the range of inlet concentrations and conversions studied at the temperature 375°C in the integral reactor, a pseudo first order equation of the type

$$\frac{k\, C_{Ao} W}{F_{Ao}} = (1+x_o) \ln \left(\frac{1}{1-X_A} \right) - x_o \cdot X_A \qquad (6.4)$$

was found to give a reasonable fit to the data. It may be emphasized here that the above equation is applicable only in a limited range of parameters studied.

6.9 EXPERIMENTAL SET UP FOR THE FLUIDIZED BED

The experimental assembly has been described earlier in Section 6.4.1 and a schematic sketch of the assembly is presented in Figure 6.3. The catalyst employed is Flyk alumina (-70 to + 120 mesh) and the catalyst mass in the bed is kept constant at 1900 g. throughout the fluid bed runs. The temperature in the fluid bed is maintained at 375°C as measured by the moveable thermocouple in the bed. Heating control is by means of variacs. The method of operation also follows a similar pattern (as described in Section 6.4.2)

except that when the flow of ethanol is begun the nitrogen flow is adjusted to the required level. Although the integral reactor experiments show formation of ether at lower conversion levels (corresponding to lower values of the time factor W/F_{Ao}), the experiments in the fluidized bed show that ether formation at 375°C is negligible in the fluid bed even at these corresponding lower conversion levels. This is in consonance with the theory as ether is formed primarily as an intermediate product and hence formation of ether in a fixed bed integral reactor is more substantial as compared to a fluid bed reactor, for the same conversion level.

Runs are conducted with increasing amounts of nitrogen in the feed stream to the fluid bed and correspondingly decreasing amounts of ethanol feed. The consequence of increasing the nitrogen inert flow rate is to mute the volume change effect. The total inlet flow rate to the bed is however kept constant for all the runs.

6.10 RESULTS OF EXPERIMENTAL RUNS IN THE FLUIDIZED BED

The data from the experimental runs in the fluidized bed reactor at a bed temperature of 375°C are presented in Table 6.5.

TABLE 6.5

RESULTS OF EXPERIMENTAL RUNS IN THE FLUIDIZED BED REACTOR

Catalyst size = -70 to +120 mesh

Catalyst mass = 1900 g

Feed = 95.6% w/w ethanol (A) + 4.4% w/w water + inert nitrogen

Temperature = 375°C

Reading No.	Ethanol flow rate, l/hr	Nitrogen flow rate (at 27°C) l/min	Total inlet flow rate at bed temp., g mole/hr	Fractional conversion at bed exit
1.	1.9	-	35.65	0.75
2.	1.7	1.5	35.56	0.77
3.	1.6	2.25	35.50	0.77
4.	1.5	3.10	35.70	0.78
5.	1.4	3.80	35.53	0.79
6.	1.3	4.60	35.60	0.79
7.	1.15	5.80	35.72	0.81

6.11 DISCUSSION OF RESULTS

The results of the experimental runs have been plotted in Figure 6.8 in terms of the fractional conversion of ethanol at the bed exit vs the mole percent of inerts in the bed. With decreasing flow of inerts in the bed (keeping total inlet flow rate constant) the effect of volume change is enhanced and this leads to a change in the conversion of ethanol at the bed exit. Water is included as an inert with nitrogen for the purpose of calculating the mole percent inerts in the feed stream.

Reading no. 7 of Table 6.5, with large flow of inert nitrogen, has been chosen as the basis on which the values of fluidized bed rate constant are obtained for the volume change model and the KL model. For the KL model this reading corresponds to conditions where the effect of change in number of moles is least perceptible. Subsequently, on the basis of these models the results have been extrapolated to the runs with decreasing nitrogen flow. The interesting conclusion obtained from this figure is that for the KL model ($\beta = 1$) the model prediction is that irrespective of the inlet concentration of the species A, the outlet conversion remains unchanged for the same residence time. Thus dilution of the feed stream with inert has an effect on the inlet and outlet concentrations but the ratio of the difference in these concentrations relative to the inlet concentration is unchanged

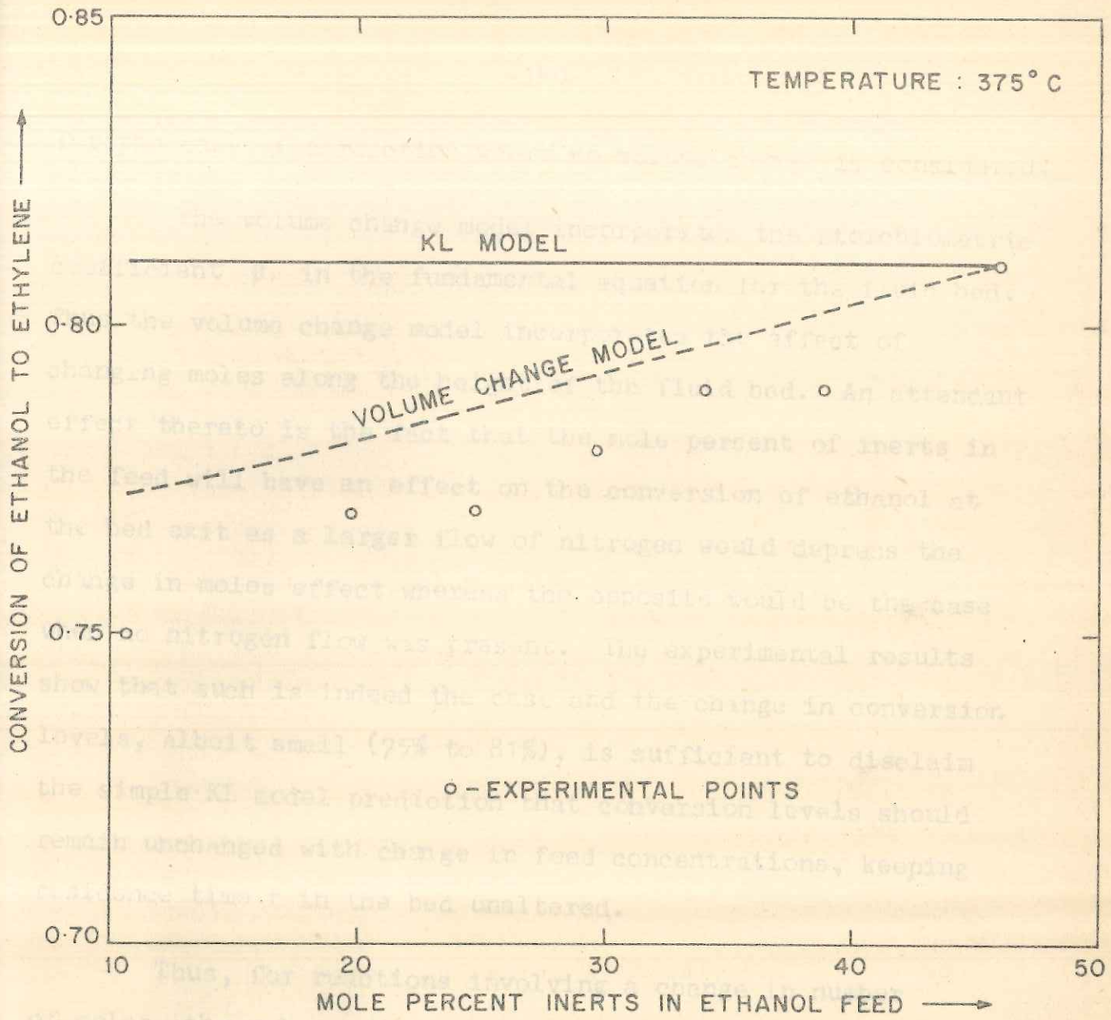

FIGURE 6·8 . COMPARISON OF EXPERIMENTAL RESULTS WITH KL AND VOLUME CHANGE MODEL PREDICTIONS.

for the case of a reaction where no volume change is considered.

The volume change model incorporates the stoichiometric coefficient β in the fundamental equation for the fluid bed. Thus the volume change model incorporates the effect of changing moles along the height of the fluid bed. An attendant effect thereto is the fact that the mole percent of inerts in the feed will have an effect on the conversion of ethanol at the bed exit as a larger flow of nitrogen would depress the change in moles effect whereas the opposite would be the case when no nitrogen flow was present. The experimental results show that such is indeed the case and the change in conversion levels, albeit small (75% to 81%), is sufficient to disclaim the simple KL model prediction that conversion levels should remain unchanged with change in feed concentrations, keeping residence time t in the bed unaltered.

Thus, for reactions involving a change in number of moles, the volume change model is seen to provide a better fit for simulation and extrapolation of data as compared to the KL model.

CHAPTER - 7

CONCLUSIONS

7. CONCLUSIONS

The models presented in the literature simulate the fluid bed reactor performance at different levels of complexity. Thus the models of Kunii and Levenspiel[2,3] and Kobayashi et al.[12] employ the concept of a single average bubble diameter whereas those of Fryer and Potter[6] and Kato and Wen[7] consider bubble coalescence in the bed. The various models are, however, primarily concerned with simple first order reactions and only a few extensions to complex reaction systems have been presented.

Industrial reactions taking place in fluidized beds are mainly complex in nature as evidenced by the production of phthalic anhydride from naphthalene or o-xylene, synthesis of acrylonitrile, ethylene by ethanol dehydration, chloromethanes, chlorofluoromethanes, high density polyethylene, per- and trichloroethylene etc. In a majority of these reactions the intermediate is the desired product and thus selectivity of intermediate formation is an important consideration.

In the present study the KL model was taken as a representative model for the fluidized bed. As a first step towards the analysis of complex reactions in a fluidized bed the KL model was extended to complex first order reversible

and irreversible reaction schemes of the type

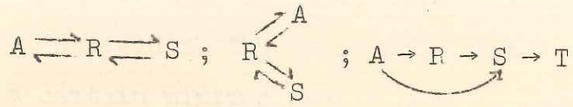

$$A \rightleftharpoons R \rightleftharpoons S \quad ; \quad R \begin{matrix} \nearrow A \\ \searrow S \end{matrix} \quad ; \quad A \rightarrow R \rightarrow S \rightarrow T \qquad (7.1)$$

and the performance equations thereof were obtained. The performance equations obtained for the fluidized bed were in analogy with the corresponding equations for a plug flow reactor, with the rate constants being replaced by effective rate constants which incorporate the independent mass transfer and resistance steps in the fluid bed. These reaction schemes, together with the special cases thereof, serve to present a comprehensive picture for simulation of the various commonly encountered complex reaction schemes that can be analyzed by the KL model. On the basis of these performance equations the conversion and product distribution in the bed were obtained along with the effect of bubble diameter and gas residence time thereon. An analysis of the performance equations obtained indicated that in the case of a fluid bed reactor the extent of $\bar{C}_{R,max}$ as well as its very presence could be controlled simply by changing the effective bubble diameter in the bed. A larger bubble diameter corresponds to a greater deviation from the ideality of plug flow conditions and thus a decrease in $\bar{C}_{R,max}$ attainable occurred with increase in the bubble diameter.

Whereas the desirability of operating the fluid bed with smaller bubble diameters is not in doubt, this often has to yield to the constraint that in industrial systems a certain minimum bubble size is involved. The ensuing analysis dealt with the interaction between gas residence time t, d_b and $\bar{C}_{R,max}$ and a technique was evolved for optimizing the production of intermediate at the bed exit for a given gas residence time or bubble diameter. For a zero first order reaction of the type

$$A \xrightarrow[\text{zero order}]{} R \xrightarrow[\text{first order}]{} S \qquad (7.2)$$

it was seen that d_b had no effect on t_{cr} at which $\bar{C}_{R,max}$ occurred, and thus the optimization of the system involved only two parameters $\bar{C}_{R,max}$ and d_b as the axes of the plot.

However, for the first first order system

$$A \xrightarrow[\text{first order}]{} R \xrightarrow[\text{first order}]{} S \qquad (7.3)$$

$\bar{C}_{R,max}$, d_b and residence time t in the bed were interrelated and thus recourse had to be taken to a three dimensional plot having these three parameters as the axes in order to optimize the production of intermediate R at the bed exit.

The related problem of selectivity of intermediate formation in fluidized beds was next considered. The conventional fluid bed is beset with the problem of lower selectivity of intermediate formation at any given conversion level for complex first order reactions, as compared to a fixed bed reactor. Catalyst dilution has been employed in fixed bed reactors as a means of affording temperature control in the bed. Dilution of catalyst in a fluid bed was shown in the present study to lead to an improvement in the efficiency E of fluidized contacting. On the basis of the performance equations developed for successive reaction schemes it was shown for a representative successive reaction of the type

$$A \xrightarrow{k_1} R \xrightarrow{k_3} S, \quad k_1 > k_3 \qquad (7.4)$$

that dilution of catalyst in a fluidized bed keeping the total mass of solids (and hence gas residence time), and other parameters unchanged, resulted in an increase in the selectivity of intermediate formation without a major loss in conversion. This was due to the fact that the fluidized bed was relatively insensitive (with respect to overall conversion) to dilution of catalyst. The contacting efficiencies of the two reaction steps were also modified to different extents and hence the ratio of the effective rate constants K_1/K_3 for the fluid bed was modified to

different extents with catalyst dilution. Thus overall production of intermediate could often be increased by employing catalyst dilution and in the limiting case of infinite dilution $\bar{C}_{R,max}$ attainable in the bed would correspond to that obtained in a plug flow reactor for the given reaction. Thus dilution of catalyst afforded a means in certain cases to overcome the main drawback of a fluid bed reactor.

Many industrially important reactions involve a change in number of moles. The conversion predicting equations hitherto arrived at for simple first order systems are inapplicable in this situation. A generalized model for the fluid bed incorporating this volume change effect along the height of the bed is yet to be presented, and based on the assumptions of the KL model a generalized model was developed which incorporated the stoichiometric coefficient β for a reaction of the type

$$A \rightarrow \beta R \qquad (7.5)$$

together with the effect of inerts in the feed stream by an equation of the type

$$\frac{-u_b}{K.L_f}\left(\frac{\beta N_{Ao}+N_j}{N_{Ao}+N_j}\right)\left[\frac{(1-\beta)(y_A-y_{Ao})}{[1-(1-\beta)y_A][1-(1-\beta)y_{Ao}]}+\ln\frac{y_A[1-(1-\beta)y_{Ao}]}{y_{Ao}[1-(1-\beta)y_A]}\right]=z \qquad (7.1)$$

Pressure variation along the bed height was also incorporated in the analysis and as this did not have any appreciable effect on the predictions of the model it could be excluded from the general equation developed. The effect of inerts in the inlet stream was to reduce the effect that the stoichiometric coefficient of volume change β had on the conversion at the bed exit. For $\beta < 1$ the conversion was always higher in the fluid bed than that which would be obtained if the reaction were considered with no attendant volume change, and for $\beta > 1$ the opposite was the case.

On the basis of the above studies an experimental verification of the volume change model and the concept of catalyst dilution was carried out. The reaction chosen was ethanol dehydration to diethyl ether and ethylene. The reaction has the advantage of being a complex reaction at lower temperatures and at higher temperatures intermediate ether formation is substantially lower so that the reaction involves a change in moles. Kinetic studies free of pore

diffusion and external mass transfer effects were carried out in an integral reactor over commercial Flyk alumina catalyst with 95.6% ethanol and nitrogen as the feed and the data on product formation were obtained at a lower (338°C) and higher (375°C) temperature. A pseudo first order equation was fitted to the data at 375°C. A 4" ø fluidized bed reactor was utilized for the dehydration reaction to verify the concept of dilution and the volume change model. Runs were carried out at 375°C with 95.6% ethanol and varying amounts of nitrogen as inert, keeping the total number of moles entering the reactor constant. On the basis of the run with largest flow of inert nitrogen (so that the volume change effect is muted) the predictions of the KL and volume change model were extrapolated to the runs with larger ethanol flow rate. The experimental results showed a change in conversion levels with changing quantity of inert nitrogen in the feed stream. This change in conversion levels with an increasing quantity of inert in the feed, albeit small (75% to 81%), was in line with the predictions of the volume change model.

Runs were also carried out in the fluidized bed at 338°C where ether formation is prevalent. Glass powder was employed as the inert diluent. The catalyst dilution

ratio was varied while keeping the residence time in the bed unchanged. At this given temperature of operation a comparison of the data obtained from the integral reactor and the fluid bed was made. At any level of conversion the selectivity of intermediate ether formation was always higher in the integral reactor as compared to that in the fluid bed reactor at the same conversion level. An optimum catalyst dilution ratio R' = 3.67 (R' - mass of catalyst in the bed undiluted bed/mass of catalyst in the diluted bed) was seen to exist at which the ether production at the bed exit was maximized for the operating conditions employed. At the optimum catalyst dilution ratio the production of intermediate ether was seen to increase more than two fold (7% to 16%) over that observed for the undiluted bed. Thus the theoretical predictions of the effect of catalyst dilution were experimentally verified.

LITERATURE CITED

LITERATURE CITED

1. Davidson, J.F. and Harrison, D. : 'Fluidized Particles', Cambridge University Press, New York, N.Y. (1963).

2. Kunii, D. and Levenspiel, O. : 'Bubbling Bed Model. Model for the Gas Flow through a Fluidized Bed', Ind.Eng.Chem.Fundam., 7, 446 (1968).

3. Kunii, D. and Levenspiel, O. : 'Bubbling Bed Model for Kinetic Processes in Fluidized Beds. Gas-Solid Mass and Heat Transfer and Catalytic Reactions', Ind.Eng.Chem.Process Des.Dev., 7, 481(1968).

4. Toor, F.D. and Calderbank, P.U. : 'Reaction Kinetics in Gas Fluidized Catalyst Beds. Mathematical Models' in 'Proceedings International Symposium on Fluidization', Netherlands University Press, Amsterdam, pp. 373-392 (1967).

5. Davidson, J.F. : 'Symposium on Fluidization - Discussion', Trans.Inst.Chem.Engrs., 39, 230 (1961).

6. Fryer, C. and Potter, O.E. : 'Bubble Size Variation in Two Phase Models of Fluidized Bed Reactors', Powder Technol., 6, 317 (1972); cf. CA, 78 : 18276 q (1973).

7. Kato, K. and Wen, C.Y. : 'Bubble Assemblage Model for Fluidized Bed Catalytic Reactors', Chem.Eng. Sci., 24, 1351 (1969).

8. Mori, S. and Wen, C.Y. : 'Simulation of Fluidized Bed Reactor Performance by a Modified Bubble Assemblage Model' in 'Fluidization Technology', Ed. Keairns, D.L., Vol.1, Hemisphere Pub.Corp., Washington, pp. 179-203 (1976).

9. Partridge, B.A. and Rowe, P.N. : 'Chemical Reaction in a Bubbling Gas Fluidized Bed','Analysis of Gas Flow in a Bubbling Fluidized Bed when Cloud Formation Occurs', Trans.Inst.Chem.Engrs., 44, T335,T349 (1966).

10. Mori, S. and Muchi, I. : 'Theoretical Analysis of Catalytic Reaction in Fluidized Bed', J.Chem.Eng.Japan, 5, 251 (1972).

11. Orcutt, J.C., Davidson, J.F. and Pigford, R.L. : 'Reaction Time Distributions in Fluidized Catalytic Reactors', Chem.Eng.Prog.Symp.Ser., 58 (38), 1(1962).

12. Kobayashi, H., Arai, F., Chiba, T. and Tanaka, Y. : 'Estimation of Catalytic Conversion in Gas-Fluidized Beds by means of a Two Phase Model. Effect of Bed Diameter', Kagaku Kogaku, 33, 27 (1969); cf. CA, 71:103630 a (1969).

13. Zenz, F.A. : 'Bubble Formation and Grid Design' in 'Proceedings of the Symposium on Fluidization, Montreal', Inst.Chem.Engrs.Symp.Ser., 30, 136 (1968).

14. Behie, L.A. and Kehoe, P. : 'The Grid Region in a Fluidized Bed Reactor', A.I.Ch.E.J., 19, 1070 (1973).

15. Miyauchi, T. : 'Concept of Successive Contact Mechanism for Catalytic Reaction in Fluid Beds', J.Chem.Eng.Japan, 7, 201 (1974).

16. Miyauchi, T. : 'Behaviour of Successive Contact Model for Catalytic Reaction in Fluid Beds', J.Chem.Eng.Japan, 7, 207 (1974).

17. Chavarie, C. and Grace, J.R. : 'Performance Analysis of a Fluidized Bed Reactor. II. Observed Reactor Behaviour Compared with Simple Two Phase Models', Ind.Eng.Chem.Fundam., 14, 79 (1975).

18. Chavarie, C. and Grace, J.R. : 'Performance Analysis of a Fluidized Bed Reactor. III. Modification and Extension of Conventional Two Phase Models', Ind.Eng.Chem.Fundam., 14, 85 (1975).

19. Spitz, P.H. : 'Phthalic Anhydride Revisited', Hydrocarbon Processing, 47(11), 162 (1968).

20. Caporali, G. : 'How Montedison Makes Acrylo',
Hydrocarbon Processing, 51(11), 144 (1972).

21. Winter, O. and Eng, M.T. :'Make Ethylene from Ethanol',
Hydrocarbon Processing, 55(11), 125 (1976).

22. Bleloch, W. : 'Industrial Production of Ethylene from Ethyl Alcohol by Fluid Catalysis in Low-Frequency Induction Heated Converter',
J.S.Africa Inst.Engrs., 45, 114 (1946);
cf. CA, 41:4091 g (1947).

23. National Chemical Laboratory : 'Chloromethanes',
Annual Report, 49 (1975).

24. Nagata, S., Matsuyama, T., Hashimoto, N. and Hase, H. : 'Studies on the Fluidized Catalyst with Mechanical Agitation',
Chem.Eng.(Japan) 16, 301 (1952);
cf. CA, 46:9747 e (1952).

25. Rasmussen, D.M. : 'High Density Polyethylene Polymerized in Gas Phase',
Chem.Eng., September 18, 104 (1972).

26. The Badger Co.Inc. : 'Isophthalonitrile',
Hydrocarbon Processing, 52(11), 139 (1973).

27. Knoop, J.F. and Neikirk, G.R. : 'Oxychlorinate for Per/Tri',
Hydrocarbon Processing, 51(11), 109 (1972).

28. Montecatini Edison Co. Inc. : 'Chlorofluoromethanes',
Hydrocarbon Processing, 50(11), 145 (1971).

29. Caldwell, A.D. and Calderbank, P.H. : 'Catalyst Dilution - A Means of Temperature Control in Packed Tubular Reactors',
Brit.Chem.Eng., 14, 1199 (1969).

30. Nashaie, S. and Yates, J.G. : 'A Model for Competing Reactions in Gas Fluidized Beds',
Chem.Eng.Sci., 27, 1757 (1972).

31. Shaw, I.D., Hoffman, T.W. and Reilly, P.M. : 'Experimental Evaluation of Two Phase Models Describing Catalytic Fluidized Bed Reactors', A.I.Ch.E. Symp.Ser., 70, No.141,41 (1974).

32. Miyauchi, T. and Furusaki, S. : 'Relative Contribution of Variables Affecting the Reaction in Fluid Bed Contactors', A.I.Ch.E.J., 20, 1087 (1974).

33. Masao, Y. : 'On the Extension of the Successive Contact Model to First Order Reversible and Consecutive Reactions', J.Chem.Eng.Japan, 8, 420 (1975).

34. Kunii, D. and Levenspiel, O. : 'Fluidization Engineering', John Wiley, New York, N.Y., pp. 249-251 (1969).

35. Carberry, J.J. : 'Catalytic and Chemical Reaction Engineering', McGraw Hill, New York, N.Y., p.575 (1976).

36. Levenspiel, O., Baden, N. and Kulkarni, B.D. : 'Complex First Order Reactions in Fluidized Reactors : Application of the KL Model', Ind.Eng.Chem.Process Des.Dev., 17, 478 (1978).

37. Rihani, D.N., Narayanan, T.K. and Doraiswamy, L.K. : 'Kinetics of Catalytic Vapor Phase Hydrogenation of Nitrobenzene to Aniline', Ind.Eng.Chem.Process Des.Dev., 4, 403 (1965).

38. Gilliatt, B.S. : Ph.D Thesis, University of Edinburgh (1967).

39. Narsimhan, G. : 'Catalyst Dilution as a Means to Establish an Optimum Temperature Profile', Ind.Eng.Chem.Process Des.Dev., 15, 302 (1976).

40. Horio, M. and Wen, C.Y. : 'An Assessment of Fluidized Bed Modelling', A.I.Ch.E. Symp.Ser., 73, No.161, 9 (1977).

41. Bukur, D., Caram, H.S. and Amundson, N.R. :'Some Model Studies of Fluidized Bed Reactors' in 'Chemical Reactor Theory :A Review', Ed. Lapidus, L. and Amundson, N.R., Prentice Hall, Englewood Cliffs, New Jersey, pp. 686-757 (1978).

42. Caram, H. C. and Amundson, N.R. : 'Fluidized Bed Gasification Reactor Modelling. I. Model Description and Numerical Results for a Single Bed', Ind.Eng.Chem.Process Des.Dev., 18, 80 (1979).

43. Chavarie, C. and Grace, J.R.: 'Interphase Mass Transfer in a Gas- Fluidized Bed', Chem.Eng.Sci., 31, 741 (1976).

44. Lehmann, J. and Schügerl, K. : 'Investigation of Gas Mixing and Gas Distributor Performance in Fluidized Beds', Chem.Eng.J., 15, 91 (1978)

45. Emmett, P.H. : 'Catalysis', Reinhold Pub.Corp., New York, N.Y., Vol.VII, p.193 (1960).

46. Ipatieff, V.: Ber., 35, 1058 (1902).

47. Ipatieff, V. : Ber., 37, 2986 (1904).

48. Clark, R.H., Graham, W.E. and Winter, A.G. : 'The Catalytic Preparation of Ether from Alcohol by Means of Aluminium Oxide', J.Am.Chem.Soc., 47, 2748 (1925).

49. Alvarado, A.M. : 'Catalytic Dehydration of Ethanol by Alumina at Various Temperatures', J.Am.Chem.Soc., 50, 790 (1928).

50. Pease, R.N. and Yung, C.C. : 'The Catalytic Dehydration of Ethyl Alcohol and Ether by Alumina' J.Am.Chem.Soc., 46, 390 (1924).

51. Brey, W.S. and Kreiger, K.A. : 'The Surface Area and Catalytic Activity of Aluminium Oxide', J.Am.Chem.Soc., 71, 3637 (1949).

52. Bork, K. H. and Kirillova, S.V. : 'Pressure Dependence of the Rate of Dehydration of Ethyl Alcohol', Zhur.Fiz. Khim., 25, 224 (1951); cf. CA, 45:5498 g (1951).

53. Topchieva, K.V. and Yun-Pin, K. : 'Mechanism of the Dehydration of Ethyl Alcohol on Alumino-Silicate Catalysts', Vestn.Mosk.Univ., 7, No.12, Ser. Fiz.Mat. i Estest. Nauk, 8, 39 (1952); cf. CA, 47:9125 g (1953).

54. Balaceanu, J.C. and Jungers, J.C. : 'Dehydration of Alcohols with Alumina',
Bull.Soc.Chim.Belges, 60, 476 (1952);
cf. CA, 47:2683 c (1953).

55. Krause, A. : 'Reaction Mechanism of the Catalytic Dehydration of Ethanol',
Bull.Soc.Amis.Sci. et lettres Poznan.Ser. B,
12, 67 (1953);
cf. CA, 47:7875 d (1953).

56. Topchieva, K.V. and Yun-Pin, K. : 'Kinetics of Ethanol and Ethyl Ether Dehydration on Alumina and Aluminium Silicate Catalysts',
Zhur.Fiz.Khim., 29, 1678 (1955);
cf. CA, 50:7558 g (1956).

57. Antipina, T.V. and Sinitsyna, M.D. : 'Ethanol Dehydration at Elevated Pressures',
Zhur.Fiz.Khim., 30, 2478 (1956);
cf. CA, 51:9471 g (1957).

58. Butt, J.B., Bliss, H. and Walker, C.A. : 'Rates of Reaction in a Recycling System : Dehydration of Ethanol and Diethyl Ether over Alumina',
A.I.Ch.E.J., 8, 42 (1962).

59. Isagulyants, G.V., Balandin, A.A., Popov, E.I. and Derbentsev, Y.I. : 'Study of the Mechanism of Dehydration of Ethyl Alcohol on Aluminium Oxide with the Aid of ^{14}C',
Zhur.Fiz.Khim., 38, 20 (1964);
cf. CA, 60 : 9121 g (1964).

60. Knoezinger, H. and Koehne, R. : 'The Dehydration of Alocohols over Alumina. I. The Reaction Scheme',
J. Catalysis, 5, 264 (1966).

61. Vasserberg, V.E. : 'Properties of an Active Complex and the Polymolecular Mechanism of Alcohol Dehydration on Alumina',
Probl. Kinet. Katal., Akad. Nauk SSSR, 12,
229 (1968);
cf. CA, 69:86020 r (1968).

62. Huang, T.C., Chen, C.C. and Tsai, F.N. : 'Pulse Chromatographic Study of Catalytic Reaction for Dehydration of Alcohol',
Hua Hsueh, 2, 38 (1973);
cf. CA, 80:41284 r (1974).

63. Wu Lian Yuan : 'Manufacture of Ethylene by Dehydration of Industrial Ethanol Using Fluid Catalyst', Chemistry (Taiwan), 1, 39 (1955); cf. CA, 50:2412 i (1956).

64. Deshpande, V. V., Bhatnagar, R.K., Venkataraman, S., Kuloor, N.R. and Daruvalla, D.N. :'A Process for the Preparation of Ethylene from Ethyl Alcohol', Indian Patent No. 57007, Nov. 27 (1957).

65. Topchieva, K.V. and Zen'kovich, I.A. : 'Effect of Hydrodynamic Process Parameters on the Kinetics of a First Order Reaction in a Fluidized Catalyst Bed', Vestn.Mosk.Univ.Khim., 24, 17 (1969). cf. CA, 71:72380 n (1969).

66. Zen'kovich, I.A. and Topchieva, K.V. : 'Effect of Hydrodynamic Parameters on the Kinetics of a Second Order Reversible Reaction in a Fluidized Catalytic Bed', Vestn. Mosk. Univ. Khim., 24, 54 (1969); cf. CA, 71 : 93089 q (1969).

67. Zen'kovich, I.A. and Topchieva, K.V. : 'Effect of Gas Phase Mixing on the Kinetics of Ethyl Alcohol Dehydration in a Fluidized Catalytic Bed', Vestn. Mosk. Univ. Khim., 11, 649 (1970); cf. CA, 74 : 87073 a (1971).

68. Ford, F.E. and Perlmutter, D.D. : 'Mass Transfer Effects in Surface Catalysis', A.I.Ch.E.J., 9, 371 (1963).

69. Antipina, T.V. and Frost, A.V.: 'Relation Between the Kinetics of Heterogeneous Reactions and the Adsorption on Catalysts. I. Determination of the Adsorption Coefficient of Water on Aluminium Oxide from Kinetic Data', Vestn. Mosk. Univ., 5, No.3, Ser.Fiz. Mat. i Estest. Nauk, 2, 81 (1950); cf. CA, 45:4541 a (1951).

70. Antipina, T.V. and Frost, A.V. : 'Relation Between the Kinetics of Heterogeneous Reactions and Adsorption on Catalysts.II. Determination of the Adsorption Coefficient of Ethylene on Aluminium Oxide and its Temperature Dependence from Kinetic Data',
Vestn. Mosk. Univ., 6, No.8, Ser.Fiz.Mat. i Estest. Nauk, 5, 69 (1951).
cf. CA, 46 : 3382 e (1952).

71. Antipina,T.V. and Frost, A.V. : 'Relation Between the Kinetics of a Heterogeneous Reaction and Adsorption on Catalysts. III. Temperature Dependence of the Adsorption Coefficient of Water on Aluminium Oxide',
Vestn. Mosk, Univ., 6, No. 10, Ser. Fiz. Mat. i Estest. Nauk, 6, 79 (1951).
cf. CA, 46 : 8487 i (1952).

72. Roy, N.C. and Bose, N.K. : 'Catalytic Dehydration of Ethanol on Activated Alumina',
Sci. and Cul., 23, 55 (1957).

73. Roy, N.C. and Bose N.K : 'Kinetics of Catalytic Dehydration on Activated Alumina',
Trans. Indian Inst.Chem.Engrs., 11, 3 (1959).

74. De Boer, J.H., Fahim, R.B., Linsen, B.G., Visseren, W.J. and De Vleesschauwer, W.F.:'Kinetics of the Dehydration of Alcohol on Alumina',
J.Catalysis, 7, 163 (1967).

APPENDIX - I

DETAILED ANALYSIS OF THE REACTION SCHEME

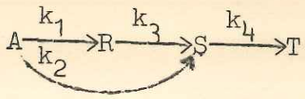

I. DETAILED ANALYSIS OF THE REACTION SCHEME

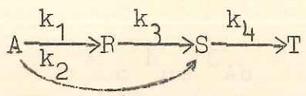

The material balance equations for this reaction scheme have been presented in Section 2.5. Rearrangement of Equation (2.55) gives

$$- u_b \frac{dC_{Ab}}{dl} = (k_1+k_2)[\gamma_b C_{Ab}+\gamma_c C_{Ac}+\gamma_e C_{Ae}] \qquad (I.1)$$

where

$$C_{Ae} = \frac{C_{Ac}\, K_{ce}}{[\gamma_e(k_1+k_2)+K_{ce}]} \qquad (I.2)$$

$$C_{Ac} = \frac{K_{bc}\, C_{Ab}}{K_{bc}+\gamma_c(k_1+k_2)+K_{ce} - \dfrac{K_{ce}^2}{[\gamma_e(k_1+k_2)+K_{ce}]}} \qquad (I.3)$$

or

$$C_{Ae} = \frac{K_{bc}\, K_{ce}\, C_{Ab}}{\left[(K_{bc}+\gamma_c(k_1+k_2)+K_{ce}) - \dfrac{K_{ce}^{\,2}}{[\gamma_e(k_1+k_2)+K_{ce}]}\right]\left[\gamma_e(k_1+k_2)+K_{ce}\right]} \qquad (I.4)$$

Neglecting the effect of solids dispersed in the bubbles ($\gamma_b=0$) Equation (2.55) may be written as

$$-u_b \frac{dC_{Ab}}{dl} = \frac{(k_1+k_2)K_{bc}}{\left[K_{bc}+\gamma_c(k_1+k_2)+K_{ce}-\dfrac{K_{ce}^{\,2}}{[\gamma_e(k_1+k_2)+K_{ce}]}\right]} \left[\gamma_c + \frac{\gamma_e K_{ce}}{[\gamma_e(k_1+k_2)+K_{ce}]}\right] C_{Ab} \qquad (I.5)$$

Rearranging the above

$$- u_b \frac{dC_{Ab}}{dl} = \left[\frac{(k_1+k_2)K_{bc}[(\gamma_e(k_1+k_2)+K_{ce})\gamma_c+\gamma_e K_{ce}]}{(K_{bc}+\gamma_c(k_1+k_2)+K_{ce})(\gamma_e(k_1+k_2)+K_{ce})-K_{ce}^2} \right] C_{Ab} \tag{I.6}$$

Consider the coefficient of C_{Ab}

$$= (k_1+k_2) \left[\frac{\gamma_c K_{bc}\gamma_e(k_1+k_2)+\gamma_c K_{bc}K_{ce}+\gamma_e K_{bc}K_{ce}}{K_{bc}\gamma_e(k_1+k_2)+K_{bc}K_{ce}+\gamma_c\gamma_e(k_1+k_2)^2+K_{ce}\gamma_c(k_1+k_2)+K_{ce}\gamma_e(k_1+k_2)} \right] \tag{I.7}$$

$$= (k_1+k_2) \left[\frac{1}{\frac{(k_1+k_2)^2\gamma_c\gamma_e+(k_1+k_2)\gamma_c K_{ce}+(k_1+k_2)\gamma_e K_{ce}+(k_1+k_2)\gamma_e K_{bc}+K_{bc}K_{ce}}{K_{bc}[(k_1+k_2)\gamma_c\gamma_e+\gamma_c K_{ce}+\gamma_e K_{ce}]}} \right] \tag{I.8}$$

$$= (k_1+k_2) \left[\frac{1}{\frac{(k_1+k_2)}{K_{bc}} + \frac{(k_1+k_2)\gamma_e + K_{ce}}{(k_1+k_2)\gamma_c\gamma_e+\gamma_c K_{ce}+\gamma_e K_{ce}}} \right] \tag{I.9}$$

$$= (k_1+k_2) \left[\frac{1}{\frac{(k_1+k_2)}{K_{bc}} + \frac{1}{\gamma_c + \frac{1}{\frac{(k_1+k_2)}{K_{ce}} + \frac{1}{\gamma_e}}}} \right] = K_{[1+2]} \qquad (I.10)$$

Thus

$$- u_b \frac{dC_{Ab}}{dl} = K_{[1+2]} C_{Ab} \qquad (I.11)$$

or rewriting in dimensionless form,

$$- \frac{d\bar{C}_{Ab}}{dz} = K_{[1+2]_{1+2}} \frac{W}{v_o \rho_s} \bar{C}_{Ab} \qquad (I.12)$$

The solution of this Equation subject to the boundary condition

$$\bar{C}_{Ab} = 1 \quad \text{at} \quad z = 0 \qquad (I.13)$$

is given by

$$\bar{C}_{Ab} = \exp \left[- K_{[1+2]_{1+2}} t \right] \qquad (I.14)$$

Rearrangement of Equation (2.56) yields

$$u_b \frac{dC_{Rb}}{dl} = k_1[\gamma_c C_{Ac} + \gamma_e C_{Ae}] - k_3[\gamma_c C_{Rc} + \gamma_e C_{Re}] \qquad (I.15)$$

In analogy with the previous analysis

$$k_1[\gamma_c C_{Ac}+\gamma_e C_{Ae}] = K_1 C_{Ab} \tag{I.16}$$

Thus Equation (I.14) becomes

$$u_b \frac{dC_{Rb}}{dl} = K_1 C_{Ab} - k_3[\gamma_c C_{Rc}+\gamma_e C_{Re}] \tag{I.17}$$

Equation (2.56) also yields the following

$$C_{Re} = \frac{K_{ce} C_{Rc} + \gamma_e k_1 C_{Ae}}{[K_{ce} + \gamma_e k_3]} \tag{I.18}$$

and

$$C_{Rc} = \frac{K_{bc} C_{Rb} + \gamma_c k_1 C_{Ac} + \frac{K_{ce}\gamma_e k_1 C_{Ae}}{(K_{ce}+\gamma_e k_3)}}{K_{bc}+\gamma_c k_3 - \frac{K_{ce}^2}{(K_{ce}+\gamma_e k_3)} + K_{ce}} \tag{I.19}$$

or

$$C_{Rc} = \frac{(K_{bc} C_{Rb}+\gamma_c k_1 C_{Ac})(K_{ce}+\gamma_e k_3) + K_{ce}\gamma_e k_1 C_{Ae}}{(K_{bc}+\gamma_c k_3+K_{ce})(K_{ce}+\gamma_e k_3) - K_{ce}^2} \tag{I.20}$$

Thus Equation (I.17) may be written as

$$u_b \frac{dC_{Rb}}{dl} = K_1 C_{Ab} - k_3 \left[\frac{\gamma_e^2 k_1 C_{Ae}}{K_{ce}+\gamma_e k_3} + \left\{ \gamma_c + \frac{\gamma_e K_{ce}}{\gamma_e k_3 + K_{ce}} \right\} \right.$$

$$\left. \left\{ \frac{(K_{bc} C_{Rb} + \gamma_c k_1 C_{Ac})(K_{ce}+\gamma_e k_3) + K_{ce} \gamma_e k_1 C_{Ae}}{(K_{bc}+\gamma_c k_3 + K_{ce})(K_{ce}+\gamma_e k_3) - K_{ce}^2} \right\} \right] \qquad (I.21)$$

Coefficient of C_{Rb} in Equation (I.21):

$$k_3 \left[\gamma_c + \frac{\gamma_e K_{ce}}{\gamma_e k_3 + K_{ce}} \right] \left[\frac{K_{bc} (K_{ce} + \gamma_e k_3)}{(K_{ce}+\gamma_e k_3)(K_{bc}+\gamma_c k_3+K_{ce}) - K_{ce}^2} \right] = K_3 \qquad (I.22)$$

Substitution for C_{Ae} and C_{Ac} in terms of C_{Ab} is effected in Equation (I.21) by employing Equations (I.3) and (I.4).

Coefficient of C_{Ab} in Equation (I.21) :

$$K_1 - \left[\frac{K_{bc}}{[K_{ce}+\gamma_e(k_1+k_2)][K_{bc}+\gamma_c(k_1+k_2)+K_{ce}]-K_{ce}^2} \right] \left[\frac{\gamma_e^2 k_1 k_3 K_{ce}}{\gamma_e k_3+K_{ce}} + \right.$$

$$\frac{\gamma_e k_1 K_{ce}^2}{(\gamma_e k_3+K_{ce})(K_{bc}+\gamma_c k_3+K_{ce})-K_{ce}^2} \left\{ \gamma_c k_3 + \frac{\gamma_e k_3 K_{ce}}{\gamma_e k_3+K_{ce}} \right\} +$$

$$\left. \left[\gamma_c k_3 + \frac{\gamma_e k_3 K_{ce}}{\gamma_e k_3+K_{ce}} \right] \left\{ \gamma_e(k_1+k_2)+K_{ce} \right\} \times \left\{ \frac{\gamma_c k_1 (\gamma_e k_3+K_{ce})}{(K_{ce}+\gamma_e k_3)(K_{bc}+\gamma_c k_3+K_{ce})-K_{ce}^2} \right\} \right]$$

$$= K_1 - \left[\frac{K_{bc}}{[K_{ce}+\gamma_e(k_1+k_2)][K_{bc}+\gamma_c(k_1+k_2)+K_{ce}]-K_{ce}^2} \right]$$

$$\left[\left[\frac{\gamma_c k_3 + \frac{\gamma_e k_3 K_{ce}}{\gamma_e k_3+K_{ce}}}{(K_{ce}+\gamma_e k_3)(K_{bc}+K_{ce}+\gamma_c k_3)-K_{ce}^2} \right] \right.$$

$$\left. \left\{ K_{ce}^2 \gamma_e k_1 + \gamma_c k_1 (K_{ce}+\gamma_e k_3)[\gamma_e(k_1+k_2)+K_{ce}] \right\} + \frac{\gamma_e^2 k_1 k_3 K_{ce}}{K_{ce}+\gamma_e k_3} \right] \quad (I.23)$$

Now in general

$$K_i = \frac{\left(\gamma_c k_i + \frac{\gamma_e k_i K_{ce}}{\gamma_e k_i + K_{ce}}\right) K_{bc}(\gamma_e k_i + K_{ce})}{(K_{ce}+\gamma_e k_i)(K_{bc}+K_{ce}+\gamma_c k_i) - K_{ce}^2} \qquad (I.24)$$

Thus rearranging Equation (I.23) gives the coefficient of C_{Ab} as

$$= K_1 - K_{[1+2]} \left[\frac{\gamma_e^2 k_1 k_3 K_{ce}}{\gamma_e k_3 + K_{ce}} + \frac{K_3 k_1}{K_{bc}} \left(\gamma_c [K_{ce} + \gamma_e (k_1+k_2)] + \frac{K_{ce}^2 \gamma_e}{K_{ce}+\gamma_e k_3} \right) \right] \Bigg/$$

$$\left[\left(\gamma_c (k_1+k_2) + \frac{\gamma_e (k_1+k_2) K_{ce}}{\gamma_e (k_1+k_2) + K_{ce}} \right) \left(K_{ce} + \gamma_e (k_1+k_2) \right) \right]$$

(I.25)

$$= K_{[1+2]} \quad \Psi_{[1+2]} = K'_{[1+2]} \qquad (I.26)$$

where

$$\Psi_{[1+2]} = \frac{K_1}{K_{[1+2]}} - \left[\frac{\gamma_e^2 k_1 k_3 K_{ce}}{\gamma_e k_3 + K_{ce}} + \frac{K_3 k_1}{K_{bc}} \left(\gamma_c [K_{ce} + \gamma_e (k_1+k_2)] + \frac{K_{ce}^2 \gamma_e}{K_{ce}+\gamma_e k_3} \right) \right] \Bigg/$$

$$\left[\left(\gamma_c (k_1+k_2) + \frac{\gamma_e (k_1+k_2) K_{ce}}{\gamma_e (k_1+k_2) + K_{ce}} \right) \left(K_{ce} + \gamma_e (k_1+k_2) \right) \right] \qquad (I.27)$$

Thus Equation (I.17) may be rewritten as

$$u_b \frac{dC_{Rb}}{dl} = K'_{[1+2]} C_{Ab} - K_3 C_{Rb} \qquad (I.28)$$

or in dimensionless form as

$$\frac{d\bar{C}_{Rb}}{dz} = \left[K'_{[1+2]}{}_{1+2} \bar{C}_{Ab} - K_{33} \bar{C}_{Rb} \right] \frac{W}{v_o \rho_s} \qquad (I.29)$$

with the boundary condition

$$\bar{C}_{Rb} = 0 \text{ at } z = 0 \qquad (I.30)$$

The solution of Equation (I.29) is then obtained to be

$$\bar{C}_{Rb} = \frac{K'_{[1+2]}}{K_3 - K_{[1+2]}} \left[\exp\left(- K_{[1+2]}{}_{1+2} t\right) - \exp\left(-K_{33} t\right) \right] \qquad (I.31)$$

Rearrangement of Equation (2.57) gives

$$u_b \frac{dC_{Sb}}{dl} = k_2[\gamma_c C_{Ac} + \gamma_e C_{Ae}] + k_3[\gamma_c C_{Rc} + \gamma_e C_{Re}] - k_4[\gamma_c C_{Sc} + \gamma_e C_{Se}] \qquad (I.32)$$

where

$$C_{Se} = \frac{\gamma_e k_2 C_{Ae} + \gamma_e k_3 C_{Re} + K_{ce} C_{Sc}}{K_{ce} + \gamma_e k_4} \qquad (I.33)$$

and

$$C_{Sc} = \frac{(\gamma_c k_2 C_{Ac} + \gamma_c k_3 C_{Rc} + K_{bc} C_{Sb})(K_{ce} + \gamma_e k_4) + K_{ce}(\gamma_e k_2 C_{Ae} + \gamma_e k_3 C_{Re})}{(K_{bc} + \gamma_c k_4 + K_{ce})(\gamma_e k_4 + K_{ce}) - K_{ce}^2} \tag{I.34}$$

Substitution for C_{Se} and C_{Sc} in terms of C_{Sb} is then carried out in Equation (I.32) by employing Equations (I.33) and (I.34).

Coefficient of C_{Sb} in Equation (I.32) :

$$- k_4 \left[\frac{\gamma_c K_{bc}(\gamma_e k_4 + K_{ce}) + \gamma_e K_{ce} K_{bc}}{(K_{bc} + \gamma_c k_4 + K_{ce})(K_{ce} + \gamma_e k_4) - K_{ce}^2} \right]$$

$$= - k_4 \left[\frac{K_{bc}\left(\gamma_c k_4 + \frac{\gamma_e k_4 K_{ce}}{\gamma_e k_4 + K_{ce}}\right)(\gamma_e k_4 + K_{ce})}{(K_{bc} + \gamma_c k_4 + K_{ce})(K_{ce} + \gamma_e k_4) - K_{ce}^2} \right] \tag{I.35}$$

$$= - K_4 \tag{I.36}$$

Coefficient of C_{Re} in Equation (I.32) :

$$\gamma_e k_3 - \left[\frac{k_3 k_4 \gamma_c \gamma_e K_{ce}}{(K_{bc}+\gamma_c k_4+K_{ce})(K_{ce}+\gamma_e k_4)-K_{ce}^2} + \frac{\gamma_e^2 k_3 k_4}{(K_{ce}+\gamma_e k_4)} \right.$$

$$\left. + \frac{K_{ce}^2 \gamma_e^2 k_3 k_4}{(K_{ce}+\gamma_e k_4)[(K_{bc}+\gamma_c k_4+K_{ce})(K_{ce}+\gamma_e k_4)-K_{ce}^2]} \right]$$

Rearranging, the above is obtained to be

$$= \frac{\gamma_e k_3 K_{ce}}{(K_{ce}+\gamma_e k_4)} \left[1 - \frac{K_4}{K_{bc}} \right] \qquad (I.37)$$

Coefficient of C_{Rc} in Equation (I.32) :

$$\gamma_c k_3 - \left[\gamma_c k_4 + \frac{\gamma_e k_4 K_{ce}}{\gamma_e k_4 + K_{ce}} \right] \left[\frac{\gamma_c k_3 (K_{ce}+\gamma_e k_4)}{(K_{bc}+\gamma_c k_4+K_{ce})(K_{ce}+\gamma_e k_4)-K_{ce}^2} \right]$$

$$= \gamma_c k_3 (1 - K_4/K_{bc}) \qquad (I.38)$$

The C_{Re} and C_{Rc} terms in Equation (I.32) may be replaced by employing Equations (I.18) and (I.19). Thus, considering all the C_R terms in Equation (I.32) we have them to be

$$= \frac{\gamma_e k_3 K_{ce}}{(K_{ce}+\gamma_e k_4)} \left[1 - \frac{K_4}{K_{bc}}\right] C_{Re} + \gamma_c k_3 \left[1 - \frac{K_4}{K_{bc}}\right] C_{Rc} \qquad (I.39)$$

$$= \frac{\gamma_e k_3 K_{ce}}{(K_{ce}+\gamma_e k_4)} \left[1 - \frac{K_4}{K_{bc}}\right] \frac{\gamma_e k_1 C_{Ae}}{(K_{ce}+\gamma_e k_3)} + \left\{ \frac{\gamma_e k_3 K_{ce}^2}{(K_{ce}+\gamma_e k_3)(K_{ce}+\gamma_e k_4)} \left[1 - \frac{K_4}{K_{bc}}\right] + \gamma_c k_3 \left[1 - \frac{K_4}{K_{bc}}\right] \right\} \left\{ \frac{K_{bc} C_{Rb} + \gamma_c k_1 C_{Ac} + \frac{K_{ce}\gamma_e k_1 C_{Ae}}{(K_{ce}+\gamma_e k_3)}}{[(K_{bc}+\gamma_c k_3+K_{ce}) - \frac{K_{ce}^2}{(K_{ce}+\gamma_e k_3)}]} \right\}$$

(I.40)

Coefficient of C_{Rb} in Equation (I.32) :

$$\left\{ \frac{\gamma_e k_3 K_{ce}^2}{(K_{ce}+\gamma_e k_3)(K_{ce}+\gamma_e k_4)} + \gamma_c k_3 \right\} \left[1 - \frac{K_4}{K_{bc}}\right]$$

$$\times \left[\frac{K_{bc}(K_{ce}+\gamma_e k_3)}{(K_{ce}+\gamma_e k_3)(K_{bc}+\gamma_c k_3+K_{ce}) - K_{ce}^2} \right]$$

Rearranging the above term it is obtained to be

$$= \quad \Psi_2 \; K_3 K_4 = K_2' \qquad \text{(I.41)}$$

where

$$\Psi_2 = \frac{\left[\dfrac{\gamma_e k_3 K_{ce}^{\,2}}{(K_{ce}+\gamma_e k_3)(K_{ce}+\gamma_e k_4)} + \gamma_c k_3 \right]}{\left[\gamma_c k_4 + \dfrac{\gamma_e k_3 K_{ce}}{K_{ce}+\gamma_e k_3}\right]\left[\gamma_c k_4 + \dfrac{\gamma_e k_4 K_{ce}}{K_{ce}+\gamma_e k_4}\right]} \qquad \text{(I.42)}$$

Coefficient of C_{Ae} in Equation (I.32) :

$$\gamma_e k_2 + \frac{\gamma_e k_3 K_{ce}}{(K_{ce}+\gamma_e k_4)} \left[1 - \frac{K_4}{K_{bc}}\right] \left[\frac{\gamma_e k_1}{(K_{ce}+\gamma_e k_3)}\right] +$$

$$\left\{ \left[\frac{\gamma_e k_3 K_{ce}^{\,2}}{(K_{ce}+\gamma_e k_4)(K_{ce}+\gamma_e k_3)} + \gamma_c k_3 \right] \left[1 - \frac{K_4}{K_{bc}}\right] \left[\frac{K_{ce}\gamma_e k_1}{(K_{bc}+\gamma_c k_3+K_{ce})(K_{ce}+\gamma_e k_3)-K_{ce}^{\,2}} \right] \right\}$$

$$- \frac{\gamma_e^{\,2} k_2 k_4}{(K_{ce}+\gamma_e k_4)} - \frac{\gamma_c \gamma_e k_2 k_4 K_{ce}}{[(K_{bc}+\gamma_c k_4+K_{ce})(K_{ce}+\gamma_e k_4)-K_{ce}^{\,2}]}$$

$$- \frac{\gamma_e^{\,2} k_2 k_4 K_{ce}^{\,2}}{(K_{ce}+\gamma_e k_4)[(K_{bc}+\gamma_c k_4+K_{ce})(K_{ce}+\gamma_e k_4)-K_{ce}^{\,2}]}$$

$$= \gamma_e k_2 + \frac{\gamma_e k_3 K_{ce}}{(K_{ce}+\gamma_e k_4)} \left[1 - \frac{K_4}{K_{bc}} \right] \frac{\gamma_e k_1}{(K_{ce}+\gamma_e k_3)} + \Psi_2 K_3 K_4 \frac{K_{ce}\gamma_e k_1}{K_{bc}(K_{ce}+\gamma_e k_3)}$$

$$- \frac{\gamma_e k_2 k_4 K_{ce}}{[(K_{bc}+\gamma_c k_4+K_{ce})(K_{ce}+\gamma_e k_4)-K_{ce}^2]} \left[\gamma_c + \frac{\gamma_e K_{ce}}{K_{ce}+\gamma_e k_4} \right] - \frac{\gamma_e^2 k_2 k_4}{(K_{ce}+\gamma_e k_4)} \qquad (I.43)$$

$$= \gamma_e k_2 + \frac{\gamma_e^2 k_1 k_3 K_{ce} K_4}{(K_{ce}+\gamma_e k_4)(K_{ce}+\gamma_e k_3)\left(\gamma_c k_4 + \frac{\gamma_e k_4 K_{ce}}{K_{ce}+\gamma_e k_4}\right)} + \frac{\Psi_2 K_3 K_4 \gamma_e k_1 K_{ce}}{K_{bc}(K_{ce}+\gamma_e k_3)}$$

$$- \frac{\gamma_e K_{ce} k_2 k_4 K_4 \left(\gamma_c + \frac{\gamma_e K_{ce}}{K_{ce}+\gamma_e k_4}\right)}{K_{bc}(K_{ce}+\gamma_e k_4)\left(\gamma_c k_4 + \frac{\gamma_e k_4 K_{ce}}{K_{ce}+\gamma_e k_4}\right)} - \frac{\gamma_e^2 k_2 k_4}{(K_{ce}+\gamma_e k_4)} \qquad (I.44)$$

Coefficient of C_{Ac} in Equation (I.32) :

$$\gamma_c k_2 + \left[\frac{\gamma_e k_3 K_{ce}^2}{(K_{ce}+\gamma_e k_4)(K_{ce}+\gamma_e k_3)} + \gamma_c k_3\right]\left[1 - \frac{K_4}{K_{bc}}\right]$$

$$\times \left[\frac{\gamma_c k_1 (K_{ce}+\gamma_e k_3)}{[(K_{bc}+\gamma_c k_3+K_{ce})(K_{ce}+\gamma_e k_3)-K_{ce}^2]}\right]$$

$$- \left[\frac{\gamma_c^2 k_2 k_4 (K_{ce}+\gamma_e k_4) + \gamma_c \gamma_e k_2 k_4 K_{ce}}{[(K_{bc}+\gamma_c k_4+K_{ce})(K_{ce}+\gamma_e k_4)-K_{ce}^2]}\right]$$

$$= \gamma_c k_2 + \frac{\gamma_c k_1 \psi_2 K_3 K_4}{K_{bc}} - \frac{\gamma_c k_2 \left[\gamma_c k_4 + \frac{\gamma_e k_4 K_{ce}}{K_{ce}+\gamma_e k_4}\right][K_{ce}+\gamma_e k_4]}{[(K_{bc}+\gamma_c k_4+K_{ce})(K_{ce}+\gamma_e k_4)-K_{ce}^2} \qquad (I.45)$$

$$= \gamma_c k_2 + \frac{\gamma_c k_1 \psi_2 K_3 K_4}{K_{bc}} - \frac{\gamma_c k_2 K_4}{K_{bc}} \qquad (I.46)$$

$$= \frac{\gamma_c k_1 \psi_2 K_3 K_4}{K_{bc}} + \gamma_c \left[1 - \frac{K_4}{K_{bc}} \right] \qquad (I.47)$$

$$= \frac{\gamma_c k_1 \psi_2 K_3 K_4}{K_{bc}} + \frac{\gamma_c k_2}{\left(\gamma_c k_4 + \frac{\gamma_e k_4 K_{ce}}{K_{ce} + \gamma_e k_4} \right)} K_4 \qquad (I.48)$$

The terms C_{Ac} and C_{Ae} may be rewritten in terms of C_{Ab} by employing Equations (I.3) and (I.4).

Coefficient of C_{Ab} in Equation (I.32):

$$\left[\begin{array}{l} \text{coefficient of } C_{Ae} \\ \text{given in Equation} \\ \text{(I.44)} \end{array} \right] \frac{K_{bc} K_{ce}}{[(K_{bc} + \gamma_c(k_1+k_2) + K_{ce})(\gamma_e(k_1+k_2) + K_{ce}) - K_{ce}^2]}$$

$$+ \left[\begin{array}{l} \text{coefficient of } C_{Ac} \\ \text{given by Equation} \\ \text{(I.48)} \end{array} \right] \frac{K_{bc}[\gamma_e(k_1+k_2) + K_{ce}]}{[(K_{bc} + \gamma_c(k_1+k_2) + K_{ce})(\gamma_e(k_1+k_2) + K_{ce}) - K_{ce}^2]}$$

$$= K_{[1+2]} \quad \psi_3 = K_{[12]} \qquad (I.49)$$

where

$$\Psi_3 = \frac{\dfrac{K_{ce}}{\gamma_e(k_1+k_2)+K_{ce}} \left[\begin{array}{l}\text{coefficient of } C_{Ae} \\ \text{given by} \\ \text{Equation (I.44)}\end{array}\right] + \left[\begin{array}{l}\text{coefficient of } C_{Ac} \\ \text{given by} \\ \text{Equation (I.48)}\end{array}\right]}{\left[\gamma_c(k_1+k_2) + \dfrac{\gamma_e(k_1+k_2)K_{ce}}{\gamma_e(k_1+k_2)+K_{ce}}\right]} \qquad (I.50)$$

Equation (I.32) may thus be rewritten in the form

$$u_b \frac{dC_{Sb}}{dl} = K_{[12]}C_{Ab} + K_2' C_{Rb} - K_4 C_{Sb} \qquad (I.51)$$

or in dimensionless form as

$$\frac{d\bar{C}_{Sb}}{dz} = \left[K_{[12]_{12}} \bar{C}_{Ab} + K_{22}' \bar{C}_{Rb} - K_{44} C_{Sb}\right] x \frac{W}{v_o \rho_s} \qquad (I.52)$$

with the boundary condition

$$\bar{C}_{Sb} = 0 \quad \text{at} \quad z = 0 \qquad (I.53)$$

The solution of Equation (I.52) is then obtained to be

$$\bar{C}_{Sb} = \exp(-K_{[1+2]_{1+2}} t) \left[\frac{K_{[12]}}{(K_4 - K_{[1+2]})} + \frac{K_2' K'_{[1+2]}}{(K_3 - K_{[1+2]})(K_4 - K_{[1+2]})} \right]$$

$$+ \exp(-K_{33} t) \left[\frac{-K_2' K_{[1+2]}}{(K_4 - K_3)(K_3 - K_{[1+2]})} \right]$$

$$+ \exp(-K_{44} t) \left[\frac{-K_2' K_{[1+2]}}{(K_4 - K_3)(K_4 - K_{[1+2]})} + \frac{K_{[12]}}{(K_4 - K_{[1+2]})} \right] \quad (I.54)$$

The height in the bed at which maximum production of intermediate R occurs can be obtained by re-setting Equation (I.29) equal to zero.

Thus

$$K'_{[1+2]} C_{Ab} - K_3 C_{Rb} = 0 \quad (I.55)$$

or

$$K'_{[1+2]} [\exp(-K_{[1+2]_{1+2}} t)] - \frac{K_3 K'_{[1+2]}}{(K_3 - K_{[1+2]})} \left[\exp(-K_{[1+2]_{1+2}} t) - \exp(-K_{33} t) \right] = 0 \quad (I.56)$$

Rearranging we obtain

$$t_{max} = \frac{W}{v_o \rho_s} \quad z_{max} = \frac{\ln \left(\frac{K_3}{K_{[1+2]}} \right)}{\left(K_{33} - K_{[1+2]_{1+2}} \right)} \qquad (I.57)$$

Equation (I.57) for t_{max} is then substituted in Equation (I.31) to give

$$\bar{C}_{R,max} = \frac{K'_{[1+2]}}{K_{[1+2]}} \left(\frac{K_{[1+2]}}{K_3} \right)^{\frac{K_3}{K_3 - K_{[1+2]}}} \qquad (I.58)$$

In this manner the general performance equations for the given reaction scheme have been developed.

APPENDIX - II

COMPUTATIONAL PROCEDURE FOR THE REACTION SCHEME

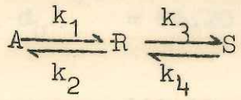

II. COMPUTATIONAL PROCEDURE FOR THE REACTION SCHEME

$$A \underset{k_2}{\overset{k_1}{\rightleftharpoons}} R \underset{k_4}{\overset{k_3}{\rightleftharpoons}} S$$

A representative bubble diameter d_b = 15 cm is considered together with the data presented in Section 2.6.

The values of the various parameters of the model are calculated as follows :

$$\bar{C}_A^* = \frac{k_2}{k_1+k_2} = 0.0909$$

$$\bar{C}_R^* = \frac{k_4}{k_3+k_4} = 0.0909$$

From the details of the model we obtain

$$u_{br} = 0.711\ (g\ d_b)^{1/2} = 86.20 \text{ cm/sec.}$$

$$u_b = u_o - u_{mf} + u_{br} = 113.20 \text{ cm/sec.}$$

$$\delta = \frac{u_o - u_{mf}}{u_b} = 0.238$$

$$K_{bc} = 4.5\ \left(\frac{u_{mf}}{d_b}\right) + 5.85\ \left(\frac{D^{1/2}\ g^{1/4}}{d_b^{5/4}}\right) = 1.395 \text{ sec}^{-1}$$

$$K_{ce} = 6.78\left[\frac{\epsilon_{mf}\ D_e\ u_b}{d_b^3}\right]^{1/2} = 0.351 \text{ sec}^{-1}$$

$$\gamma_c = (1-\epsilon_{mf}) \left[\frac{3u_{mf}/\epsilon_{mf}}{u_{br} - u_{mf}/\epsilon_{mf}} + V_w/V_b \right] = 0.351$$

$$\gamma_e = (1-\epsilon_{mf}) \left[\frac{1-\delta}{\delta} \right] - \gamma_c = 1.563$$

Substituting these values in Equation (2.13) gives

$$K_1 = 1.025 \text{ sec}^{-1}$$

$$K_3 = 0.438 \text{ sec}^{-1}$$

From Equation (2.24) and (2.23) then

$$\Psi_1 = 0.85 \; ; \; K_1 = 0.652 \text{ sec}^{-1}$$

Substitution in Equations (2.26), (2.27) and (2.25) respectively results in

$$\phi_2 = 14.23 \text{ sec}^{-1}$$

$$\phi_3 = 14.76 \text{ sec}^{-1}$$

$$\phi_1' = 0.49 \text{ sec}^{-1}$$

and from Equation (2.31)

$$K_{11} = 0.594 \text{ sec}^{-1}; \; K_{11}' = 0.378 \text{ sec}^{-1}; \; K_{33} = 0.254 \text{ sec}^{-1}$$

The concentration profiles as well as $\bar{C}_{R,max}$ and t_{max} are then calculated on the basis of Equations (2.33) and (2.34). Thus

$$\bar{C}_{Ab} = 0.909 \exp(-0.594\ t) + 0.091$$

$$\bar{C}_{Rb} = 1.01 \exp(-0.594\ t) + 0.887 \exp(-0.254t) + 0.123$$

These equations have been plotted in Figure 2.3 for $d_b = 15$ cm. From a material balance we obtain

$$\bar{C}_{Sb} = 1.0 - (\bar{C}_{Ab} + \bar{C}_{Rb})$$

$C_{R,max}$ and t_{max} are then calculated as follows :

Equations (2.37), (2.40), (2.41) and (2.42) respectively give

$$P = 0.373$$

$$P_1 = -1.01$$

$$P_2 = 0.887$$

$$P_3 = 0.123$$

Substitution of these parameters in Equation (2.36) and (2.39) yield

$$t_{max} = \frac{\ln P}{K_{33} - K_{11}} = 2.88 \text{ sec}$$

$$C_{R,max} = (PP_1 + P_2)\ P^{-\frac{K_3}{K_3 - K_1}} + P_3 = 0.368$$

The above is the computational procedure for the given complex reaction scheme.

ACKNOWLEDGEMENTS

I am deeply indebted to Dr. L. K. Doraiswamy, Director, National Chemical Laboratory, Poona, and Prof. S. Z. Hussain, Indian Institute of Technology, Bombay, for their inspiring joint guidance and constant encouragement throughout the course of this investigation.

I am grateful to the Council of Scientific and Industrial Research for the award of a research fellowship and to the Directors, Indian Institute of Technology and National Chemical Laboratory, for permitting me to submit this work in the form of a thesis.

My sincere thanks are due to Dr. B. D. Kulkarni for stimulating discussions and my colleagues for their whole-hearted co-operation.

Raiomond K. Irani

July 1980

SUMMARY

Industrial reactions taking place in fluidized beds are mainly complex in nature and in a majority of these reactions the intermediate is the desired product. However, only a few extensions to complex reaction systems have been presented of the various models appearing in the literature. The fluidized bed also yields a lower selectivity of intermediate at a given conversion level as compared to a tubular reactor. Many reactions involve a change in volume of the gas phase due to reaction. The simple first order reaction models are inapplicable for predicting the conversion in this case and a generalized model that takes into account the volume change due to reaction is yet to be published.

It is the object of the present work to carry out an analysis of complex reaction schemes in a fluid bed. The drawback of reduced selectivity is further sought to be remedied by propounding the concept of catalyst dilution in fluid beds. A generalized model incorporating volume change due to reaction is developed and experimentally tested, together with the catalyst dilution concept, for the reaction system pertaining to the dehydration of ethanol.

The Kunii-Levenspiel model has been taken as a representative model for the fluidized bed reactor in the

present study. Based on this model a unified development for bothconversion and product distribution is presented for complex first order reaction schemes of the type

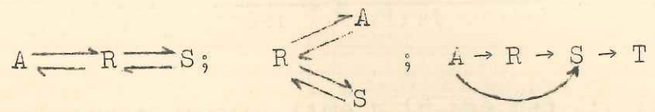

The influence of bubble diameter on the maximum concentration ($C_{R,max}$) and selectivity of intermediate R for successive reversible reactions is shown. An increase in the effective bubble diameter d_b in the bed is seen to result in a decrease in $C_{R,\ max}$ attainable, and the extent of the maximum as well as its very presence in the bed can be controlled by changing the bubble diameter. The above reaction schemes, together with their special cases, provide a reasonably extensive coverage of complex first order networks of practical relevance.

Although operating the fluid bed with smaller bubble diameters is preferable, physical constraints in operating systems lead to a certain minimum bubble size being involved. A technique has been evolved for optimizing the production of intermediate at the bed exit for a given gas residence time t or bubble diameter. For a reaction of the type

$$A \xrightarrow[\text{zero order}]{} R \xrightarrow[\text{first order}]{} S$$

d_b has no effect on t_{cr} at which $C_{R,max}$ occurs. However, for a system of the type

$$A \xrightarrow[\text{first order}]{} R \xrightarrow[\text{first order}]{} S$$

$C_{R,max}$, d_b and residence time t in the bed are interrelated and a three dimensional plot with these parameters as axes is employed to optimize the production of R at the bed exit.

The concept of dilution of catalyst has been applied to simple and complex first order reaction schemes in a fluidized bed reactor on the basis of the performance equations developed. Dilution of catalyst is seen to result in an improvement in the efficiency E of fluidized contacting and thus the fluid bed is relatively insensitive (with respect to overall conversion) to catalyst dilution. For a representative reaction scheme

$$A \xrightarrow{k_1} R \xrightarrow{k_3} S \ , \quad k_1 > k_3$$

dilution of catalyst keeping the total mass of solids and other parameters unchanged, is shown to result in an increase in the selectivity of intermediate formation without

a major loss in conversion. This is due to the fact that the contacting efficiencies of the two reaction steps are modified to different extents. Thus catalyst dilution affords a means to overcome the main drawback of a fluid bed reactor.

A model equation for calculating the conversion in a fluid bed reactor for a generalized reaction scheme of the type

$$A \rightarrow \beta R$$

where β is the stoichiometric coefficient of volume change, is next developed. Whereas pressure variation along the bed height does not have any appreciable effect on the model predictions, the effect of inerts in the feed stream is to mute the volume change effect. For $\beta < 1$ and $\beta > 1$ the conversions in the fluid bed are respectively higher and lower than that which would be obtained if no attendant volume change were considered.

The dehydration of ethanol to diethyl ether and ethylene, free of external and pore diffusion effects, has next been studied in an integral reactor reactor at 338°C and 375°C. The catalyst is commercial alumina and 95.6% ethanol and nitrogen are employed as the feed. A pseudo

first order equation is fitted to the data at 375°C. Runs have been carried out in a 4" ø fluid bed reactor at 375°C with varying amounts of nitrogen as inert in the feed, keeping the total number of moles entering the reactor constant. On the basis of the run with largest flow of nitrogen the predictions of the Kunii-Levenspiel and volume change model are extrapolated to the runs with larger ethanol flow rate and the volume change model is seen to give a better fit to the data.

Runs have also been carried out in the fluidized bed at 338°C where ether is formed principally as an intermediate. Glass powder is the inert diluent. A comparison of the fluid bed and integral reactor data shows that at any level of conversion the selectivity of intermediate formation is always higher in the fixed bed. The catalyst dilution ratio is varied keeping the residence time in the bed unchanged. An optimum catalyst dilution ratio F' = 3.67 (F' - mass of catalyst in the undiluted bed/mass of catalyst in the diluted bed) is shown to exist at which the ether production at the bed exit is maximized, and is seen to increase more than twofold (7% to 16%) as compared to that for the undiluted bed. An experimental verification of the theoretical predictions of the effect of catalyst dilution is thus obtained.

LIST OF PUBLICATIONS

1. 'Analysis of Complex Reaction Schemes in a Fluidized Bed. Application of the Kunii-Levenspiel Model',
Ind.Eng.Chem.Process Des.Dev., 19, 24(1980).

2. 'Optimal Production of Intermediate for Zero First and First First Order Reaction Sequences in Fluidized Bed Reactors',
Chem.Eng.Sci., in press (1980).

3. 'Effect of Catalyst Dilution on the Performance of a Fluid Bed Reactor for Complex First Order Reactions',
Ind.Eng.Chem.Process Des.Dev., 18, 648 (1979).

4. 'Analysis of Fluid Bed Reactors for Reactions Involving a Change in Volume',
Ind.Eng.Chem.Fundam., in press (1980).

5. 'Studies in the Dilution of Catalyst in a Fluidized Bed : Dehydration of Ethanol',
Ind.Eng.Chem.Fundam., communicated (1980).